Novel Multiple Antenna Techniques for Improved Diversity in Wireless Communication Systems

Thesis submitted to Cardiff University in candidature for the degree of Doctor of Philosophy.

Cheng Shen

Centre of Digital Signal Processing
Cardiff University
2009

UMI Number: U585229

All rights reserved

INFORMATION TO ALL USERS
The quality of this reproduction is dependent upon the quality of the copy submitted.

In the unlikely event that the author did not send a complete manuscript
and there are missing pages, these will be noted. Also, if material had to be removed,
a note will indicate the deletion.

UMI U585229
Published by ProQuest LLC 2013. Copyright in the Dissertation held by the Author.
Microform Edition © ProQuest LLC.
All rights reserved. This work is protected against
unauthorized copying under Title 17, United States Code.

ProQuest LLC
789 East Eisenhower Parkway
P.O. Box 1346
Ann Arbor, MI 48106-1346

DECLARATION

This work has not previously been accepted in substance for any degree and is not being concurrently submitted in candidature for any degree.

Signed..Cheng Shen..(candidate) Date ..30/06/09.....

STATEMENT 1

This thesis is being submitted in partial fulfillment of the requirements for the degree of PhD.

Signed ...Cheng Shen... (candidate) Date ..30/06/09.....

STATEMENT 2

This thesis is the result of my own investigation, except where otherwise stated. Other sources are acknowledged by giving explicit reference.

Signed ...Cheng Shen..... (candidate) Date ..30/06/09.....

STATEMENT 3

I hereby give consent for my thesis, if accepted, to be available for photocopying and for inter-library loan, and for the title and summary to be made available to outside organizations.

Signed .....Cheng Shen... (candidate) Date ..30/06/09.....

STATEMENT 4

I hereby give consent for my thesis, if accepted, to be available for photocopying and for inter-library loan, after expiry of a bar on access approved by the Graduate Development Committee.

Signed.....Cheng Shen(candidate) Date ....30/06/09.....

ABSTRACT

The focus of this thesis is to enhance the performance of wireless communication systems through the exploitation of multiple antennas at both the transmitter and the receiver ends of a communication link. Such a multiple-input multiple-output (MIMO) connection can theoretically provide spatially independent channels which can be exploited to provide diversity gain and thereby mitigate the problem of channel fading. To integrate such MIMO technology with emerging wireless systems such as third generation code division multiple access (CDMA) and fourth generation orthogonal division multiple access (OFDMA) based-approaches novel advanced signal processing techniques are required.

The major advantages of MIMO systems, including array, diversity and multiplexing gains, are initially reviewed. Diversity gain is identified as the key property, which leverages the spatial independent channels to increase the robustness of the communication link. The family of space-time block codes is then introduced as a low computational complexity scheme to benefit from diversity gain within wireless systems. In particular, extended-orthogonal and quasi-orthogonal space-time block codes (EO-/QO-STBCs) are introduced for systems with four transmit antennas which can operate either in open or closed-loop forms.

New EO-STBC and QO-STBC wideband CDMA transmission schemes

are proposed which when operating in closed-loop mode, i.e. channel state information is exploited at the transmitter, is shown to attain full diversity and thereby outperform previous schemes in terms of attainable symbol error rate performance. This advantage is then utilized in MIMO-OFDM transmission schemes and similar frame error rate (FER) performance advantage is attained.

Finally, to mitigate multiuser interference within the proposed MIMO-OFDM system a novel two-step combined parallel interference canceller and multiuser detection scheme is proposed. Simulation studies based upon FER confirm the efficacy of the technique.

To my loving wife Liyun, my son Ruoshu

and to my parents

ACKNOWLEDGEMENTS

I would like to give my great thanks to my supervisor Prof. Jonathon A. Chambers, who spent much time consulting with me. Thanks for his great enthusiasm and patience with me. Without his invaluable support and encouragement, this thesis would have not been accomplished. I feel lucky to have been inspired by his extraordinary motivation, great intuition and hard work. He is an example for my future career and has my deepest respect professionally and personally.

I would also like to thank my second supervisor Dr. Sangarapillai Lambotharan, who also supervised me during my second and third year PhD study. Dr. Saeid Sanei, and Dr. Zhuo Zhang have given much help and many suggestions on not only my research and study, but also my life in Cardiff. I would also like to express sincere gratitude to them.

The thanks also go to my dear colleagues in the Center of Digital Signal Processing (CDSP). It has been my great honour to work with them: Andrew Aubrey, Clive Cheong Took, Yonggang Zhang, Li Zhang, Qiang Yu, Yue Zheng and many others. Cardiff has been wonderful for me mainly because of all these friends.

My wife Liyun Zhang who accompanied me to Cardiff during the last two years, is greatly appreciated. I would like to thank for her love and encouragement.

Finally, I would like to thank my parents for their unconditional

patience and support while we have been separated for many years.

MAIN CONTRIBUTIONS AND PUBLICATIONS

Main Contributions

In this thesis, some new digital signal processing algorithms for implementation of the transmitters and receivers within MIMO-WCDMA and MIMO-OFDM systems are proposed, with and without feedback schemes. As by-products of this study, further research on iterative detection and interference cancellation techniques is also performed. The main contributions of this thesis can be summarized as follows:

1. WCDMA is a proven technology to reach the higher data rate and high quality signal. To further improve such a system's performance, a target system which is the WCDMA receiver architecture with MIMO extensions was considered. The combination system is a very interesting approach to combat the impairments of wireless multiuser channels. In recent research, a modified version of the Alamouti scheme has been preciously explored for a WCDMA system in [1]. Thus, a transmit diversity technique based on O-STBC has been proposed for a CDMA system in [2]. In the work in this chapter, novel QO-STBCs and EO-STBCs for such a WCDMA system is considered with a practically inspired

number of antennas both at the base station and the mobile station. A low complexity feedback algorithm, is therefore further developed, which will improve the performance. The simulation results indicate that the proposed scheme is robust in terms of bit error performance as compared with the previous single antenna scheme.

2. Certain physical layer processing issues relating to the implementation of both MIMO and OFDM systems are presented in this thesis. In particular, facilitating multiuser operation for certain MIMO-OFDM baseband systems is a focus. The QOSTBC with feedback method for the OFDM system is considered and confirmed to improve link performance.

3. The idea of two-step interference cancellation was first introduced in [3]. In this thesis, a two-step hard-decision interference cancellation receiver is investigated for a multiuser MIMO-OFDM synchronous uplink system which employs STBC over frequency selection channels in two and four antennas systems. The STBC is implemented either over adjacent tones or adjacent OFDM symbols. The two-step receiver structure uses a combined interference suppression scheme based on minimum mean-squared error (MMSE) and symbol-wise maximum likelihood detectors, which is then followed by an interference cancellation step. The receiver can suppress and cancel the interference from the co-channel users effectively without increasing the complexity significantly. The performance of the system is shown by simulation to be significantly improved in a low SNR environment.

List of Publications

- C. Shen, and J. A. Chambers, "A New Approach to Joint Full-Rate STBC and Long-Code WCDMA for Four Transmit Antenna MIMO Systems," *Proc. 8th IEEE International Conference on Signal Processing (ICSP2006)*, Guilin, P.R.China, Nov. 2006.

- C. Shen, and J. A. Chambers, "A Novel Closed-Loop Quasi-Orthogonal Space-Time Block Coding Scheme for Long-Code WCDMA," *Proc. 7th International Conference on Mathematics in Signal Processing (IMA2006)*, pp. 175-179, Cirencester, UK, Dec. 2006.

- C. Shen, L. Zhang, and J. A. Chambers, "A Two-Step Interference Cancellation Technique for a MIMO-OFDM System with Four Transmit Antennas," *Proc. 2007 15th International Conference on Digital Signal Processing*, pp. 351-354, Cardiff, UK, July 2007.

- C. Shen, L. Zhang, and J. A. Chambers,"An Enhanced Two-Step Interference Cancellation Technique for a Multiuser MIMO-OFDM Systems with Four Transmit Antennas," *IEEE Signal Processing Lett.*, submitted, May 2009.

- L. Zhang, C. Shen, M. Sellathurai, and J. A. Chambers,"Low Complexity Sequential Iterative Cancellation Technique for Multi-user MIMO-OFDM Systems," *IEEE Signal Processing Lett.*, submitted, Apr. 2009.

LIST OF ACRONYMS

3GPP	3rd Generation Partnership Project
4G	Fourth-Generation
AWNG	Additive White Gaussian Noise
BER	Bit Error Rate
BLAST	Bell-Labs Layered Space-Time Architecture
BPSK	Binary Phase Shift Keying
CCI	Co-Channel Interference
CDF	Cumulative Distribution Function
CDMA	Code Division Multiple Access
CP	Cyclic Prefix
CSI	Channel State Information
DAB	Digital Audio Broadcasting
DFT	Discrete Fourier Transform
DSRC	Dedicated Short-Range Communications
EGC	Equal Gain Combining

ENF	Equivalent Noise Floor
EO-STBCs	Extended-Orthogonal Space-Time Blocks
EVCM	Equivalent Virtual Channel Matrix
FDM	Frequency Division Multiplexing
FER	Frame Error Rate
FFT	Fast Fourier Transform
IC	Interference Cancellation
ICI	Inter-Carrier Interference
IDFT	Inverse Discrete Fourier Transform
IFFT	Inverse Fast Fourier Transform
ISI	Inter-Symbol Interference
LAN	Local Area Network
L-MMSE	Linear Minimum Mean Square Error
MAI	Multiple Access Interference
MAIFB	MAI-Free Bound
MAP	Maximum A Posterior
MAN	Metropolitan Area Network
MF	Matched Filter
MIMO	Multiple-Input Multiple-Output
ML	Maximum-Likelihood

MMSE	Minimum Mean-Squared Error
MRC	Maximal-Ratio Combining
MRRC	Maximum Ratio Receiver Combiner
MUD	Multiuser Detection
OFDM	Orthogonal Frequency Division Multiplexing
OFDMA	Orthogonal Division Multiple Access
OSTBC	Orthogonal Space-time Block Codes
PAM	Phase Amplitude Modulation
PIC	Parallel Interference Cancellation
PSK	Phase Shift Keying
QO-STBCs	Quasi-Orthogonal Space-Time Blocks
QAM	Quadrature Amplitude Modulation
QPSK	Quadrature Phase Shift Keying
SER	Symbol Error Rate
SISO	Single-Input Single-Output
STBC	Space-Time Block Coding
STC	Space-Time Coding
STTC	Space-Time Trellis Codes
SNR	Signal-to-Noise Ratio
SVD	Singular Value Decomposition

TDMA	Time Division Multiple Access
WCDMA	Wideband Code Division Multiple Access
WLANs	Wireless Local Area Networks
ZF	Zero-Forcing

MATHEMATICAL NOTATIONS

x	Scalar quantity
$\mathbf{x}$	Vector quantity
$\mathbf{X}$	Matrix quantity
$\mathbf{x}_n$, $\mathbf{x}(n)$	Value of $\mathbf{x}$ at discrete time n
$\mathbf{X}_{qj}$	The qj-th element of the matrix quantity $\mathbf{X}$
$\bar{\mathbf{x}}$	Mean vector
$\hat{\mathbf{x}}$	Estimate of original quantity $\mathbf{x}$
$\mathbf{0}$	Vector of zeros
$\mathbf{I}$	Identity matrix
$\mathbf{A} \otimes \mathbf{B}$	Kronecker product of matrix $\mathbf{A}$ and matrix $\mathbf{B}$
$(\cdot)^T$	Transpose operator
$(\cdot)^H$	Hermitian transpose operator
$(\cdot)^{-1}$	Matrix inverse

$(\cdot)^*$	Complex conjugate operator
$\|\cdot\|$	Absolute magnitude value
$\|\|\cdot\|\|$	Euclidean norm
$\angle(\cdot)$	Angle operation
$det(\cdot)$	Matrix determinant
$min(a, b)$	Minimum value of a or b
$max(a, b)$	Maximum value of a or b
$Re(\cdot)$	Real part of the symbol
$E\{\cdot\}$	Statistical expectation

CONTENTS

ABSTRACT iii

ACKNOWLEDGEMENTS vi

MAIN CONTRIBUTIONS AND PUBLICATIONS viii

LIST OF ACRONYMS xi

MATHEMATICAL NOTATIONS xv

LIST OF FIGURES xxiii

LIST OF TABLES xxviii

1 INTRODUCTION 1

1.1 Benefits of Multiple Antennas for Wireless Communications 2

1.1.1 Higher Bit Rates with Spatial Multiplexing 3

1.1.2 Smaller Error Rates through Spatial Diversity 3

1.1.3 Improved Signal-to-Noise Ratios with Smart Antennas 4

1.2 Focus of the Thesis 5

1.3 Outline of the Thesis 7

2 MULTIPLE ANTENNA WIRELESS COMMUNICATION AND DIVERSITY 9

2.1 Introduction 9

2.2 System Model 10

2.3 MIMO Capacity 12

2.4 Diversity Techniques 15

2.4.1 Diversity Combining Techniques 16

2.4.2 Diversity Gain 19

2.4.3 Array Gain 22

2.5 Summary 22

3 SPACE TIME BLOCK CODES 23

3.1 Introduction 23

3.2 Space-Time Block Code Encoding and Code Rate 24

3.3 Alamouti Code 26

3.3.1 Equivalent Virtual Channel Matrix (EVCM) of the Alamouti Code 28

3.3.2 Linear Signal Combining and Maximum Likelihood Decoding of the Alamouti Code 30

3.4 Orthogonal Space-Time Block Codes (OSTBCs) 33

3.5 Quasi-Orthogonal Space-Time Block Codes (QO-STBCs) 34

3.5.1 Transmission with Channel Feedback 37

3.5.2 Two Phase Feedback 38

3.5.3 Single Phase Feedback 40

3.5.4 Quantization 41

3.5.5 Simulation 42

3.6 Extended Orthogonal Space Time Block Codes (EO-STBCs) 43

3.6.1 Channel Matched Filtering 45

3.6.2 Transmission with Channel Feedback 46

3.6.3 Simulation and Results 49

3.7 MIMO in Current and Future Wireless Communication System 50

3.7.1 MIMO in OFDM 50

3.8 Summary 52

4 CLOSED-LOOP MIMO SCHEMES FOR WCDMA SYSTEM 53

4.1 Introduction 53

4.2 WCDMA System 54

4.2.1 WCDMA Detection Techniques 57

4.3 Orthogonal Space Time Coded WCDMA 60

4.3.1 Space Time Receiver 61

4.3.2 Simulation and Results 64

4.4 QO-STBC MIMO-WCDMA Transceiver Design with Four Antennas 66

4.4.1 Simple Linear Matrix Transform Method in the Receiver 68

4.4.2 Transmission with Channel Feedback 69

4.4.3 Simulations 71

4.5 EO-STBC MIMO-WCDMA Transceiver Design with Four Antennas 73

4.5.1 Transmission with Channel Feedback 75

4.5.2 Simulations 76

4.6 Summary 77

5 CLOSED-LOOP MIMO SCHEMES FOR OFDM SYSTEMS 78

5.1 A Brief Overview of the OFDM Technique 79

5.2 OFDM Principles 80

5.2.1 OFDM Employing FFT 82

5.2.2 Bandwidth Efficiency 83

5.2.3 Modulation 84

5.2.4 Guard Interval 85

5.3 OFDM System Model 86

5.3.1 Signal Processing of OFDM Model in a Static Channel 88

5.4 Introduction to MIMO-OFDM Systems 92

5.5 Capacity of MIMO-OFDM Systems 95

5.6 Space-Time Block Coded MIMO-OFDM Transceiver Design with Two Antennas 97

5.6.1 Simulations 102

5.7 QO-STBC MIMO-OFDM Transceiver Design with Four Antennas 104

5.7.1 Transmission with Channel Feedback 106

5.7.2 Simulation 108

5.8 EO-STBC MIMO-OFDM Transceiver Design with Four Antennas 109

5.8.1 Transmission with Channel Feedback 112

5.8.2 Simulation 114

5.9 Summary 114

6 TWO-STEP MULTIUSER DETECTION SCHEME FOR QO-STBC MIMO-OFDM SYSTEMS 116

6.1 Introduction 116

6.2 Multiuser Interference and Multiuser Detection 117

6.2.1 Multiuser Detection 117

6.2.2 Multiuser Interference Cancellation 118

6.3 PIC scheme in Multiuser Detection 119

6.4 Two-Step PIC MUD for QO-STBC MIMO-OFDM Systems 123

6.4.1 System Model 123

6.4.2 Linear MMSE IC Suppression and ML Decoding 127

6.4.3 Two-step Approach for IC and ML Decoding 129

6.4.4 Simulations and Results 130

6.5 Summary 136

7 CONCLUSION 138

7.1 Summary of the Thesis 138

7.2 Future Work 140

7.2.1 Robustness of Space Time Codes 140

7.2.2 Robustness of STBC MIMO-OFDM system 141

BIBLIOGRAPHY 143

List of Figures

1.1 Diagrammatic overview of multiple antenna techniques for wireless communication systems and their benefits for link level performance 2

2.1 MIMO model with n_t transmit antennas and n_r receive antennas. 10

2.2 A single-input single-output (SISO) channel. 12

2.3 Ergodic MIMO channel capacity vs. SISO channel capacity. 14

2.4 Diagram showing four types of diversity combining techniques can be employed as receive diversity. 17

2.5 Block diagram of switched combining for n_r branches/antenna elements with only one receiver 17

2.6 Block diagram of selection combining for n_r branches/antenna elements. 18

2.7 Block diagram of equal gain combining for n_r branches/antenna elements. 19

2.8 Block diagram of maximum ratio combining for N branches/antenna elements. 20

2.9 CDF of Rayleigh fading signals for a different number of diversity branch. 21

3.1 A block diagram of the Alamouti space-time encoder. 26

3.2 The BER performance of Alamouti schemes with one and two receivers compared with when there is no diversity and MRRC schemes 32

3.3 Block diagram of the baseband model of an four transmit and one receive system based two-phase feedback STBC scheme with four transmit antennas 39

3.4 Performance of quasi-orthogonal STBC scheme. 43

3.5 Baseband representation of the proposed closed-loop EO-STBC system with four transmit and one receiver antennas 44

3.6 Performance of extended orthogonal STBC scheme 49

4.1 Noiseless single symbol output y_{im}. 55

4.2 Structure of the code matrix **T**, **H** and **S**. 56

4.3 WCDMA system with space-time coded scheme using two transmit antennas and one receiver antenna. 61

4.4 Performance comparison for WCDMA system and STBC-WCDMA system with two transmit antennas and one receive antenna. 65

4.5 WCDMA system with space-time coded scheme using four transmit antennas and one receiver antenna. 66

4.6 Block diagram of the baseband model of an WCDMA based two-phase feedback STBC scheme with four transmit antennas 70

4.7 The BER vs. SNR performance for QO-STBC-WCDMA system 72

4.8 The BER vs. SNR performance for EO-STBC-WCDMA system 77

5.1 OFDM modulation block diagram. 81

5.2 Guard interval by cyclic extension 85

5.3 OFDM transceiver diagram consisting of the transmitter, channel and receiver. 87

5.4 The average SER vs. SNR performance for an OFDM system: the simulation is implemented over a static channel and performs ZF channel equalization. 90

5.5 The average SER vs. SNR performance for an OFDM system: the simulation is implemented over static channels and performs L-MMSE channel equalization. 92

5.6 The block diagram of MIMO OFDM scheme with four transmit antennas. 93

5.7 The block diagram of an MIMO OFDM receiver with one receive antenna. 94

5.8 Average channel capacity for different MIMO-OFDM configurations. 97

5.9 STBC MIMO-OFDM baseband transmitter diagram consisting of two transmit antennas. 100

5.10 FER performance for an OFDM based STBC scheme with two transmit antennas and one receive antenna. 103

5.11 FER performance comparison between MIMO-OFDM system, O-STBC scheme and close-loop QO-STBC scheme with feedback. 109

5.12 FER performance comparison for MIMO-OFDM system with O-STBC scheme, feedback close-loop QO-STBC scheme and feedback close-loop EO-STBC scheme. 115

6.1 The structure of the parallel interference cancellation (PIC) scheme for the two user signal detection. 121

6.2 Multiuser QO-STBC MIMO-OFDM transmitters for K users, where each user terminal is equipped with $n_t = 4$ transmit antennas. 124

6.3 Two-step PIC Multiuser QO-STBC MIMO-OFDM receiver for two users, which is equipped with m receive antennas. 127

6.4 The FER vs. SNR performance comparison for two user QO-STBC-OFDM system: LMMSE and two-step schemes over slow fading MIMO channels where channel tap length $L = 3$ and Doppler frequency $f_d = 20Hz$. MAI-free bound is also shown. 133

6.5 The FER vs. SNR performance comparison for two user QO-STBC-OFDM system: implements between LMMSE and two-step processing over various fading rates (maximum Doppler frequencies f_d are 20Hz, 50Hz and 200Hz respectively), and MAIFB is also performed at 20Hz for comparison. 134

6.6 The FER vs. SNR performance comparison for two user STBC-OFDM system: implements LMMSE and two-step scheme between O-STBC scheme and QO-STBC scheme respectively, over slow fading channel (maximum Doppler frequencies f_d are 20Hz, and also shows MAIFB curve for comparison. 135

List of Tables

6.1 Two-step PIC algorithm for two user QO-STBC-OFDM Detection. 131

Chapter 1

INTRODUCTION

The telecommunications industry has experienced a tremendous growth over the past few years, specifically in wireless communications, which has become a very important part of everyone's life [4]. This expansion has been supported by the wide spread usage of mobile telephones and wireless devices. Even though the throughput data rate of such systems is limited when compared to that of wired systems, recent developments in wireless technology are able to provide competitive solutions. But, bandwidth limitations, propagation loss, time variations, noise, interference, and multipath fading make the wireless channel a particularly challenging communication pipe that does not easily accommodate large data rates. Further challenges arise from power limitation as well as size and speed of devices in wireless portables. The research community has generated a number of promising solutions for significant improvements in link performance. One of the most promising future technologies in mobile radio communications to improve link performance is multiple antenna elements at the transmitter and at the receiver, benefits of which are next described.

1.1 Benefits of Multiple Antennas for Wireless Communications

The great potential of using multiple antennas for wireless communications has only become apparent during the last 20 years. At the end of the 1990*s* [5], multiple antenna techniques were shown to provide a novel means to achieve both higher bit rates and smaller error rates. Correspondingly, they constitute an important technology for modern wireless communications [6, 7]. The benefits of multiple antennas for the physical layer of wireless communication systems are summarized in Figure 1.1. In the sequel, they are characterized in more detail.

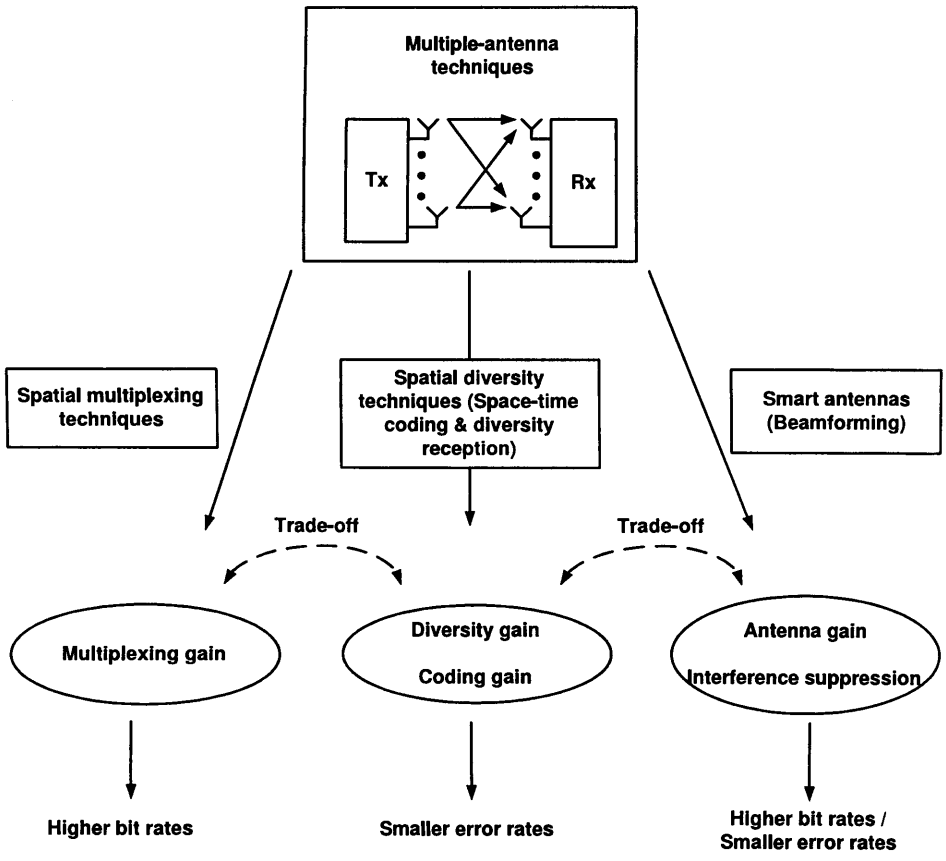

Figure 1.1. Diagrammatic overview of multiple antenna techniques for wireless communication systems and their benefits for link level performance

1.1.1 Higher Bit Rates with Spatial Multiplexing

Spatial multiplexing techniques simultaneously transmit independent information sequences, often called layers, over multiple antennas. Using M transmit antennas, the overall bit rate compared to a single-antenna system is thus theoretically enhanced by a factor of M without requiring extra bandwidth or extra transmission power. A well-known spatial multiplexing scheme is the Bell-Labs Layered Space-Time Architecture (BLAST) [8]. The achieved gain in terms of bit rate (in comparison to a single-antenna system) is called multiplexing gain [9].

1.1.2 Smaller Error Rates through Spatial Diversity

Similar to channel coding, multiple antennas can also be used to improve the average bit error rate (BER) of a system, by transmitting or receiving redundant signals representing the same information sequence. By means of two-dimensional coding in time and space, commonly referred to as space-time coding, the information sequence is spread out over multiple transmit antennas. At the receiver, an appropriate combining (such as maximum ratio receiver combiner (MRRC) architecture) of the redundant signals has to be performed [5]. Optionally, multiple receive antennas can be used, in order to further improve the average BER performance (diversity reception). The advantage over conventional channel coding is that redundancy can be accommodated in the spatial domain, rather than in the time domain. Correspondingly, a coding gain (and thus an improved error performance) can be achieved without lowering the effective bit rate compared to a single-antenna transmission. Additionally, a spatial diversity gain is achieved which also contributes to an improved error performance.

Although the major goal of spatial diversity techniques is to improve average BER performance (or, equivalently, to reduce the transmit power required to achieve a certain error performance), they can also be used to increase the bit rate of a system, when employed in conjunction with an adaptive modulation/channel coding scheme [10]. Well-known spatial diversity techniques for systems with multiple transmit antennas are, for example, Alamouti's transmit diversity scheme [5] as well as the higher complexity space-time trellis codes [11] invented by Tarokh, Seshadri, and Calderbank. For systems, where multiple antennas are available only at the receiver, there are well-established linear diversity combining techniques dating back to the 1950s [12].

1.1.3 Improved Signal-to-Noise Ratios with Smart Antennas

In addition to higher bit rates and smaller error rates, multiple-antenna techniques can also be utilized to improve the signal-to-noise ratio (SNR) at the receiver and to suppress co-channel interferers in a multi-user scenario. This is achieved by means of adaptive antenna arrays, also called smart antennas or software antennas in the literature [13–15]. Using beamforming techniques, the beam patterns of the transmit and receive antenna array can be steered in certain desired directions, whereas undesired directions (e.g., directions of significant interferers) can be suppressed. Beamforming can be interpreted as linear filtering in the spatial domain. The SNR gains achieved by beamforming are often called antenna gains or array gains. Beamforming techniques can also be beneficial in scenarios with strong spatial fading correlations due to insufficient antenna spacings. The concept of antenna arrays with adaptive beam patterns is not new and has its

origins in the field of radar (e.g., for target tracking) and aerospace technology. However, intensive research on smart antennas for wireless communication systems started only in the 1990s.

1.2 Focus of the Thesis

The above families of multiple-antenna techniques are, in fact, quite different. Spatial multiplexing is closely related to the field of multiuser communications. Space-time coding is more in the field of modulation and channel coding, and beamforming techniques belong more to the area of signal processing and filtering. There are also composite transmission schemes that aim at a combination of the different gains mentioned above. However, given a fixed number of transmit and receive antennas, there are certain trade-offs between multiplexing gains, diversity gains, and SNR gains [16]. The core idea in MIMO transmission is space-time (frequency) signal processing in which signal processing in time (frequency) is complemented by signal processing in the spatial dimension by using multiple, spatially distributed antennas generally at both link ends.

Space-time coding (STC), introduced first by Tarokh et al. [11], is a promising method where the number of the transmitted code symbols per time slot is equal to the number of transmit antennas. These code symbols are generated by the space-time encoder in such a way that diversity gain, coding gain, as well as high spectral efficiency are achieved. After a while, Alamouti [5] proposed a simple transmitter diversity scheme which provided full diversity in a two-transmit antenna channel with simple maximum-likelihood (ML) decoding. The good properties of this code inspired Tarokh [17] to examine the exis-

tence of similar designs for numbers of transmit antennas. In the case of complex codes, i.e. modulation schemes using complex constellation members, the authors proposed a structured modulation scheme, called orthogonal space-time block codes (OSTBCs) that could send on average two symbols in every two time slots, and achieved full diversity and full rate as well as simple symbol wise ML decoding. They presented examples for three and four transmit antennas with average rate of $3/4$, or in the case of real constellations they presented rate one codes for four and eight transmit antennas. It was shown in that paper that for complex constellation there is no other square rate one code, i.e. a code for which the time length of the block equals the number of transmit antennas as that of Alamouti, for more than two transmit antennas. The Alamouti code is therefore the only square full-rate complex orthogonal space time block code.

In the last few years the research community has made an enormous effort to understand space-time codes, their performance and their limitations. The purpose of these works were to explain the concept of space-time (frequency) block coding in a systematic way [18–25]. In this thesis, the main focus is devoted to so-called quasi-orthogonal space-time block codes (QO-STBCs) and extended-orthogonal space-time block codes (EO-STBCs), since they allow full-rate orthogonal codes to be produced through the exploitation of channel state feedback. The goal is to analyze their performance on current and next generation wireless communication system, with and without adopting the phase feedback method at the transmitter.

1.3 Outline of the Thesis

The thesis is organized in seven chapters as follows:

Chapter 2: This chapter covers the introduction to MIMO systems and diversity techniques. Multiple antenna systems are described and the corresponding statistical parameters [26–31]. The potential of MIMO systems as well as their problems are described. Within this chapter, the most important parameter of a MIMO system, the channel capacity, together with diversity combining techniques and the notion of diversity gain are presented. Orthogonal and quasi-orthogonal space time block codes designs are presented and their performances are evaluated by simulations.

Chapter 3 : A review of space-time coding techniques for wireless communication system is detailed in this chapter. The performance of these schemes is introduced. A more systematic discussion of space-time block coding (STBC) is provided. The Alamouti STBC that provides a transmit diversity of two is highlighted. The analysis of other space codes is considered, such as QO-STBCs in open-loop or closed-loop transmission systems together with EO-STBCs in closed-loop mode, and their performance is evaluated by simulation.

Chapter 4: A novel combination of STBCs and the current third generation communication system – wideband code division multiple access (WCDMA) is proposed in this chapter. The chapter starts with an STBC-WCDMA system model. A novel combination of the EO-STBCs or the QO-STBCs and the WCDMA system is introduced to combat the impairments of wireless multiuser channels and thereby increase capacity. As a nobel contribution, an open-loop mode of operation is considered initially. Next, a transmit antenna phase rotation

method based on feedback is presented and then EO-STBCs are introduced to yield the best performance. By Monte Carlo simulations the BER performances of the two different space time block codes are evaluated.

Chapter 5: In this chapter, the previous schemes are successfully extended as full rate space time block codes within a $4G$ communication multiuser system, i.e an orthogonal frequency division multiplexing (OFDM) system. The simulation results show that the new novel system can improve the frame error rate performance, especially the closed-loop method.

Chapter 6: Finally, this chapter presents a design of a two-step interference cancellation scheme for a MIMO-OFDM wireless communication system which adopts full-rate STBC in the transmission. Four transmit antennas are used in each terminal user and two receive antennas are exploited in the receiver. The receiver is based on a linear MMSE interference suppression in the first step and a two-step interference cancellation approach is also considered. Simulation results confirm the success of the scheme.

Chapter 7: This chapter concludes the research and suggestions for future work are also given.

Chapter 2

MULTIPLE ANTENNA WIRELESS COMMUNICATION AND DIVERSITY

2.1 Introduction

Rapid growth in mobile computing and other wireless multimedia services is inspiring many research and development activities on high-speed wireless communication systems [32]. The main challenge in this area include the development of efficient coding and modulation signal processing techniques to improve the quality and spectral efficiency of the link level of wireless systems. The recently emerging signal processing techniques for wireless communication systems employing multiple transmit and receive antennas offer a powerful paradigm for meeting these challenges. Information theoretic results show that multiple-input multiple-output (MIMO) systems can theoretically offer significant capacity gains over traditional single-input single-output (SISO) channels [8, 11, 26, 33]. This increase in capacity is enabled by the fact that

in rich scattering wireless environments, the signals from each individual transmitter appear highly uncorrelated at each of the receive antennas. When conveyed through uncorrelated channels between the transmitter and the receiver, the signals corresponding to each of the individual transmit antennas have attained different spatial signatures. The receiver can exploit these differences in spatial signatures to separate the signals originated from different transmit antennas.

2.2 System Model

Let us consider a point-to-point MIMO communication system with n_t transmit antennas and n_r receive antennas. The block diagram is given in Figure 2.1.

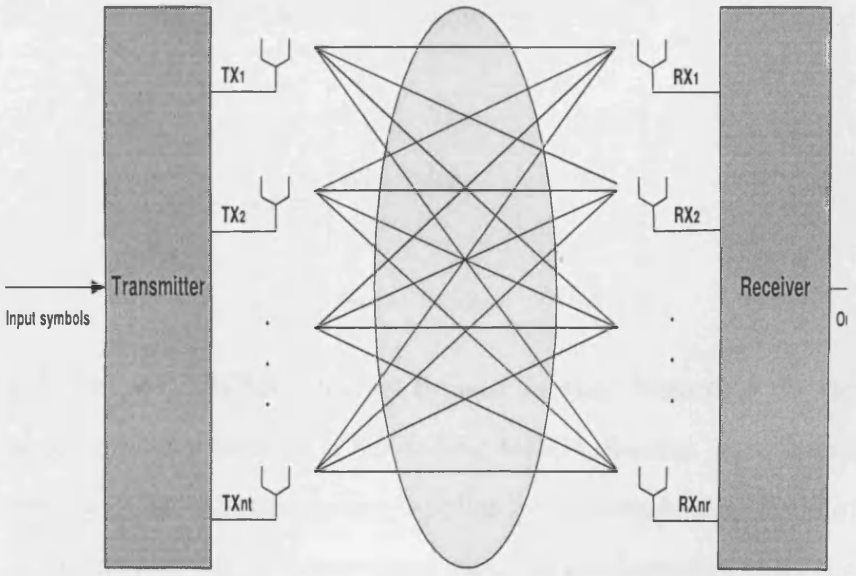

Figure 2.1. MIMO model with n_t transmit antennas and n_r receive antennas.

Let $h_{i,j}$ be a complex number corresponding to the channel gain between the element $j \in [1, \ldots, n_t]$ at the transmitter and element $i \in [1, \ldots, n_r]$ at the receiver. The received signal at antenna i can be

expressed as:

$$y_i = \sum_{j=1}^{n_t} h_{i,j} x_j + n_i \tag{2.2.1}$$

where n_i is an additive noise term, typically zero mean white Gaussian noise. The vector $\mathbf{x} = [x_1, x_2, \cdots, x_{n_t}]^T$ is the complex transmitted signal vector which contains the symbols transmitted via the n_t transmit antennas. Combining all receive signals in a vector $\mathbf{y}$, Equation (2.2.1) can be easily expressed in matrix form as

$$\mathbf{y} = \mathbf{H}\mathbf{x} + \mathbf{n} \tag{2.2.2}$$

where $\mathbf{y} = [y_1, y_2, \cdots, y_{n_r}]^T$ is the $n_r \times 1$ received signal vector, $\mathbf{n} = [n_1, n_2, \cdots, n_{n_r}]^T$ is the received noise vector and

$$\mathbf{H} = \begin{bmatrix} h_{1,1} & h_{1,2} & \cdots & h_{1,nt} \\ h_{2,1} & h_{2,2} & \cdots & h_{2,nt} \\ \vdots & \vdots & \ddots & \vdots \\ h_{nr,1} & h_{nr,2} & \cdots & h_{nr,nt} \end{bmatrix} \tag{2.2.3}$$

is the $(n_r \times n_t)$ MIMO channel transfer matrix. Note that the system model implicity assumes a flat fading MIMO channel. Flat fading, or frequency non-selective fading, applies by definition to systems where the bandwidth of the transmitted signal is much smaller than the coherence bandwidth of the channel. All the frequency components of the transmitted signal undergo the same attenuation and phase shift propagation through the channel.

2.3 MIMO Capacity

The motivation for using MIMO systems is the possibility to achieve orthogonal subchannels between the transmitters and receivers through a rich scattering environment and consequently to increase the offered capacity. Mathematically, the number of independent subchannels can be estimated by using the singular value decomposition (SVD) of the channel coefficient matrix $\mathbf{H}$ as

$$\mathbf{H} = U\Sigma V^H \tag{2.3.1}$$

where U is a unitary matrix of dimension $(n_t \times n_r)$, V is a unitary matrix of dimension $(n_t \times n_r)$ and Σ is a $(n_r \times n_t)$ diagonal matrices, and the superscript H denotes conjugate transpose.

The maximum error-free data rate that a channel can support is called the channel capacity. Before investigating MIMO capacity, the capacity of single-input single-output (SISO) fading channels is briefly examined, which is shown in Figure 2.2. The channel capacity for SISO additive white Gaussion noise (AWGN) channels was first derived by Claude Shannon [34]. In contrast to SISO AWGN channels, multiple antenna channels combat fading by exploiting a spatial dimension.

Figure 2.2. A single-input single-output (SISO) channel.

The capacity C of a deterministic SISO channel for the input-output

relation $y(t) = h(t)x(t) + n(t)$ is shown to be [28]:

$$C = log_2(1 + \rho|h|^2) \quad [bits/s/Hz] \tag{2.3.2}$$

where the average signal-to-noise ratio at receiver is $\rho = P/\sigma_n^2$, and P is the average power at the output of receiver antennas. h is the channel coefficient.

Conceptually, the MIMO system enables multiple data streams to be transmitted simultaneously on the same frequency, hence increasing the bandwidth efficiency by the number of data streams employed. The channel capacity of a deterministic non-ergodic MIMO channel is shown to be [28]:

$$C = log_2[det(\boldsymbol{I}_{n_r} + \frac{\rho}{n_t}\mathbf{H}\mathbf{H}^H)] \quad [bits/s/Hz] \tag{2.3.3}$$

where ρ is the total signal-to-noise ratio across the n_r receivers, $det(\cdot)$ mean the matrix determinant and $\boldsymbol{I}_{n_r}$ is an $n_r \times n_r$ identity matrix. For random MIMO channel, the mean channel capacity, also called the ergodic capacity, is given by

$$C = E_H\{log_2[det(\boldsymbol{I}_{n_r} + \frac{\rho}{n_t}\mathbf{H}\mathbf{H}^H)]\} \quad [bits/s/Hz] \tag{2.3.4}$$

where E_H denotes statistical expectation with respect to $\mathbf{H}$. The ergodic capacity grows with the number n of antennas (under the assumption $n_t = n_r = n$), which results in a significant capacity gain of MIMO fading channels compared to a wireless SISO channel as will be next shown.

Example Channel Capacity of the MIMO Systems

In Figure 2.2 the ergodic channel vs. the mean SNR is plotted for MIMO systems with $n_t = n_r = n$. The channel capacity for the SISO system ($n_t = n_r = 1$) at $SNR = 10dB$ is approximately 3.1 bits/s/Hz. By applying multiple antennas, it is obvious that the channel capacity increases substantially. A (2×2) MIMO system (with two transmit and two receive antennas) can theoretically transmit more than 6.2 bits/s/Hz, the (4×4) MIMO system (with four transmit and four receive antennas) can transmit more than 12.1 bits/s/Hz, the MIMO system with eight transmit and eight receive antennas (8×8 MIMO) promises almost a seven fold increase in capacity (20.9 bits/s/Hz) over the SISO channel at this SNR value.

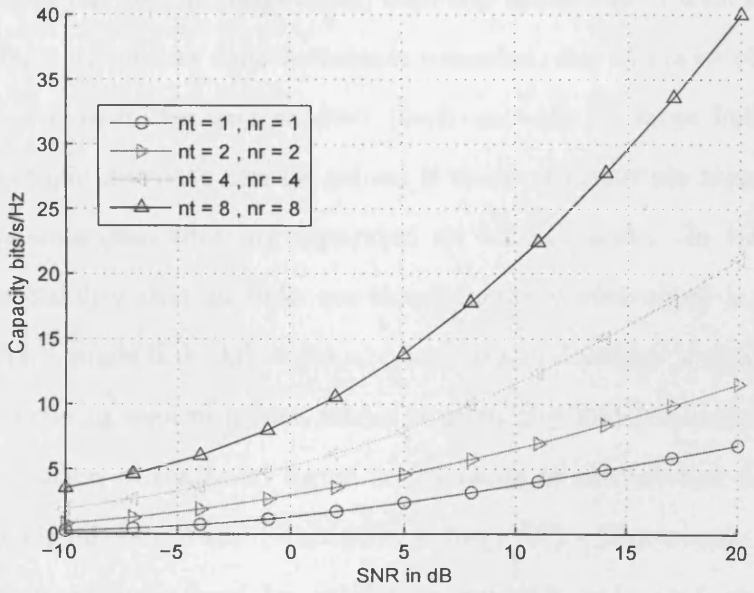

Figure 2.3. Ergodic MIMO channel capacity vs. SISO channel capacity.

Methods to exploit the potential capacity gain of a MIMO system which is proportional to the $min(n_t, n_r)$ [35] are next considered.

2.4 Diversity Techniques

Diversity is described as a powerful communication receiver technique that provides wireless link improvement at relatively low cost, which exploits the randomness of the radio propagation in a wireless channel [4]. The basic principle of diversity is that the receiver should have more than one version of the transmitted signal available, where each version is received through a different uncorrelated channel. Though the system complexity increases, diversity systems provide performance improvements without additional requirements of power or bandwidth.

Diversity methods can be employed either at the base station (macroscopic diversity) or at the mobile station (microscopic diversity), although the antenna separation required differs for each case [36]. In practice, macroscopic (large-scale) diversity is associated with shadowing effects in wireless communication scenarios, due to major obstacles between transmitter and receiver (such as walls or large buildings). Macroscopic diversity can be gained if there are multiple transmit or receive antennas, that are separated on a large scale. In this case, the probability that all links are simultaneously obstructed is smaller than for a single link. Microscopic (small-scale) diversity is available in rich-scattering environments, where constructive and non-constructive superposition of scattered signal components at the receiver causes a fading signal amplitude (multipath fading) [37]. Microscopic spatial diversity can be gained by employing multiple co-located antennas. Typically, antenna spacings of just a few wavelengths are sufficient, in order to obtain links that fade more or less independently. Similar to macroscopic diversity, the diversity gains are due to the fact that the probability of all links being simultaneously in a deep fade decreases

with the number of antennas used. An excellent survey of the value of spatial diversity for wireless communication systems can be found in [38].

There are five categories of diversities, i.e. frequency, time diversity, spatial diversity, pattern diversity and polarization diversity. Frequency diversity implies transmitting the message on multiple carrier frequencies spaced sufficiently far apart so as to provide independent fading versions of the channel. Time diversity transmits the message in different time slots, providing signal repetition such as in GSM, second generation mobile system [4]. Both of these methods are wasteful in that they use up excessive channel bandwidth. With spatial diversity, multiple receiving antennas are spaced at least half a wavelength of the carrier frequency apart to ensure that the signals reaching them are statistically independent [5]. The advantage of spatial diversity over frequency and time diversity is that the message carrying signal does not have to be rebroadcast.

2.4.1 Diversity Combining Techniques

Diversity schemes can be classified according to the type of combining employed at the receiver, namely, switched diversity, selection diversity, equal gain combining (EGC) and maximal-ratio combining (MRC), which are illustrated in Figure 2.4.

Switched Combining

The switched combining technique requires only one receiver radio between the N branches as shown in Figure 2.5.

The receiver is switched to other branches only when the SNR on

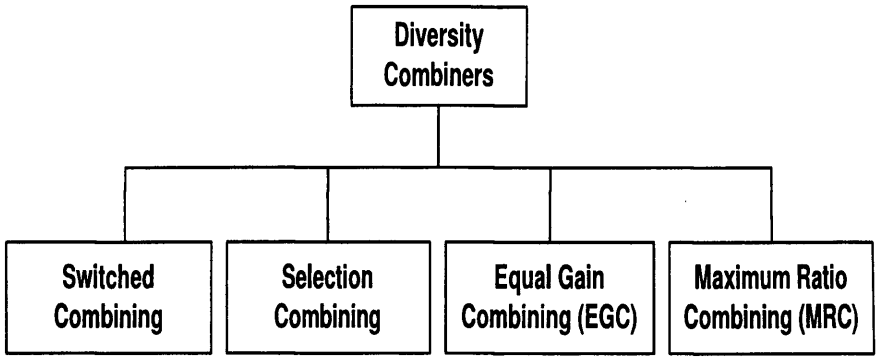

Figure 2.4. Diagram showing four types of diversity combining techniques can be employed as receive diversity.

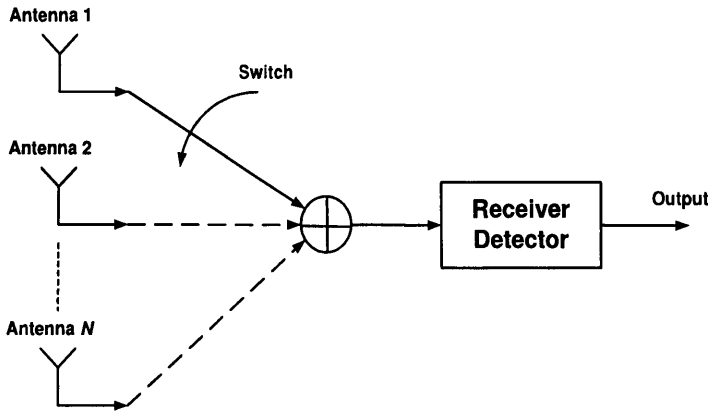

Figure 2.5. Block diagram of switched combining for n_r branches/antenna elements with only one receiver

the current branch is lower than a predefined threshold. Other combining techniques, on the other hand, require N receivers to monitor the received instantaneous signals level of every branch when there are N element antennas. Due to size restrictions, battery life and complexity, the switched combining technique is presently implemented in mobile terminals with diversity antennas [39].

Selection Combining

The selection combining technique is similar to the switched combining technique except that N receivers are required to monitor instantaneous SNR at all branches, which is shown in Figure 2.6. The branch with the highest SNR is selected as the output signal.

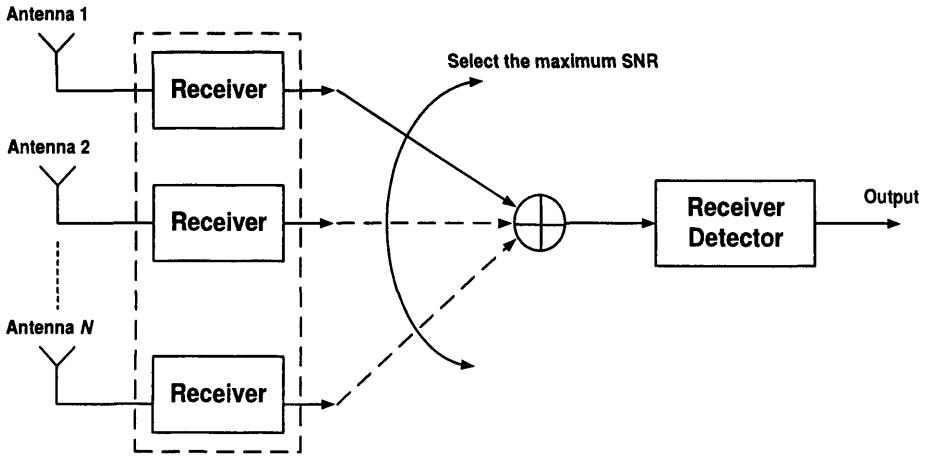

Figure 2.6. Block diagram of selection combining for n_r branches/antenna elements.

Equal Gain Combining

Both switched and selection combining techniques only use the signal from one of the branches as the output signal. In order to improve SNR at the output, the signals from all branches are combined to form the output signal. However, the signal from each branch is not in-phase. Therefore, each branch must be multiplied by a complex phasor having a phase -θ_i, where θ_i is the phase of the channel corresponding to branch i (i.e. co-phased) as shown in Figure 2.7. When this is achieved, all signals will have zero phase and are combined coherently.

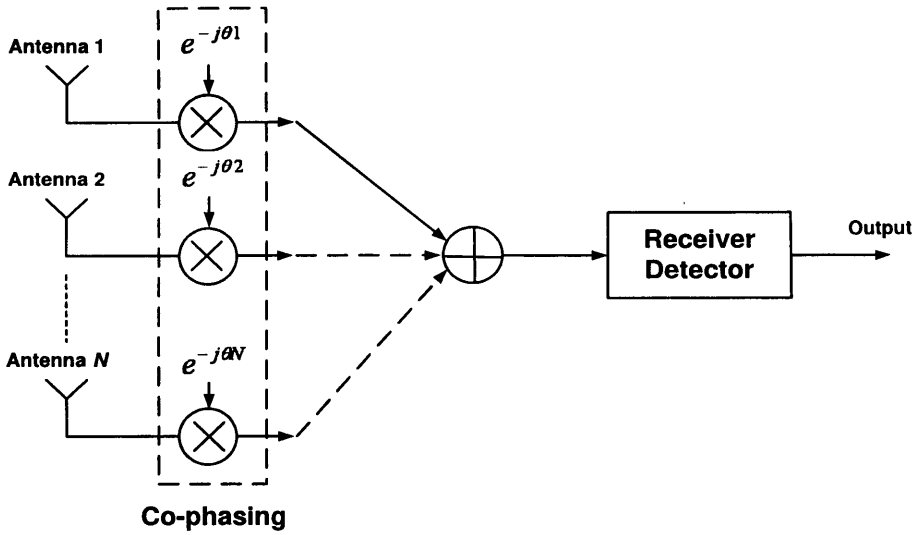

Figure 2.7. Block diagram of equal gain combining for n_r branches/antenna elements.

Maximum Ratio Combining

In the equal gain combining technique, all the branches may not have a similar SNR. Sometimes one of the branches has a much lower SNR than the other branches and this will reduce the overall SNR to a lower value at the output. In order to maximise the SNR at the output, each branch is applied with a weight, wi before all the signals are combined coherently as shown in Figure 2.8. In order to maximise the SNR at the output, a branch with a higher SNR will be given a higher weighting.

2.4.2 Diversity Gain

Diversity gain is defined as the improvement in the SNR of the combined signals relative to the SNR from a single antenna element. The cumulative distribution function (CDF) of a Rayleigh channel is given

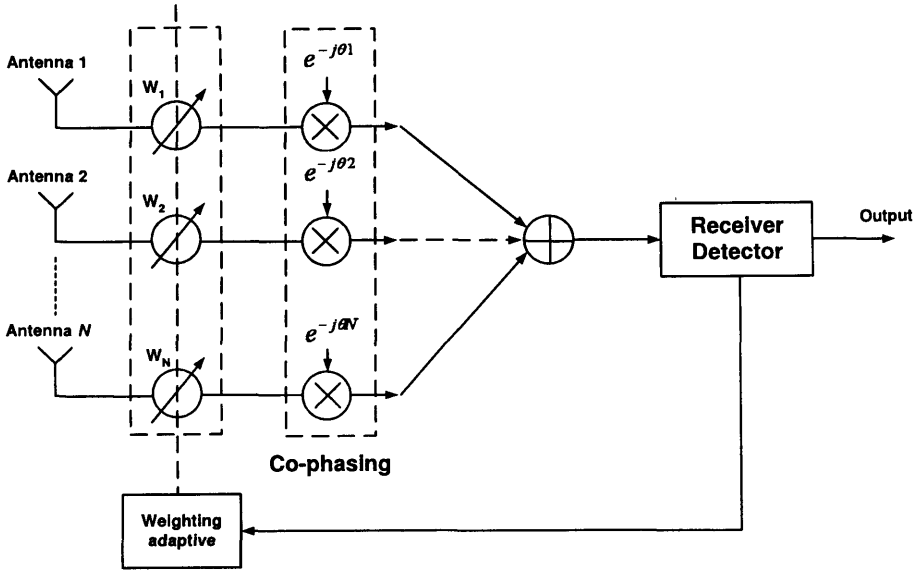

Figure 2.8. Block diagram of maximum ratio combining for N branches/antenna elements.

as [26, 40]:

$$P(\gamma < \gamma_s) = (1 - e^{-\gamma_s/\Gamma}) \tag{2.4.1}$$

where Γ is the mean SNR, γ is the instantaneous SNR, $P(\gamma < \gamma_s)$ is the probability that the SNR will fall below the given threshold, γ_s. For a selection combiner with n_r independent branches, assuming that the n_r branches have independent signals and equal mean SNRs, the probability of all branches having a SNR below γ_s is equivalent to the probability for a single branch raised to the power n_r as:

$$P(\gamma < \gamma_s)_{n_r} = (1 - e^{-\gamma_s/\Gamma})^{n_r} \tag{2.4.2}$$

where n_r is the number of antennas/branches.

Equations (2.4.1) and (2.4.2) are plotted in Figure 2.9 so it can be seen how increasing the number of branches, n_r, reduces the probability

of fades below a given threshold. Also shown here is the diversity gain, which is the increase in SNR of a combined output compared to a single branch. In this case, the diversity gain is evaluated when there is a $P(\gamma < \gamma_s)$ of 1% (i.e. 99% reliability). Analysis of diversity receivers from Figure 2.9 shows that there is $10dB$ and $16dB$ respectively of diversity gain for the two branches and four branches selection combiner respectively. This advantage of moving from two to four antennas to increase the diversity gain is a key point in this thesis. Such diversity gain can also be achieved by increasing the number of transmit antennas from two to four and is exploited in the following chapters.

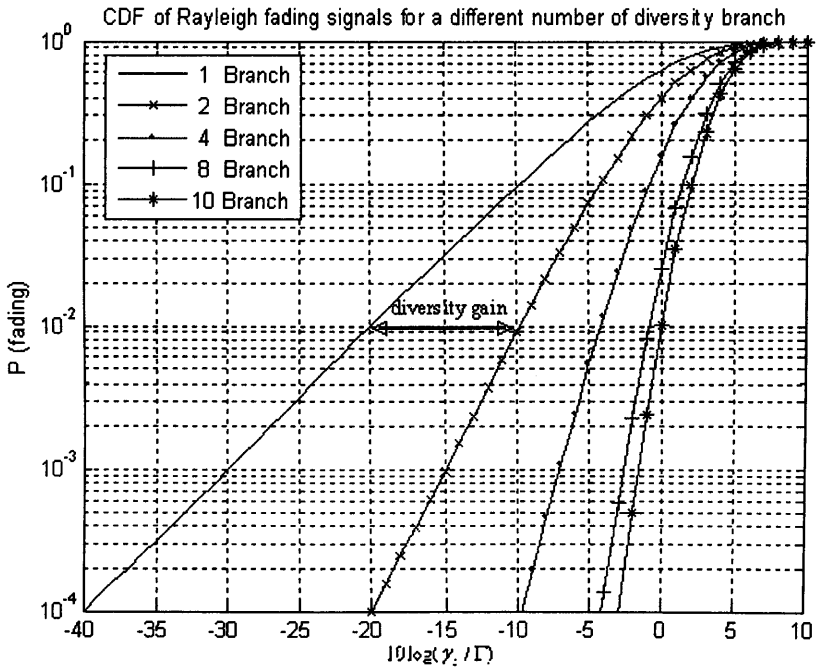

Figure 2.9. CDF of Rayleigh fading signals for a different number of diversity branch.

2.4.3 Array Gain

Refers to the average increase in SNR at the receiver that arises from the coherent combining effect of multiple antennas at the receiver and/or transmitter [41]. In MIMO channels, array gain exploitation requires channel knowledge at the transmitter.

2.5 Summary

This chapter has shown that a MIMO system can increase the channel capacity significantly without increasing the bandwidth and transmission power when compared to a SISO system. The system model has also been addressed. One of the most important parameters of a MIMO system, the channel capacity, has been studied. The basic concepts which are relevant to understanding the MIMO channel capacity have been given. By means of one example the capacity of different MIMO systems have been compared with a SISO system. Diversity combining techniques which have received considerable attention in recently years to combat multipath fading have also been described. The concept of array gain has also been introduced.

Chapter 3

SPACE TIME BLOCK CODES

3.1 Introduction

Space-time codes (STCs) have been implemented in cellular communications as well as in wireless local area networks (WLANs). STCs is performed in both the spatial and temporal domains introducing redundancy between signals transmitted from various antennas at various time periods. This can achieve transmit diversity and antenna gain over spatially uncoded systems without sacrificing bandwidth. The research on STC focuses on improving the system performance by employing extra transmit antennas. In general, the design of STC amounts to finding transmit matrices that satisfy certain optimality criteria. Constructing a STC, a researcher has to trade-off between three goals: simple decoding, minimizing the error probability, and maximizing the information rate. The essential question is: How can the transmitted data rate be maximized using a simple coding and decoding algorithm at the same time as the bit error probability be minimized? There are two major categories of space-time codes: space-time trellis codes (STTC) and space-time block codes (STBC).

Within an STTC scheme, the coding processing is based on a trellis rule for the transmitted symbols over multiple antennas and multiple

time-slots, and both full diversity gain and coding gain can be achieved by a maximum likelihood (ML) receiver [11].

Within an orthogonal STBC scheme, the key feature is that it achieves a full diversity gain with a simple maximum likelihood decoding algorithm. The STBC design is based on the fundamental principles of orthogonal designs originated by Randon [42] in the early 20 century and refined by Geramita and Seberry [43] in the late 1970's. Based on these mathematical frameworks, Tarokh has developed the orthogonal design theories for space-time block code in the late 1990's [17]. The STBC encoding scheme will be introduced first.

3.2 Space-Time Block Code Encoding and Code Rate

In general a space-time block code is defined by an $n_t \times t_o$ transmission matrix $\mathbf{X}$. Here n_t represents the number of transmit antennas and t_o represents the number of time periods for transmission of one block of coded symbols.

Assume the signal constellation consists of 2^m points. During each modulating operation, every block of m information bits is mapped into a constellation point, i.e., each modulated signal represents m bits. Then every block of t_i modulated signals is encoded by a space-time block code encoder that generates n_t parallel signal sequences, each of which has length t_o, according to the transmission matrix $\mathbf{X}$. These sequences are transmitted through n_t transmit antennas simultaneously in t_o time periods.

In the space-time block code, the number of symbols the encoder takes as its input in each encoding operation is t_i. The number of transmission periods required to transmit the space-time coded symbols

through the multiple transmit antennas is t_o. In other words, there are t_o space-time symbols transmitted from each antenna for each block of t_i input symbols. The rate of a space-time block code is defined as the ratio between the number of symbols the encoder takes as its input and the number of space-time coded symbols transmitted from each antenna. This rate is given by

$$R_{stbc} = t_i/t_o \tag{3.2.1}$$

The entries of the transmission matrix $\mathbf{X}$ are linear combinations of the t_i modulated symbols $x_1, x_2, \ldots, x_{t_i}$ and their conjugates $x_1^*, x_2^*, \ldots, x_{t_i}^*$. In order to achieve full transmit diversity of n_t, the transmission matrix $\mathbf{X}$ is constructed based on the orthogonal designs developed by Tarokh [17] which implies that $\mathbf{X}$ satisfies

$$\mathbf{X} \cdot \mathbf{X}^H = c(|s_1|^2 + |s_2|^2 + \cdots + |s_k|^2)\boldsymbol{I}_{n_t} \tag{3.2.2}$$

where c is a constant, $\mathbf{X}^H$ is the Hermitian of $\mathbf{X}$ and $\boldsymbol{I}_{n_t}$ is an $n_t \times n_t$ identity matrix. The *i-th* row of $\mathbf{X}$ represents the symbols transmitted from the *i-th* transmit antenna consecutively in t_o transmission periods, while the *t-th* column of $\mathbf{X}$ represents the symbols transmitted simultaneously through n_t transmit antennas at time t. The *t-th* column of $\mathbf{X}$ is regarded as a space-time symbol transmitted at time t. The element of $\mathbf{X}$ in the *i-th* row and *t-th* column, $x_{i,t}, i = 1, 2, \ldots, n_t, t = 1, 2, \ldots, t_o$, represents the signal transmitted from antenna i at time t.

It has been shown that the rate of a space time block code with full transmit diversity is less than or equal to one, $R_{stbc} \leq 1$ [17]. The code with full rate $R_{stbc} = 1$ requires no bandwidth expansion, while the code

with rate $R \leq 1$ requires a bandwidth expansion of $1/R$. For space-time block codes with n_t transmit antennas, the transmission matrix is denoted as $\mathbf{X}_{n_t}$. The code is called the space-time block code with size n_t.

3.3 Alamouti Code

Historically, the Alamouti code is the first STBC that provides full diversity at full data rate for two transmit antennas [5]. It is the only open-loop STBC that can achieve both full diversity and full code rate for complex constellations. A block diagram of an Alamouti space-time encoder is shown in Figure 3.1.

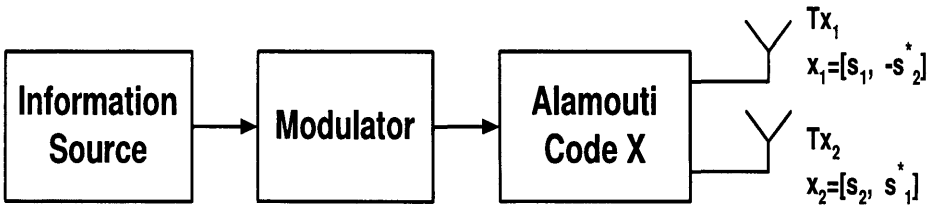

Figure 3.1. A block diagram of the Alamouti space-time encoder.

To transmit B bits/channel user, a modulation scheme that maps every b bits to one symbol from a constellation with 2b symbols is used. The constellation can be any real or complex constellation, for example PAM, PSK, QAM, and higher order constellations. First, the transmitter picks two symbols from the constellation using a block of 2b bits. If s_1 and s_2 are the selected symbols for a block of $2b$ bits, the transmitter sends s_1 from antenna one and s_2 from antenna two at time one. In the second transmission period, the symbol $-s_2^*$ is transmitted from antenna one and the symbol s_1^* from transmit antenna two. Therefore, the encoder takes the block of two modulated symbols

s_1 and s_2 in each encoding operation and hands it to the transmit antennas according to the code matrix

$$\mathbf{X} = \begin{bmatrix} s_1 & s_2 \\ -s_2^* & s_1^* \end{bmatrix} \tag{3.3.1}$$

It is clear that the encoding is performed in both the time (two transmission intervals) and space domains (across two transmit antennas). The two rows and columns of $\mathbf{X}$ are orthogonal to each other and the code matrix 3.3.1 is orthogonal:

$$\begin{aligned} \mathbf{X}\mathbf{X}^H &= \begin{bmatrix} s_1 & s_2 \\ -s_2^* & s_1^* \end{bmatrix} \begin{bmatrix} s_1^* & -s_2 \\ s_2^* & s_1 \end{bmatrix} \\ &= \begin{bmatrix} |s_1|^2 + |s_2|^2 & 0 \\ 0 & |s_1|^2 + |s_2|^2 \end{bmatrix} \\ &= (|s_1|^2 + |s_2|^2)\mathbf{I}_2 \end{aligned} \tag{3.3.2}$$

where $\boldsymbol{I}_2$ is a (2×2) identity matrix. This property enables the receiver to detect s_1 and s_2 by a simple linear signal processing operation.

The receiver side is examined now. Only one receive antenna is assumed to be available. The channel at time t may be modelled by a complex multiplicative distortion $h_1(t)$ for transmit antenna one and $h_2(t)$ for transmit antenna two. Assuming that the fading is constant across two consecutive transmit periods of duration T, then

$$h_1(t) = h_1(t+T) = h1 = |h_1|e^{j\theta_1} \tag{3.3.3}$$

$$h_2(t) = h_2(t+T) = h1 = |h_2|e^{j\theta_2} \tag{3.3.4}$$

where $|h_i|$ and $\theta_i, i = 1, 2$ are the amplitude gain and phase shift for the path from transmit antenna i to the receive antenna. The received signals at time t and $t + T$ can then be expressed as:

$$r_1 = s_1 h_1 + s_2 h_2 + n_1 \tag{3.3.5}$$

$$r_2 = -s_2^* h_1 + s_1^* h_2 + n_2 \tag{3.3.6}$$

where r_1 and r_2 are the received signals at time t and $t+T$, n_1 and n_2 are complex random variables representing receiver noise and interference. This can be written in matrix form as:

$$\mathbf{r} = \mathbf{X}\mathbf{h} + \mathbf{n} \tag{3.3.7}$$

3.3.1 Equivalent Virtual Channel Matrix (EVCM) of the Alamouti Code

Conjugating the signal r_2 in (3.4.6) that is received in the second symbol period, the received signal may be written equivalently as

$$\begin{aligned} r_1 &= h_1 s_1 + h_2 s_2 + \tilde{n}_1 \\ r_2^* &= -h_1^* s_2 + h_2^* s_1 + \tilde{n}_2 \end{aligned} \tag{3.3.8}$$

Thus equation 3.3.8 can be written as

$$\begin{bmatrix} r_1 \\ r_2^* \end{bmatrix} = \begin{bmatrix} h_1 & h_2 \\ h_2^* & -h_1^* \end{bmatrix} \begin{bmatrix} s_1 \\ s_2 \end{bmatrix} + \begin{bmatrix} \tilde{n}_1 \\ \tilde{n}_2 \end{bmatrix} \tag{3.3.9}$$

or in short notation:

$$\mathbf{y} = \mathbf{H_v}\mathbf{s} + \tilde{\mathbf{n}} \tag{3.3.10}$$

where the modified receive vector $\mathbf{y} = [r_1, r_2^*]^T$ has been introduced. $\mathbf{H_v}$ will be termed equivalent virtual MIMO channel matrix (EVCM) of the Alamouti STBC scheme. It is given by:

$$\mathbf{H_v} = \begin{bmatrix} h_1 & h_2 \\ h_2^* & -h_1^* \end{bmatrix} \tag{3.3.11}$$

Thus, by considering the elements of $\mathbf{y}$ in Equation (3.3.10) as originating from two virtual receive antennas (instead of received samples at one antenna at two time slots) the (2×1) Alamouti STBC can be interpreted as a (2×2) spatial multiplexing transmission using one time slot. The key difference between the Alamouti scheme and a true (2×2) multiplexing system lies in the specific structure of $\mathbf{H_v}$. Unlike a general i.i.d. MIMO channel matrix, the rows and columns of the virtual channel matrix are orthogonal:

$$\mathbf{H_v}\mathbf{H_v}^H = \mathbf{H_v}^H\mathbf{H_v} = (|h_1|^2 + |h_2|^2)I_2 = |h|^2 I_2 \tag{3.3.12}$$

where I_2 is the (2×2) identity matrix and $|h|^2$ is the power gain of the equivalent MIMO channel with $|h|^2 = |h_1|^2 + |h_2|^2$. Due to this orthogonality the receiver of the Alamouti scheme (discussed in detail in the following subsection) decouples the MISO channel into two virtually independent channels each with channel gain $|h|^2$ and diversity $d = 2$.

It is obvious that the EVCM depends on the structure of the code

and the channel coefficients. The concept of the EVCM simplifies the analysis of the STBC transmission scheme. The existence of an EVCM is one of the important characteristics of STBCs and will be frequently used in this thesis.

3.3.2 Linear Signal Combining and Maximum Likelihood Decoding of the Alamouti Code

If the channel coefficient h_1 and h_2 can be perfectly estimated at the receiver, the decoder can use them as channel state information (CSI). Assuming that all the signals in the modulation constellation are equiprobable, a maximum likelihood (ML) detector for that pair of signals $(\hat{s}_1, \hat{s}_2)$ from the signal modulation constellation that minimizes the decision metric:

$$d^2(r_1, h_1 s_1 + h_2 s_2) + d^2(r_2, -h_1 s_2^* + h_2 s_1^*) = \\ |r_1 - h_1 s_1 - h_2 s_2|^2 + |r_2 + h_1 s_2^* - h_2 s_1^*|^2 \quad (3.3.13)$$

where $d(z_1, z_2) = |z_1 - z_2|$. On the other hand, using a linear receiver, the signal combiner at the receiver combines the received signals r_1 and r_2 as follows

$$\tilde{s}_1 = h_1^* r_1 + h_2 r_2^* = (|h_1|^2 + |h_2|^2) s_1 + h_1^* n_1 + h_2 n_2^* \\ \tilde{s}_2 = h_2^* r_1 - h_1 r_2^* = (|h_1|^2 + |h_2|^2) s_2 - h_1 n_2^* + h_2^* n_1 \quad (3.3.14)$$

Hence $\tilde{s}_1$ and $\tilde{s}_2$ are two decisions statistics constructed by combining the received signals with coefficients derived from the channel state information. These noisy signals are sent to ML detectors and thus

the ML decoding rule 3.3.14 can be separated into two independent decoding rules for s_1 and s_2, namely

$$\hat{s}_1 = \arg\min_{\hat{s}_1 \in S} d^2(\tilde{s}_1, s_1) \tag{3.3.15}$$

for detecting s_1, and

$$\hat{s}_2 = \arg\min_{\hat{s}_2 \in S} d^2(\tilde{s}_2, s_2) \tag{3.3.16}$$

for detecting s_2.

The Alamouti transmission scheme is a simple transmit diversity scheme which improves the signal quality at the receiver using a simple signal processing algorithm (STC) at the transmitter. The diversity order obtained is equal to that one applying maximal ratio combining (MRC) with one antenna at the transmitter and two antennas at the receiver where the resulting signals at the receiver are:

$$r_1 = h_1 s_1 + n_1 \tag{3.3.17}$$

$$r_2 = h_2 s_1 + n_2 \tag{3.3.18}$$

and the combined signal is

$$\begin{aligned} \tilde{s}_1 &= h_1^* r_1 + h_2^* r_2 \\ &= (|h_1|^2 + |h_2|^2) s_1 + h_1^* n_1 + h_2^* n_2 \end{aligned} \tag{3.3.19}$$

The resulting combined signals in Equation (3.3.14) are equivalent to those obtained from a two-branch MRC in Equation (3.3.19). The only differences are phase rotations on the noise components which do

not degrade the effective SNR. Therefore, the resulting diversity order obtained by the Alamouti scheme with one receiver is equal to that of a two-branch MRC at the receiver. This statement can be confirmed by simulating the BER performance of the Alamouti scheme.

The performance of the Alamouti scheme over a quasi-static flat fading is provided in Figure 3.2. It is assumed that the total transmit power from the two antennas used with the Alamouti scheme is the same as the transmit power sent from a single transmit antenna to two receive antennas and applying an MRC at the receiver. Further, it is assumed that the receiver has perfect knowledge of the channel. The BER performance of the Alamouti scheme is compared with a (1×1) system scheme (no diversity) and with a (1×2) MRC scheme.

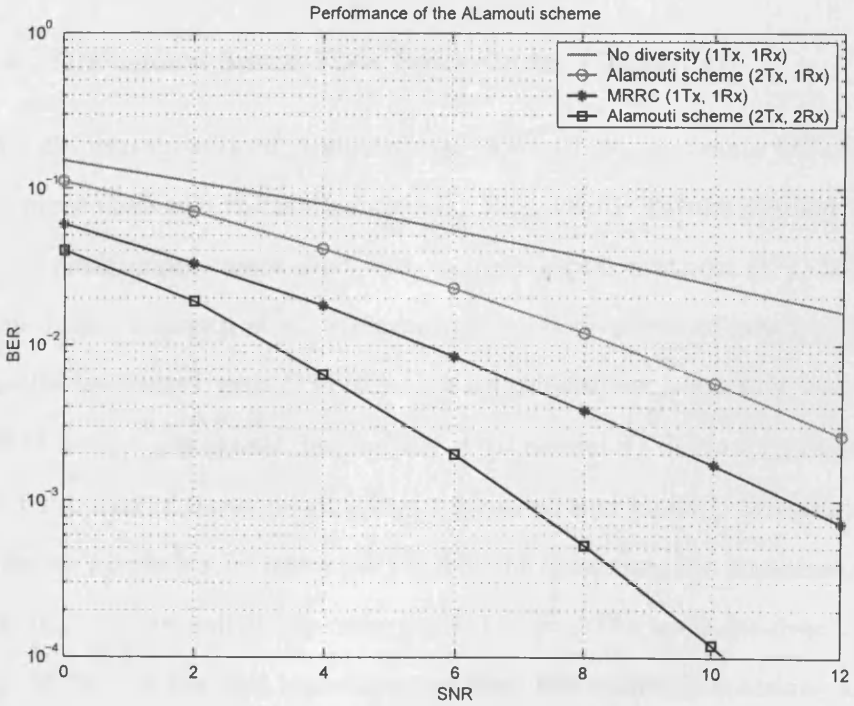

Figure 3.2. The BER performance of Alamouti schemes with one and two receivers compared with when there is no diversity and MRRC schemes

The simulation results show that the Alamouti (2×1) scheme achieves the same diversity as the (1×2) scheme using MRC. However, the performance of Alamouti scheme is $3dB$ worse due to the fact that the power radiated from each transmit antenna in the Alamouti scheme is half of that radiated from the single antenna and sent to two receive antennas and using MRC. In this way, the two schemes have the same total transmit power [5]. The (2×2) Alamouti scheme shows a better performance than either of the other curves because the order of diversity in this case is $n_t n_r = 4$. In general, the Alamouti scheme with two transmit and n_r receive antennas has the same diversity gain as an MRC receive diversity scheme with one transmit and $2n_r$ receive antennas [17].

3.4 Orthogonal Space-Time Block Codes (OSTBCs)

The pioneering work of Alamouti has been a basis to create OSTBCs for more than two transmit antennas. First of all, Tarokh studied the error performance associated with unitary signal matrices [17]. Some time later, Ganesan et al. streamlined the derivations of many of the results associated with OSTBCs and established an important link to the theory of orthogonal designs [20]. Orthogonal STBCs are an important subclass of linear STBCs that guarantee that the ML detection of different symbols s_n is decoupled and at the same time the transmission scheme achieves a diversity order equal to $n_t n_r$. The main disadvantage of OSTBCs is the fact that for more than two transmit antennas and complex-valued signals, OSTBCs only exist for code rates smaller than one symbol per time slot.

Next, a general survey on orthogonal design and various properties

of OSTBCs will be provided. There exist real orthogonal and complex orthogonal designs. Focus will be here on complex orthogonal designs. More about real orthogonal design can be found in [44–46].

Definition: *Orthogonal Design*

An OSTBC is a linear space-time block code $\mathbf{X}$ that has the following unitary property:

$$\mathbf{X}^H\mathbf{X} = \sum_{n=1}^{N} |s_n|^2 I \tag{3.4.1}$$

The *i-th* row of $\mathbf{X}$ corresponds to the symbols transmitted from the *i-th* transmit antenna in N transmission periods, while the *j-th* column of $\mathbf{X}$ represents the symbols transmitted simultaneously through n_t transmit antennas at time *j*.

According to Equation (3.4.1) the columns of the transmission matrix $\mathbf{X}$ are orthogonal to each other. That means that in each block, the signal sequences from any two transmit antennas are orthogonal.

3.5 Quasi-Orthogonal Space-Time Block Codes (QO-STBCs)

The main characteristic of the code design methods explained in the previous sections is the orthogonality of the codes. The codes are designed using transmission matrices with orthogonal columns. It has been shown how simple decoding which can separately recover transmit symbols, is possible using an orthogonal design. However, in [17] it is proved that a complex orthogonal design of STBCs which provides full diversity and full transmission rate is not possible for more than two transmit antennas.

In [21–23,47–49] so called Quasi Orthogonal Space-Time Block Codes (QO-STBC) have been introduced as a new family of STBCs. These codes achieve full data rate at the expense of a slightly reduced diversity. In the proposed quasi-orthogonal code designs, the columns of the transmission matrix are divided into groups. While the columns within each group are not orthogonal to each other, different groups are orthogonal to each other. Using quasi-orthogonal design, pairs of transmitted symbols can be decoded independently and the loss of diversity in QO-STBC is due to some coupling term between the estimated symbols.

A Straightforward extension of Alamouti's STBC is to construct the code matrix using two 2×2 Alamouti codes [5], $\mathbf{X}_{12}$ and $\mathbf{X}_{34}$ with

$$\mathbf{X_{12}} = \begin{bmatrix} s_1 & s_2 \\ -s_2^* & s_1^* \end{bmatrix} \quad and \quad \mathbf{X_{34}} = \begin{bmatrix} s_3 & s_4 \\ -s_4^* & s_3^* \end{bmatrix} \tag{3.5.1}$$

which are used in a block structure resulting in the so called QO-STBC scheme for four transmit antennas:

$$\mathbf{X_{QO}} = \begin{bmatrix} \mathbf{X}_{12} & \mathbf{X}_{34} \\ -\mathbf{X}_{34}^* & \mathbf{X}_{12}^* \end{bmatrix} = \begin{bmatrix} s_1 & s_2 & s_3 & s_4 \\ -s_2^* & s_1^* & -s_4^* & s_3^* \\ -s_3^* & -s_4^* & s_1^* & s_2^* \\ s_4 & -s_3 & -s_2 & s_1 \end{bmatrix} \tag{3.5.2}$$

For simplicity, assume that the above codeword is transmitted through a four transmit and one receive antenna in a flat fading environment, by taking the complex conjugate of the second and third row of the matrix in Equation (3.5.2), the received signal vector can be written explicitly in terms of the transmitted symbols as follows

$$\begin{bmatrix} r_1 \\ r_2^* \\ r_3^* \\ r_4 \end{bmatrix} = \begin{bmatrix} h_1 & h_2 & h_3 & h_4 \\ h_2^* & -h_1^* & h_4^* & -h_3^* \\ h_3^* & h_4^* & -h_1^* & -h_2^* \\ h_4 & -h_3 & -h_2 & h_1 \end{bmatrix} \begin{bmatrix} s_1 \\ s_2 \\ s_3 \\ s_4 \end{bmatrix} + \begin{bmatrix} n_1 \\ n_2^* \\ n_3^* \\ n_4 \end{bmatrix} \tag{3.5.3}$$

$$\mathbf{r} = \mathbf{H}\mathbf{x} + \mathbf{n} \tag{3.5.4}$$

where h_i and n_i, $i = 1, 2, 3, 4$ are the complex channel impulse response coefficients and zero-mean, circularly symmetric, complex valued Gaussian noise terms with variance σ_n^2 respectively.

In the receiver, the pairwise decoding is used for decoding of the QO-STBC. Similar to the decoding formulas in the previous section, the maximum-likelihood decoding for the QO-STBC is [23]

$$min\{\mathbf{H}^H\mathbf{X}^H\mathbf{X}\mathbf{H} - \mathbf{H}^H\mathbf{X}^H\mathbf{r} - \mathbf{r}^H\mathbf{X}\mathbf{H}\} \tag{3.5.5}$$

Algebraic manipulation shows that maximum-likelihood decoding is equal to minimizing the following sum [23]:

$$f_{14}(s_1, s_4) + f_{23}(s_2, s_3) \tag{3.5.6}$$

where

$$\begin{aligned} f_{14}(s_1, s_4) = & \sum_{m=1}^{M}[(|s_1|^2 + |s_4|^2)(\sum_{n=1}^{4}|\alpha_{n,m}|^2) \\ & + 2Re\{(-\alpha_{1,m}r_{1,m}^* - \alpha_{2,m}^* r_{2,m} - \alpha_{3,m}^* r_{3,m} - \alpha_{4,m} r_{4,m}^*)s_1\} \\ & + 2Re\{(-\alpha_{4,m}r_{1,m}^* - \alpha_{3,m}^* r_{2,m} - \alpha_{2,m}^* r_{3,m} - \alpha_{1,m} r_{4,m}^*)s_4\} \\ & + 4Re\{(\alpha_{1,m}\alpha_{4,m}^* - \alpha_{2,m}^*\alpha_{3,m}\}Re\{s_1 s_4^*\}] \end{aligned} \tag{3.5.7}$$

and

$$\begin{aligned} f_{23}(s_2, s_3) &= \sum_{m=1}^{M}[(|s_2|^2 + |s_3|^2)(\sum_{n=1}^{4}|\alpha_{n,m}|^2) \\ &+ 2Re\{(-\alpha_{2,m}r_{1,m}^* + \alpha_{1,m}^* r_{2,m} - \alpha_{4,m}^* r_{3,m} + \alpha_{3,m}r_{4,m}^*)s_1\} \\ &+ 2Re\{(-\alpha_{3,m}r_{1,m}^* - \alpha_{4,m}^* r_{2,m} + \alpha_{1,m}^* r_{3,m} + \alpha_{1,m}r_{4,m}^*)s_4\} \\ &+ 4Re\{(\alpha_{2,m}\alpha_{3,m}^* - \alpha_{1,m}^*\alpha_{4,m}\}Re\{s_2 s_3^*\}] \end{aligned} \tag{3.5.8}$$

Since $f_{14}(s_1, s_4)$ is independent of (s_2, s_3) and $f_{23}(s_2, s_3)$ is independent of (s_1, s_4), the pairs (s_1, s_4) and (s_2, s_3) can be decoded separately.

3.5.1 Transmission with Channel Feedback

Clearly, the code rate in Equation (3.5.4) is unity, since four data symbols are transmitted over four time slots. As it will be shown later, however, the diversity order of this code is two. Hence in contrast to O-STBC, while QO-STBC achieves full code rate, it suffers from diversity loss. This can be explained as follows.

Matched filtering is performed by $\mathbf{H}^H$, therefore, the estimates of the transmitted symbols become [50]

$$\tilde{\mathbf{x}} = \mathbf{H}^H\mathbf{r} = \Delta\mathbf{x} + \mathbf{H}^H\mathbf{n} \tag{3.5.9}$$

$$\tilde{\mathbf{x}} = \begin{bmatrix} \gamma & 0 & 0 & \alpha \\ 0 & \gamma & -\alpha & 0 \\ 0 & -\alpha & \gamma & 0 \\ \alpha & 0 & 0 & \gamma \end{bmatrix} \begin{bmatrix} s_1 \\ s_2 \\ s_3 \\ s_4 \end{bmatrix} + \tilde{\mathbf{n}} \tag{3.5.10}$$

where $\gamma = |h_1^2| + |h_2^2| + |h_3^2| + |h_4^2|$ and $\alpha = Re\{h_1^* h_4 - h_2^* h_3\}$.

Hence, it is easily seen that due to the term α there is a form

of coupling. For example, the fourth symbol interferes with the first symbol, while the second interferes with the third symbol. The cause of the diversity loss is due to this coupling of symbols. In this scheme, the channel is assumed to be frequency selective and remains constant over four symbol intervals, i.e. a quasi-static channel. The original QO-STBC scheme provides full code rate at the expense of loss in diversity. A proposed scheme in [50] is called closed-loop QO-STBC is to provide full diversity while achieving full code rate. The principle of the later scheme or what is called closed-loop QO-STBC is to rotate the signal which in radiated from one/two of the antennas by phased defined by the feedback from the receiver. The performance advantage of the scheme is confirmed when the feedback information is quantized and even when feedback is completely lost.

3.5.2 Two Phase Feedback

Without loss of generality, consider that the signals from the third and fourth transmit antennas are rotated by phases θ and ϕ respectively and the rotation angle is selected from a range $\theta, \phi \in [0, 2\pi]$, the system diagram is illustrated in Figure 3.3, which is equivalent to multiplying the first and second terms in Equation (3.5.3) by $e^{j\theta}$ and $e^{j\phi}$,

$$\alpha' = Re\{h_1^* h_4 e^{j\theta} - h_2^* h_3 e^{j\phi}\} \tag{3.5.11}$$

Let $\kappa = h_1^* h_4$ and $\lambda = h_2^* h_3$

$$\alpha' = |\kappa| cos(\theta + \angle\kappa) - |\lambda| cos(\phi + \angle\beta) \tag{3.5.12}$$

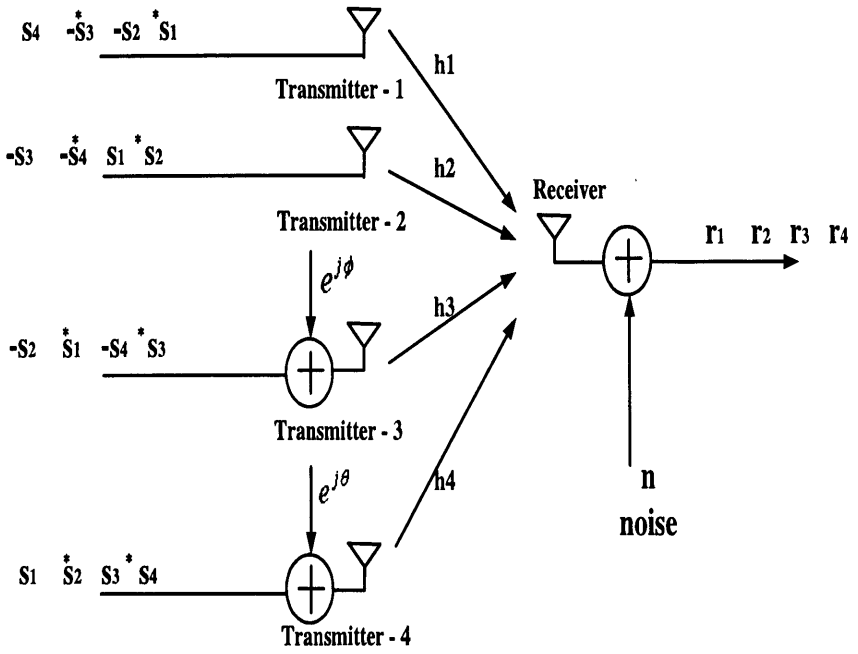

Figure 3.3. Block diagram of the baseband model of an four transmit and one receive system based two-phase feedback STBC scheme with four transmit antennas

where $|\cdot|$ and $\angle$ denote the absolute value and the angle (arctan) operators, respectively.

Then it is easily to find the rotated phasor parameter θ and ϕ after trigonometric manipulations (let $\alpha' = 0$). The solution are

$$\theta = arccos(\frac{|\lambda|}{|\kappa|}cos(\phi + \angle\lambda)) - \angle\kappa \tag{3.5.13}$$

provided that

$$\phi \in \begin{cases} [0, 2\pi), & \text{when } |\lambda| < |\kappa| \\ [\pi\text{-}\xi\text{-}\angle\lambda,\ \xi\text{-}\angle\lambda] & \\ \bigcup[2\pi - \xi - \angle\lambda, \pi + \xi - \angle\lambda], & \text{otherwise} \end{cases} \tag{3.5.14}$$

where $\xi = \frac{|\kappa|}{|\lambda|}$.

3.5.3 Single Phase Feedback

The number of feedback bits required from the receiver to the transmitter has to be small because of practical constraints. Reduction in feedback bits can be achieved by reducing the number of phase rotations at the transmitter antennas.

There are two methods proposed by Toker et al. [50] which are as follows:

1. One way to reduce the amount of information needed to be fed back is to rotate the signal of one antenna only.

2. Another way is to quantize the feedback phase information according to the number of feedback bits available.

It is possible to reduce the off diagonal terms of the matrix 3.5.10 just by rotating a single antenna instead of rotating two antennas. For example rotation is applied only at the fourth antenna, the coupling term α can be rewritten as

$$\begin{aligned} \alpha'' &= Re\{h_1^* h_4 e^{j\theta} - h_2^* h_3\} \\ &= |\kappa| cos(\theta + \angle\kappa) - \lambda_{real} \end{aligned} \tag{3.5.15}$$

where $\kappa = h_1^* h_4$,$\lambda = h_2^* h_3$, the parameter λ_{real} is the real part of λ and $|\kappa|$ is the absolute value.

From the Equation (3.5.15), it is clear that the cosine wave is a function of θ, scaled by κ, phase shift by $\angle\kappa$ and biased by $-\lambda_{real}$.

Under the condition $|\lambda_{real}| \leq |\kappa|$, $\alpha = 0$ has two solutions for θ.

$$\begin{aligned}\theta_1 &= acrcos(\frac{\lambda_{real}}{|\kappa|} - \angle\kappa) \\ \theta_2 &= -acrcos(\frac{\lambda_{real}}{|\kappa|} - \angle\kappa)\end{aligned} \tag{3.5.16}$$

On the other hand, if $\lambda_{real} > |\kappa|$, there is no solution for $\alpha = 0$ and $|\alpha|$ can only be minimized at the following phase value

$$\begin{aligned}\theta &= -\angle\kappa, \lambda_{real} > |\kappa| \\ \theta &= \pi - \angle\kappa, -\lambda_{real} > |\kappa|\end{aligned} \tag{3.5.17}$$

with the minimum value

$$\begin{aligned}\alpha''_{min} &= -\lambda_{real} + |\kappa|, \lambda_{real} > |\kappa| \\ \alpha''_{min} &= -\lambda_{real} - |\kappa|, -\lambda_{real} > |\kappa|\end{aligned} \tag{3.5.18}$$

3.5.4 Quantization

In practice only a finite number of bits is allowed for the feedback, which is assumed to equal to P bits. For the single antenna phase adjustment, the discrete estimated feedback information corresponding to the phase θ will be an element of the set ($\theta' \in \Omega = \frac{2\pi n}{2^P}, n = 0, 1, \ldots, 2^P - 1$)

$$\theta' = argmin(|h_1^* h_4 e^{j\theta} - h_2^* h_3|) \tag{3.5.19}$$

Similarly, for the dual antenna phase adjustment, the discrete estimated feedback information for the phase θ and ϕ are the elements of

the set $((\theta', \phi') \in \Omega = \frac{2\pi n}{2^{P-1}}, n = 0, 1, \ldots, 2^{P-1} - 1)$

$$(\theta', \phi') = argmin(|(\sum_{m=1}^{n_r} h_1^* h_4 e^{j\theta'}) - (\sum_{m=1}^{n_r} h_2^* h_3 e^{j\phi'})|^2) \tag{3.5.20}$$

$$\phi \in \begin{cases} [0, 2\pi), & \text{when } |\beta| < |\kappa| \\ [\pi\text{-}\xi\text{-}\angle\beta,\ \xi\text{-}\angle\beta] & \\ \bigcup[2\pi - \xi - \angle\beta, \pi + \xi - \angle\beta], & \text{otherwise} \end{cases} \tag{3.5.21}$$

3.5.5 Simulation

Figure 3.4 provides simulation results for the transmission of QO-STBC for four transmit antennas and one receive antenna using a QPSK modulation scheme.

Simulation results show that QO-STBC with four transmit antennas is much better than that of the system with one transmit antenna. A rotated QO-STBC with feedback loop provides the advantages of full diversity and full code rate is successful in reducing the off-diagonal term of the matrix Equation (3.5.10). At a BER of 10^{-2}, the QO-STBC provides more than $7dB$ improvement compared with the system with one transmit antenna. It is also observed that there is about $0.6dB$ degradation at 10^{-2} in the performance of the one phase feedback scheme compared with the open loop scheme, and nearly $0.7dB$ degradation in the performance between the two phase feedback scheme and one phase method.

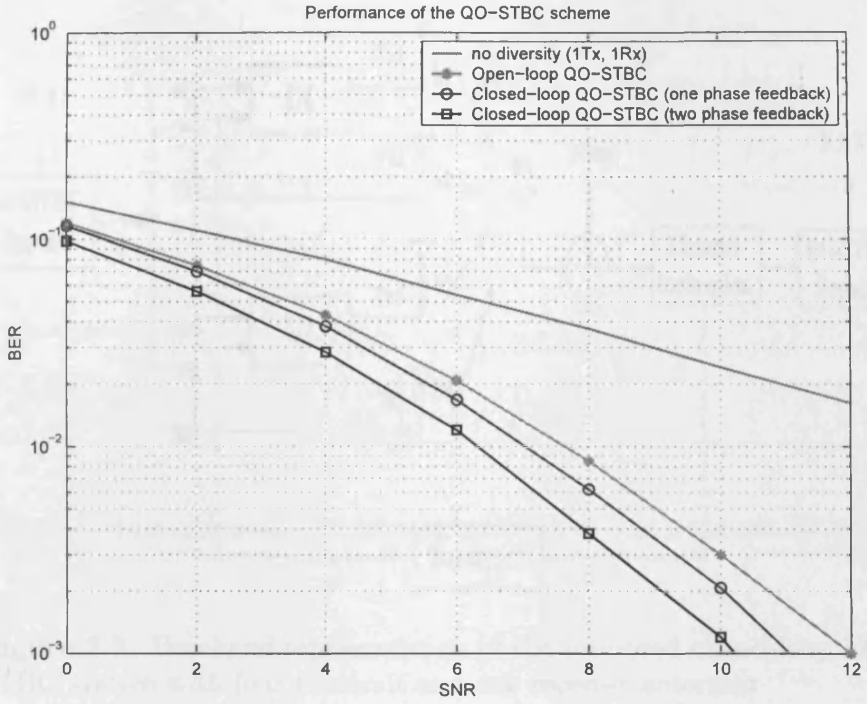

Figure 3.4. Performance of quasi-orthogonal STBC scheme.

3.6 Extended Orthogonal Space Time Block Codes (EO-STBCs)

The Alamouti scheme can be also used as a building block to design the EO-STBC with four transmit antennas and full rate [51]. The scheme can achieve a full transmit diversity with simple detection, given by

$$\mathbf{X_{EO}} = \xi \begin{bmatrix} s_1 & s_1 & s_2 & s_2 \\ -s_2^* & -s_2^* & s_1^* & s_1^* \end{bmatrix} \tag{3.6.1}$$

where ξ is a constant value equal to $1/2$, which is always ignored for simplicity. The Horizontal axis corresponds to the temporal dimension, whereas the vertical axis corresponds to the spatial dimension. That is at each time slot t, $[X_{EO}]_{t,n}$ is transmitted from the n-th transmit antenna.

As shown in Figure 3.5, for one receive antenna, the received signals

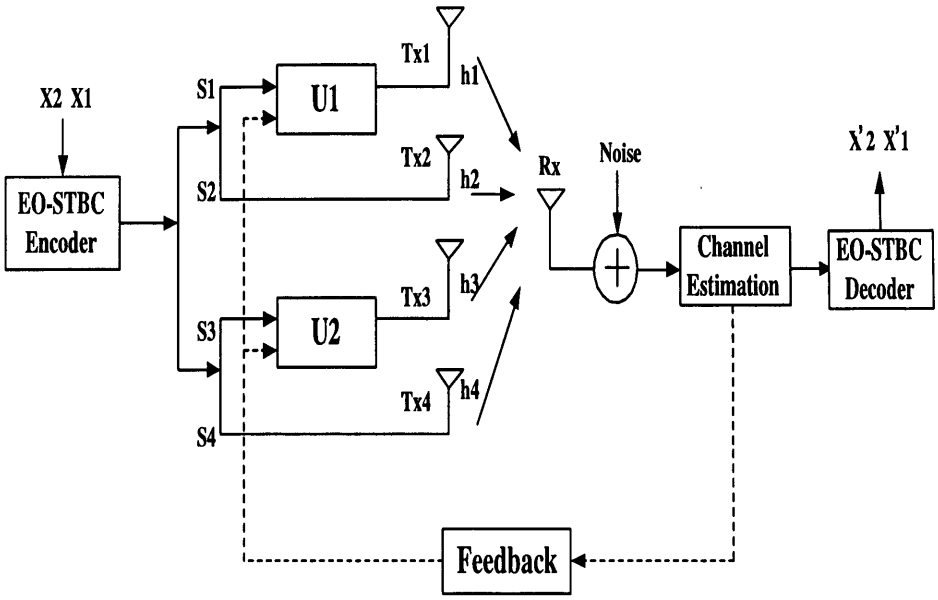

Figure 3.5. Baseband representation of the proposed closed-loop EO-STBC system with four transmit and one receiver antennas

at the first and second signalling intervals denoted as r_1 and r_2 are

$$\begin{aligned} r_1 &= \frac{1}{2}[h_1 s_1 + h_2 s_2 + h_3 s_3 + h_4 s_4] + n_1 \\ r_2 &= \frac{1}{2}[-h_1 s_2^* - h_2 s_2^* + h_3 s_1^* + h_4 s_1^*] + n_2 \end{aligned} \tag{3.6.2}$$

where the frequency flat fading channel coefficients $h_n, n = 1, \ldots, 4$ are assumed to be independent zero-mean complex Gaussian random variance $1/2$ per real dimension and constant over two time intervals, moreover the noise terms $n_t, t = 1, 2$ are assumed to be independent zero-mean circularly symmetric complex Gaussian random variance $N_o/2$ per real dimension. Furthermore, the Equation (3.6.2) can be written as the matrix notation,

$$\mathbf{r} = \begin{bmatrix} r_1 \\ r_2^* \end{bmatrix} = \begin{bmatrix} h_1 + h_2 & h_3 + h_4 \\ h_3^* + h_4^* & -h_1^* - h_2^* \end{bmatrix} \begin{bmatrix} s_1 \\ s_2 \end{bmatrix} + \begin{bmatrix} n_1 \\ n_2^* \end{bmatrix} \tag{3.6.3}$$

$$\mathbf{r} = \mathbf{H}\mathbf{x} + \mathbf{n} \tag{3.6.4}$$

3.6.1 Channel Matched Filtering

Applying the matched filtering $\mathbf{H}^H$ at the receiver, the Equation (3.6.4) is transform as:

$$\mathbf{H}^H\mathbf{r} = \mathbf{H}^H\mathbf{H}\mathbf{x} + \mathbf{H}^H\mathbf{n} \tag{3.6.5}$$

$$\mathbf{r}_{mf} = \Delta\mathbf{x} + \mathbf{n}_{mf} \tag{3.6.6}$$

where the 2×2 matrix Δ can be obtained as follows.

$$\begin{aligned}
\Delta &= \begin{bmatrix} h_1^* + h_2^* & h_3 + h_4 \\ h_3^* + h_4^* & -h_1 - h_2 \end{bmatrix} \begin{bmatrix} h_1 + h_2 & h_3 + h_4 \\ h_3^* + h_4^* & -h_1^* - h_2^* \end{bmatrix} \\
&= \begin{bmatrix} |h_1 + h_2|^2 + |h_3 + h_4|^2 & 0 \\ 0 & |h_1 + h_2|^2 + |h_3 + h_4|^2 \end{bmatrix} \\
&= \begin{bmatrix} (\sum_{i=1}^{4} |h_i|^2 + \varrho) & 0 \\ 0 & (\sum_{i=1}^{4} |h_i|^2 + \varrho) \end{bmatrix} \\
&= (\sum_{i=1}^{4} |h_i|^2)\mathbf{I}_2 + \varrho \begin{bmatrix} 1 & 0 \\ 0 & 1 \end{bmatrix}
\end{aligned} \tag{3.6.7}$$

where

$$\varrho = 2Re\{h_1 h_2^* + h_3 h_4^*\} \tag{3.6.8}$$

It is clear that the matrix $\mathbf{H}$ of the EO-STBC is proportional to an orthogonal matrix in the sense that $\mathbf{H}^H\mathbf{H}$ is diagonal, which indicates that the code can be decoded with a simple receiver. In particular, with linear processing, the detected signals $\tilde{s_1}$ and $\tilde{s_2}$ can be obtained as

$$\begin{bmatrix} \tilde{s_1} \\ \tilde{s_2} \end{bmatrix} = \Delta \begin{bmatrix} s_1 \\ s_2 \end{bmatrix} + \begin{bmatrix} (h_1^* + h_2^*)n_1 + (h_3 + h_4)n_2^* \\ (h_3^* + h_4^*)n_1 - (h_1 + h_2)n_2^* \end{bmatrix} \tag{3.6.9}$$

Although the decoding complexity is low, the β term may be negative which leads to some diversity loss. In order to achieve full diversity, two feedback bits can be used to rotate the phase of the signals for certain antennas to ensure that β is positive during the transmission block. The proposed feedback schemes are explained in the following section.

3.6.2 Transmission with Channel Feedback

Assume that channel state information (CSI) is available at the EO-STBC transmitter. At first, by rotating the signals from the first and third antennas in the transmission were adopted to force the β to be positive and maximum magnitude, as seen in Figure 3.5, where the rotation is define by the following phasors

$$\mathbf{U} = [U_1, U_2]^T \tag{3.6.10}$$

In order to achieve full diversity, the signals s_1 and s_3 are multiplied by $U_1 = (-1)^i$ and $U_2 = (-1)^k$, where $i, k = 0, 1$, before they are transmitted from first and third antennas, respectively. Here i and k are two feedback parameters determined by the channel condition. In particular, when $i(ork) = 1$, $U_1(orU_2) = -1$, which means that s_1 and s_3 will be phase rotated by 180° before transmission. Otherwise, they can be directly transmitted.

The phase rotation on the transmitted symbols in importantly effectively equivalent to rotating the phases of the corresponding channel coefficients. Since the channel is assumed to be constant over a transmission block, hence the received signal becomes

$$\begin{bmatrix} r_1 \\ r_2^* \end{bmatrix} = \begin{bmatrix} h_1' + h_2 & h_3' + h_4 \\ h_3'^* + h_4^* & -h_1'^* - h_2^* \end{bmatrix} \begin{bmatrix} s_1 \\ s_2 \end{bmatrix} + \begin{bmatrix} n_1 \\ n_2^* \end{bmatrix} \tag{3.6.11}$$

where h_1' and h_3' represent $U_1 h_1$ and $U_2 h_3$, respectively. Furthermore, the new matrix $\tilde{\Delta}$ can be written as

$$\tilde{\Delta} = \begin{bmatrix} |h_1' + h_2|^2 + |h_3' + h_4|^2 & 0 \\ 0 & |h_1' + h_2|^2 + |h_3' + h_4|^2 \end{bmatrix} \tag{3.6.12}$$

From Equation (3.6.11) and (3.6.12), the decision vector $\tilde{\mathbf{X}} = [\tilde{s_1}, \tilde{s_2}]^T$ with the receive vector $\mathbf{R} = [r_1, r_2^*]^T$ can be calculated as

$$\begin{aligned} \tilde{\mathbf{X}} = \tilde{\mathbf{H}}^H \mathbf{R} = (|U_1|^2 |h_1|^2 + |h_2|^2 + |U_2|^2 |h_3|^2 + |h_4|^2 \\ + (2Re(U_1 h_1 h_2^*) + 2Re(U_2 h_3 h_4^*))\mathbf{X} + \mathbf{V} \end{aligned} \tag{3.6.13}$$

where $\mathbf{V} = \tilde{\mathbf{H}}^H \tilde{\mathbf{N}}$ is a noise component with the covariance matrix $(|h_1' + h_2|^2 + |h_3' + h_4|^2)\mathbf{I}_2 N_o$. Since $|U_1|^2 = |U_2|^2 = 1$

$$\alpha = \sum_{i=1}^{4} |h_i|^2 \tag{3.6.14}$$

which α corresponds to the conventional diversity gain for the four transmit and one receive antenna case. The feedback performance gain is

$$\varrho' = 2Re((U_1 h_1 h_2^*) + 2Re(U_2 h_3 h_4^*)) \tag{3.6.15}$$

Moreover, the SNR at the receiver can be calculated as follows:

$$\gamma = \frac{\alpha + \varrho'}{4}\gamma_o \tag{3.6.16}$$

where $\gamma_o = E_s/N_o$ is the SNR without the diversity. It is obvious that if $\varrho' > 0$, the designed closed-loop system can obtain additional performance gain, which leads to an improved SNR at the receiver. According to the above analysis, the design criterion of the two-bit feedback scheme can be proposed. That is, each element of the feedback performance gain in Equation (3.6.15) should be nonnegative

$$(i,k) = \begin{cases} (0,0), & if\, Re(h_1 h_2^*) \geq 0 \quad and \quad Re(h_3 h_4^*) \geq 0 \\ (0,1), & if\, Re(h_1 h_2^*) \geq 0 \quad and \quad Re(h_3 h_4^*) < 0 \\ (1,0), & if\, Re(h_1 h_2^*) < 0 \quad and \quad Re(h_3 h_4^*) \geq 0 \\ (1,1), & if\, Re(h_1 h_2^*) < 0 \quad and \quad Re(h_3 h_4^*) < 0 \end{cases} \tag{3.6.17}$$

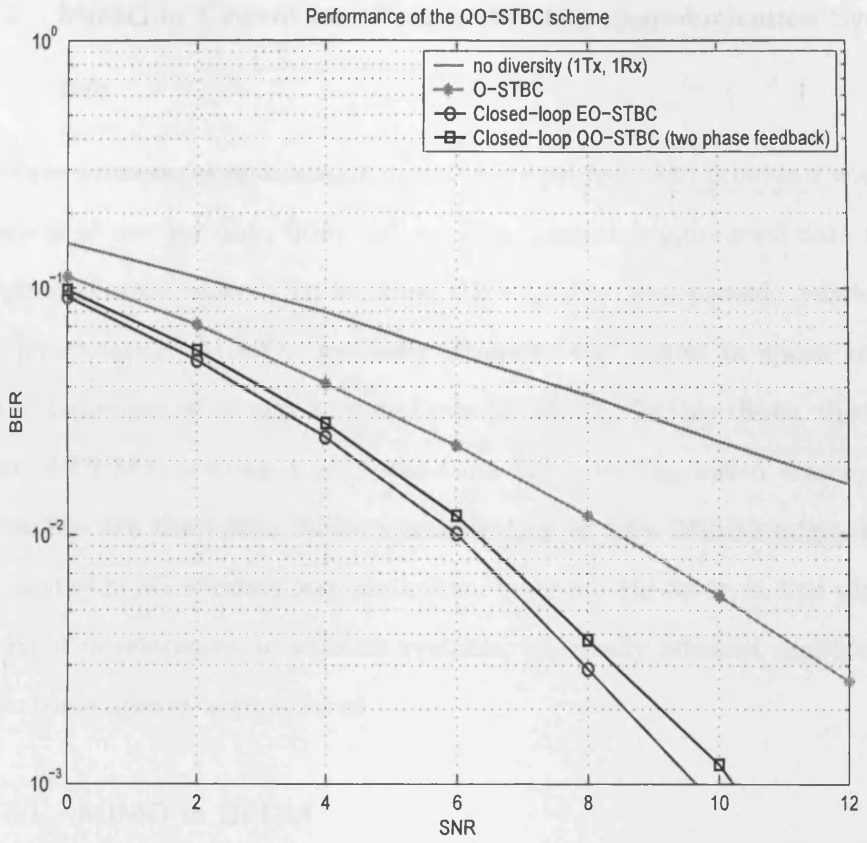

Figure 3.6. Performance of extended orthogonal STBC scheme

3.6.3 Simulation and Results

Here, the channel is still assumed to be constant (or at least does not change significantly) for a sufficiently long period. In this simulation both QO-STBC and EO-STBC with feedback outperform the Alamouti scheme, which is illustrated in Figure 3.6. The EO-STBC achieves the best performance due to the additional array gain, In particular, at 10^{-3}, the improvement is nearly 1dB than the QO-STBC scheme.

3.7 MIMO in Current and Future Wireless Communication System

Future wireless communication systems are projected to provide a wide variety of new services, from high quality voice and high-speed data to high-resolution video. To increase the capacity and provide reliable communication, MIMO, especially diversity techniques in space and time are expected to play a crucial role [26,28,52]. In this thesis, therefore WCDMA systems with space-time block coding based transmit diversity are the initial focus corresponding to how MIMO might be exploited in 3G wireless communication systems. However, in line with current development in wireless systems, spectrally efficient multicarrier transmission is considered.

3.7.1 MIMO in OFDM

Orthogonal frequency division multiplexing (OFDM) has become a popular technique for transmission of signals over wireless channels. OFDM has been adopted in several wireless standards such as digital audio broadcasting (DAB), digital video broadcasting (DVB-T), the IEEE 802.11a local area network (LAN) standard and the IEEE 802.16a metropolitan area network (MAN) standard. OFDM is also being pursued for dedicated short-range communications (DSRC) for road side to vehicle communications and as a potential candidate for fourth-generation (4G) mobile wireless systems.

OFDM converts a frequency-selective channel into a parallel collection of frequency flat subchannels. The subcarriers have the minimum frequency separation required to maintain orthogonality of their

corresponding time domain waveforms, yet the signal spectra corresponding to the different subcarriers overlap in frequency. Hence, the available bandwidth is used very efficiently. If knowledge of the channel is available at the transmitter, then the OFDM transmitter can adapt its signaling strategy to match the channel. Due to the fact that OFDM uses a large collection of narrowly spaced subchannels, these adaptive strategies can approach the ideal water pouring capacity of a frequency- selective channel. In practice this is achieved by using adaptive bit loading techniques, where different sized signal constellations are transmitted on the subcarriers.

The use of multiple antennas at both ends of a wireless link (MIMO technology) offers the potential ability to improve considerably the spectral efficiency and link reliability in future wireless communications systems [35]. However, most MIMO schemes, in fact, realize both spatial-multiplexing and diversity gain in some form of trade-off [53]. Hence, by combining OFDM with MIMO, OFDM can be adopted to reinforce a multi-antenna scheme by transferring a frequency-selective MIMO channel into a set of parallel frequency-flat MIMO channels. As a result, receiver complexity decreases and the advantages of each technique are still retained. Compared with the analyses in [54] and [8] experienced on flat fading MIMO channels, the OFDM-based multi-antenna scheme is robust with respect to multipath induced frequency-selective fading [55, 56]. Furthermore, frequency-selective fading can be further beneficial for these OFDM-based MIMO solutions in terms of spatial-multiplexing gain [56]. These features make combination of MIMO technology with OFDM be considered as one of the promising candidates for next-generation fixed and mobile wireless systems.

This design is motivated by the growing demand for broadband wireless communications.

3.8 Summary

Space-time block codes improve the performance of communication systems by introducing the transmit diversity. This chapter introduced the basic concepts of space-time block codes schemes to the readers and provided simulation results for their BER performance.

Space-time block codes are methods which utilize a special codeword to encode the transmitted symbols over both spatial and temporal dimensions thereby benefiting from diversity. Such codes include O-STBCs, QO-STBCs and EO-STBCs that were described in detail in this chapter. O-STBCs have simple decoding algorithms and can achieve full diversity gains. But they can not provide full rate and full diversity for a MIMO system with more than two transmit antennas. QO-STBCs and EO-STBCs can have the same full-rates and thereby further improve the error rate performance, when adopted with feedback, i.e. closed-loop operation. These versatile codes are applied widely in later chapters of this thesis.

Chapter 4

CLOSED-LOOP MIMO SCHEMES FOR WCDMA SYSTEM

4.1 Introduction

In modern wireless communication systems, the high transmission quality and transmission rates are rapidly growing to support multiple users. One promising technique to achieve this goal is the code-division multiple access (CDMA) with space-time processing, which is considered for third-generation (3G) and beyond the wideband CDMA (WCDMA) standard [57]. The focus of this chapter is on the application of WCDMA technology to MIMO communication systems denoted as MIMO-WCDMA. The aim is to develop advanced signal processing techniques applicable to a MIMO system operating under the WCDMA protocol with two transmit antennas. In addition, we will describe the transmitter model for the MIMO-WCDMA system with the different space-time block codes models related to four transmit antennas system will be described. A special closed-loop MIMO-WCDMA system with four transmit antennas system will be considered.

4.2 WCDMA System

The same data model as in [58] is adopted. The context is the uplink of a slotted system with K asynchronous users. In a slot, the ith user transmits a vector $\mathbf{s}_i$ consisting of M_i symbols s_{ik}. Each symbol s_{ik} is spread by an aperiodic code (vector) c_{ik} of length G_i. After multipath propagation over a channel with length L_i chips and relative delay D_i, pulse-shaped matched filtering and chip-rate sampling, the receiver stacks the received samples in a slot in a vector $\mathbf{y}$. The contribution of s_{ik} to $\mathbf{y}$ is a linear combination of the transmitted signal $c_{ik}s_{ik}$, plus a delay of it, properly scaled by the L_i channel coefficients collected in a vector $\mathbf{h}_i$, or

$$\mathbf{y}_{ik} = \mathbf{T}_{ik}\mathbf{h}_i s_{ik}, k = 1, \ldots, M_i \tag{4.2.1}$$

which is illustrated in Figure 4.1.

$\mathbf{T}_{ik}$ is a Toeplitz matrix whose first column is made of $(k-1)G_i + d_i$ zeros following by the code vector c_{ik}(the kth segment of G_i) chips of the spreading code of user i) and additional zeros that make the size of y_{ik} the total number of chips of the entire slot plus $\max\{d_i, i = 1, \ldots, M_i\}$.

Including all K users and the noise, yields

$$\mathbf{y} = \mathbf{THS} + \mathbf{w} \tag{4.2.2}$$

$$\mathbf{T} := [\mathbf{T}_1, \ldots, \mathbf{T}_k] \tag{4.2.3}$$

$$\mathbf{H} := diag(\boldsymbol{I}_{M_1} \otimes \mathbf{h}_1, \ldots, \boldsymbol{I}_{M_K} \otimes \mathbf{h}_K) \tag{4.2.4}$$

where matrix $\mathbf{H}$ is block diagonal with $\boldsymbol{I}_{M_i} \otimes \mathbf{h}_i$ as the $i\text{-}th$ block, the $\boldsymbol{I}_{M_i} \otimes \mathbf{h}_i$ is the the Kronecker product of $\boldsymbol{I}_{M_i}$ and $\mathbf{h}_i$, and $\mathbf{w}$ is a vector

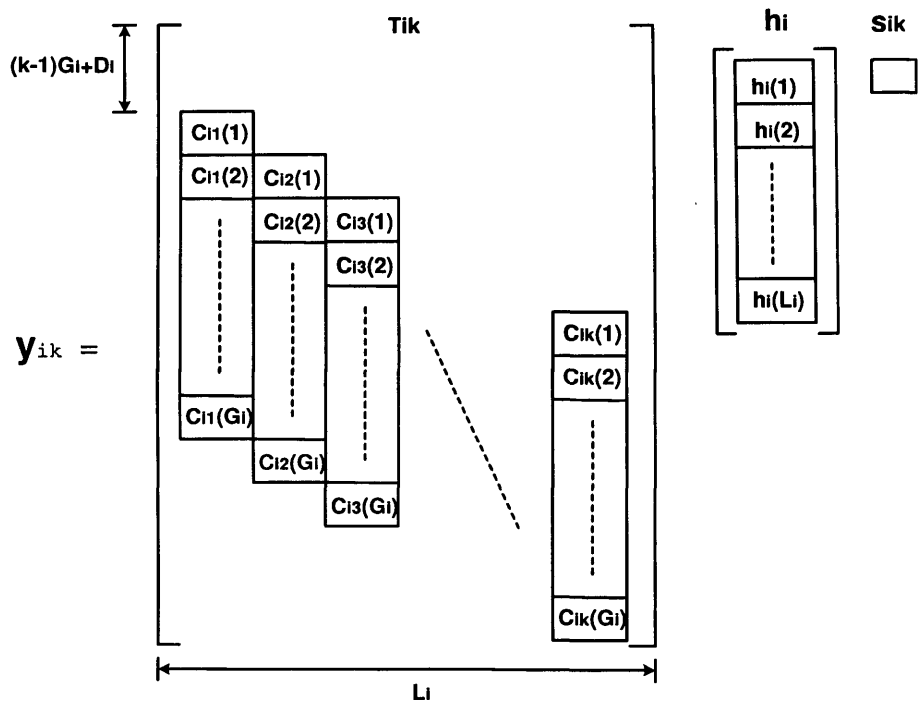

Figure 4.1. Noiseless single symbol output y_{im}.

representing the additive white Gaussian noise, the users' code matrix $\mathbf{T}$, the channel matrix $\mathbf{H}$ and stacking of all symbol vectors of all users are illustrated in Figure 4.2 .

It is clearly shown that the code matrix $\mathbf{T}$ has the size $max(M_iG_i + D_i + L_i - 1) \times \Sigma_1^K(M_iL_i)$, the channel matrix $\mathbf{H}$ has the size $\Sigma_1^K(M_iL_i) \times \Sigma_1^K(M_i)$ and the symbol vectors $\mathbf{S}$ have the size $\Sigma_1^K M_i \times 1$.

In the derivations of the algorithms, the following assumptions are made:

(1) The code matrix $\mathbf{T}$ has full column rank.

(2) The channel matrix $\mathbf{H}$ has full column rank.

(3) The code matrix $\mathbf{T}$ is known.

(4) The noise vector is white Gaussian with possibly unknown variance σ^2.

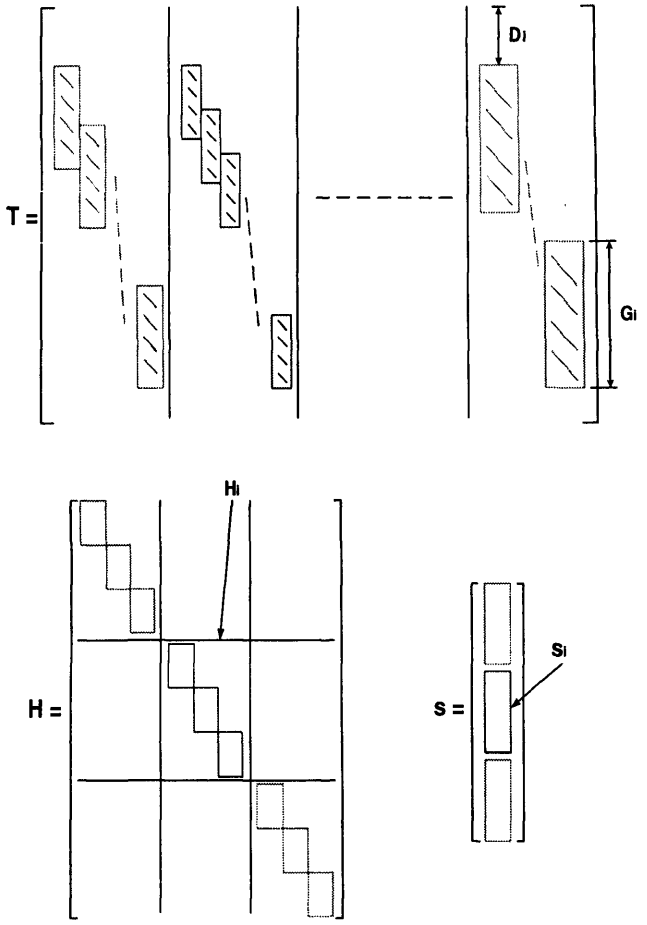

Figure 4.2. Structure of the code matrix **T**, **H** and **S**.

Assumption (1) implies that the receiver knows the codes, the delay offset D_i, and the number of channel coefficients L_i of all users. If D_i is unknown, it may be set it to 0 and model all paths. L_i is a model parameter, and its coefficient i is allowed to be zero, one can over parameterize the channel to accommodate channel length and delay uncertainties and pay a price for the lack of modelling details. If the channel is known to be sparse, it is more efficient to model the channel as separate clusters of fingers. In that case, the approximate locations of these clusters are assumed to be known.

Assumption (2) is sufficient but not necessary for the channel to be identifiable and for the proposed algorithm to produce good estimates. When (2) fails, the channel may still be identifiable. In practice, one may only include a limited number of dominant interferers and significant fingers in the data model.

4.2.1 WCDMA Detection Techniques

It is well known that the simple receiver for a SISO communication signal corrupted by AWGN is a Matched Filter (MF) sampled periodically at the symbol rate. These samples constitute a set of sufficient statistics for estimating the digital information that was transmitted. If the signal samples at the output of the MF are corrupted by ISI, an equalizer will further process the symbol space samples. In the presence of channel distortion, such as channel multipath, the MF must also be matched to the CIR. However, in practice, the CIR is usually unknown. One approach is to estimate the CIR from the transmission of a sequence of known symbols and to implement the MF using the estimate of the CIR.

Conventional matched filter, decorrelator, and regularized decorrelator as are considered the front end. The conventional detector for CDMA systems over SISO channels is a matched filter. However, the conventional MF detector is not optimal due to the multiple access interference (MAI) and is also not near-far resistant. Power control is introduced to alleviate the near-far effect. Although ideal power control is difficult to implement, stringent power control is necessary to ensure that users have almost identical signal power at the base station. The conventional detector treats the MAI as AWGN. This is a

reasonable approach because CDMA interference consists of contributions from independent interferers. The MAI can be defined through the cross-correlation matrix amongst users. Verdu [59] showed that the near-far effect is overwhelming on other users' signal power over the desired user's signal power, and is a limitation of the CDMA system. He also showed that this problem could be solved using an optimal multiuser ML detector, and provides a significant capacity improvement over the conventional MF or single-user detector. However, it comes at the cost of huge computational complexity. The computational complexity increases exponentially with the number of active users and the data block length, and leads to impractical implementation. Therefore, a number of sub-optimal multiuser receivers to enhance the detection performance have been studied.

The decorrelator is basically assumed for the algorithm construction. However, other front ends can be applied to the same algorithm depending on the situation.

Conventional RAKE Receiver

The conventional RAKE receiver consists of a bank of matched filters and projects the received signal into the code domains of the individual users, by correlating with several shifts of the code vectors, or $\mathbf{r} = \mathbf{T}^H\mathbf{y}$, the structure for single input single output (SISO) CDMA MF is found in [59]. Since the codes are not exactly orthogonal (let alone shift-orthogonal), $\mathbf{T}^H\mathbf{T} \neq I$, and contributions of each user overlaps the projections of other users, this makes the performance interference-limited.

Decorrlating RAKE Receiver

The proposed decorrelating RAKE uses a decorrelating matched filter, or $\mathbf{T}^{\dagger} = (\mathbf{T}^H\mathbf{T})^{-1}\mathbf{T}^H$. This removes all multiuser interference. The output of the decorrelating matched filter is given by [58]

$$\mathbf{u} = \mathbf{T}^{\dagger}\mathbf{y} = diag(\boldsymbol{I}\otimes \mathbf{h}_1, \ldots . \boldsymbol{I}\otimes \mathbf{h}_I)\mathbf{s} + \mathbf{n} \tag{4.2.5}$$

MMSE Receiver

Based on the data model Equation (4.2.2), the estimated data sequence by a linear minimum mean square error (MMSE) receiver is known to be [58]

$$\widetilde{\mathbf{s}} = (\mathbf{H}^H\mathbf{T}^H\mathbf{T}\mathbf{H} + \sigma^2\boldsymbol{I})^{-1}\mathbf{H}^H\mathbf{T}^H\mathbf{y} \tag{4.2.6}$$

Regularized decorrelating RAKE Receiver

The decorrelating matched filter $T^{\dagger}$ leads to exact channel identification in the absence of noise. However, it has the drawback of noise enhancement when T is ill-conditioned. A remedy is to use a regularized decorrelating matched filter given by [58]

$$\mathbf{F} = (\mathbf{T}^H\mathbf{T} + \sigma^2\mathbf{I})^{-1}\mathbf{T}^H \tag{4.2.7}$$

Such a front end does not eliminate multiple access interference, and the derivation of the channel estimator is now an approximation. It does improve the performance at low SNR in simulations.

4.3 Orthogonal Space Time Coded WCDMA

To facilitate the performance of the WCDMA communication system, the above WCDMA system with space time bock coded based transmit diversity should be formulated. Specifically, a WCDMA system with the Alamouti orthogonal space time block coded scheme was considered [5]. Two transmit antennas and one signal receive antenna, K asynchronous users with aperiodic spreading codes, and slotted transmissions were assumed.

At the transmitter, user i transmits two data sequences $\{s_{im}^{(1)}\}_{m=1}^{M_i}$ and $\{s_{im}^{(2)}\}_{m=1}^{M_i}$, one for each transmitter, in each slot, the data sequence for user i is space time encoded as

$$\begin{aligned} s_{im}^{(1)} &= s_{im} \\ s_{i,m+1}^{(1)} &= s_{i,m+1} \\ s_{i,m}^{(2)} &= -s_{i,m+1}^{(1)*} \\ s_{i,m+1}^{(2)} &= s_{i,m}^{(1)*}, \qquad m = 1, 3, \ldots, M_i - 1 \end{aligned} \tag{4.3.1}$$

where $s_{i,m}$ is the input data sequence, $s_{i,m}^{(j)}$, $j = 1, 2$ denote the encoded data sequence for transmit antenna j. Following this, signals from each transmit antenna are all spread by the same spreading code c_{ik}, and followed by a chip rate pulse-shaping filter. A quasi-static time-varying channel for each transmit and receiver antenna pair is considered, i.e., that the channel doesn't change in a slot period. Here, an FIR channel model with channel impulse response $h(i), i \in \{0, \ldots, L_i\}$ has been considered. The continuous-time channel impulse response of the path

from transmitter j to the single receiver for user i is given by

$$h_i^{(j)}(\tau) = \Sigma_{l=1}^{L_i^{(j)}} h_{il}^{(j)} \delta(\tau - lTc - d_i^{(j)} Tc) \tag{4.3.2}$$

where $h_{il}^{(j)}$ is the $l-th$ path gain for transmit-receiver pair j for user i and Tc is the chip interval. Simultaneously, the delay $d_i^{(j)}$ and the channel order $L_i^{(j)}$ from the slot reference are assumed known. The maximum value of ${L_i^{(j)}}_{j=1,2}$ is set as L_i, and the minimum of ${d_i^{(j)}}_{j=1,2}$ as d_i for the system analyze. The transmitted signal is corrupted by other user interference and additive noise in the channel. This gives us the long-code WCDMA system model as illustrated in Figure 4.3.

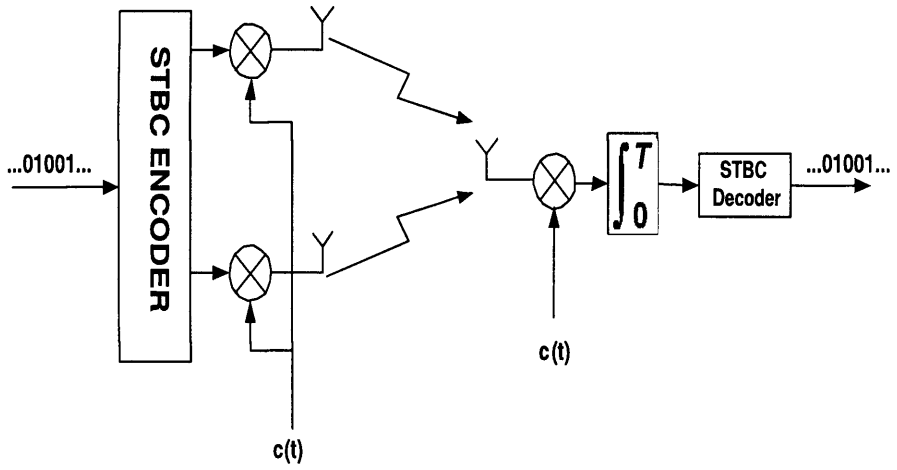

Figure 4.3. WCDMA system with space-time coded scheme using two transmit antennas and one receiver antenna.

4.3.1 Space Time Receiver

A decorrelator, conventional matched filter, and regularized decorrelator as are again considered the front end. The decorrelator is basically assumed for the algorithm construction. However, other front ends can be applied to the same algorithm depending on the situation.

The proposed decorrelating RAKE uses a decorrelating matched filter, or $\mathbf{T}^{\dagger} = (\mathbf{T}^H\mathbf{T})^{(-1)}\mathbf{T}^H$. This removes all multi-user interference. At the receiver, let $\mathbf{y}(t)$ pass through the chip-matched filter, and sample it at the chip rate. Stacking the chip rate sample, the discrete-time received signal vector can be obtained. The noiseless output y_{im} corresponding to the mth symbol of use i is given by

$$\mathbf{y}_{im} = \mathbf{T}_{im}[\mathbf{h}_i^{(1)} s_{im}^{(1)} + \mathbf{h}_i^{(2)} s_{im}^{(2)}] \tag{4.3.3}$$

where $h_i^{(j)} = [h_{i1}^j, \ldots, h_{iLi}^{(j)}]^T$ is the vector containing all multipath coefficients of antenna pair j and T_{im} is the Toeplitz matrix of the spread code vector c_{im} (the m-th segment of G_i chips of the spreading code of user i) and additional zeros that make the size of y_{im} the total number of chips of the entire slot plus $maxd_i, i = 1, \ldots, K$. Here, all the slot size is assumed to be fixed for different spreading gains, that is, $G_1 M_1 = \cdots = G_K M_K$.

Since the channel is linear, the total received noiseless signal for using i is given by the sum of $y_{im}, m = 1, \ldots, M_i$, as

$$\begin{aligned}
\mathbf{y}_i &= \sum_{m=1}^{M_i} \mathbf{T}_{im}[\mathbf{h}_i^{(1)} s_{im}^{(1)} + \mathbf{h}_i^{(2)} s_{im}^{(2)}] \\
&= \mathbf{T}_i(\boldsymbol{I}_{M_i} \otimes [\mathbf{h}_i^{(1)} \quad \mathbf{h}_i^{(2)}])\mathbf{s}_i \\
\mathbf{s}_i &= [s_{i1}^{(1)}, s_{i1}^{(2)}, s_{i2}^{(1)}, s_{i2}^{(2)} \ldots, s_{iM_i}^{(2)}] \\
\mathbf{T}_i &= [\mathbf{T}_{i1}, \mathbf{T}_{i2}, \ldots, \mathbf{T}_{iM_i}]
\end{aligned} \tag{4.3.4}$$

where $\mathbf{T}_i$ is the code matrix of user i and has a special block shifting structure.

Including all users and noise, the complete matrix model is given by

$$\begin{aligned}\mathbf{y} &= [\mathbf{T}_1 \cdots \mathbf{T}_K] diag(\boldsymbol{I}_{M_1} \otimes \mathbf{H}_1, \ldots, \boldsymbol{I}_{M_K} \otimes \mathbf{H}_K)\mathbf{S} + \mathbf{w} \\ &= \mathbf{T}\boldsymbol{D}(\mathbf{H})\mathbf{S} + \mathbf{w} \end{aligned} \tag{4.3.5}$$

The output of the decorrelating matched filter is given in vector form by

$$\mathbf{z} = \mathbf{T}^{\dagger}\mathbf{y} = \boldsymbol{D}(\mathbf{H})\mathbf{S} + \mathbf{n} = diag(\boldsymbol{I}_{M_1} \otimes \mathbf{H}_1, \ldots \boldsymbol{I}_{M_K} \otimes \mathbf{H}_K)\mathbf{s} + \mathbf{n} \tag{4.3.6}$$

where $\mathbf{n} = \mathbf{T}^{\dagger}\mathbf{w}$ is now colored, The vector $\mathbf{z}$ is segmented to obtain subvectors $\mathbf{z}_{im}$ of size L_i, $m = 1, 2, \ldots, M_i$. In the case of equal spreading gain and equal channel order ($M_1 = \cdots = M_K = M$ and $L_1 = \cdots = L_K = L$), z_{im} is the $((i-1)M + m)th$ L-dimensional subvector of z. The subvector corresponding to two consecutive symbols $2n-1, 2n$ of user i are given by

$$\begin{aligned}\mathbf{z}_{i,2n-1} &= \mathbf{H}_i \begin{bmatrix} s_{i,2n-1} \\ -s^*_{i,2n} \end{bmatrix} + \mathbf{n}_{i,2n-1} \\ \mathbf{z}_{i,2n} &= \mathbf{H}_i \begin{bmatrix} s_{i,2n} \\ s^*_{i,2n-1} \end{bmatrix} + \mathbf{n}_{i,2n} \end{aligned} \tag{4.3.7}$$

where $n = 1, 2, \ldots, M_i/2$. Rewriting the two vectors in a matrix form yields

$$\mathbf{Z}_{in} = [\mathbf{z}_{i,2n-1}^T, \mathbf{z}_{i,2n}^T]^T = \mathbf{H}_i\mathbf{S}_{in} + \mathbf{N}_{in} \tag{4.3.8}$$

where $\mathbf{H}_i$ contains the channel vector each transmit-receive pair, $\mathbf{N}_i n = [n_{i,2n-1}^T, n_{i,2n}^T]^T$, and

$$\mathbf{S}_{in} = \begin{bmatrix} s_{i,2n-1} & s_{i,2n} \\ -s_{i,2n}^* & s_{i,2n-1}^* \end{bmatrix} \tag{4.3.9}$$

Here, $\mathbf{S}_{in}$ belongs to the space-time code. Notice that the rearranged front-end output of Equation (4.3.5) in the CDMA with multipaths has an equivalent signal structure for MIMO channel for two transmit antennas and L_i receive antennas with flat fading for each transmit-receive pair.

4.3.2 Simulation and Results

In this section, the error performance of the proposed schemes in quasi-static frequency selective channels independently from one frame to another is assessed. For the previous system, the average bit error rate (BER) against signal-to-noise ratio (SNR) is simulated using BPSK symbols, which was calculated using Monte Carlo runs. An uplink WCDMA system with two transmit antennas and a single receive antenna was adopted. Single user ($K = 1$) was considered. The spreading codes were randomly generated with spreading gain $G = 32$ and fixed throughout the Monte Carlo simulation for BER. The slot size was $M = 80$. The symbol sequences were generated randomly for each Monte

Carlo run in the simulation. The channel for each Tx-Rx pair had three fingers $L = 3$. The SNR is defined by $(\|\mathbf{h}^{(1)}\|^2 + \|\mathbf{h}^{(2)}\|^2)GE_c/\sigma^2$, where E_c it the chip energy and σ^2 is the chip noise variance. Each frame consists of 1000 symbols.

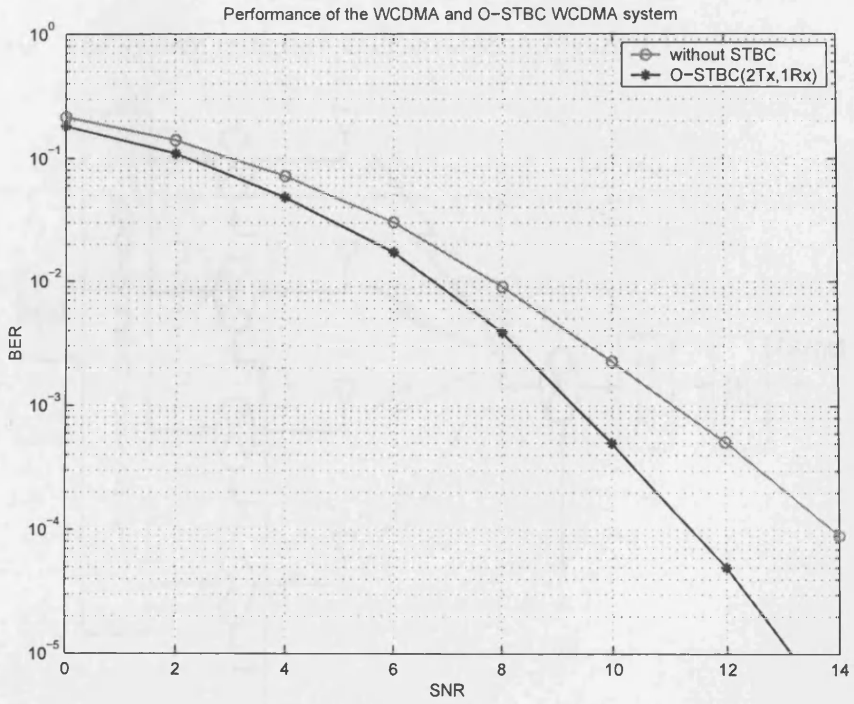

Figure 4.4. Performance comparison for WCDMA system and STBC-WCDMA system with two transmit antennas and one receive antenna.

In Figure 4.4, the performance of the proposed O-STBC WCDMA system with two transmit antennas is shown. The WCDMA system without STBC is also shown in Figure 4.4 for comparison. This set of results allow the performance advantage attained using O-STBC with two transmit antennas to be qualified in a WCDMA system, at the BER of 10^{-4}, there is near $2.8dB$ improvement.

4.4 QO-STBC MIMO-WCDMA Transceiver Design with Four Antennas

In this section, the space time coded WCDMA system will be developed for the four transmit antennas using the quasi-orthogonal space time code. The system structure is illustrated in Figure 4.5.

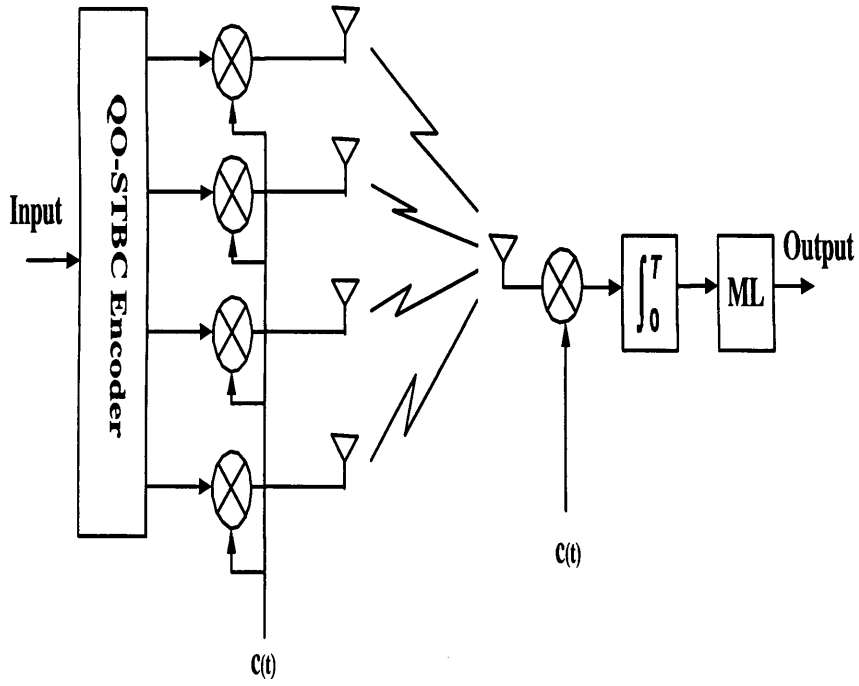

Figure 4.5. WCDMA system with space-time coded scheme using four transmit antennas and one receiver antenna.

At the transmitter, the *i-th* user's data sequences are denoted $s_{i,m_{m=1}}^{(1)\,M_i}$, $s_{i,m_{m=1}}^{(2)\,M_i}$, $s_{i,m_{m=1}}^{(3)\,M_i}$ and $s_{i,m_{m=1}}^{(4)\,M_i}$, one for each transmitter, in each slot, where M_i denotes the slot size for user i. The data for user i are quasi-orthogonal space-time encoded as:

$$
\begin{aligned}
s_{i,m}^{(1)} &= s_{i,m}, s_{i,m+1}^{(1)} = s_{i,m+1}, s_{i,m+2}^{(1)} = s_{i,m+2}, s_{i,m+3}^{(1)} = s_{i,m+3} \\
s_{i,m}^{(2)} &= -s_{i,m+1}^{*}, s_{i,m+1}^{(2)} = s_{i,m}^{*}, s_{i,m+2}^{(2)} = -s_{i,m+3}^{*}, s_{i,m+3}^{(2)} = s_{i,m+2}^{*} \\
s_{i,m}^{(3)} &= -s_{i,m+2}^{*}, s_{i,m+1}^{(3)} = -s_{i,m+3}^{*}, s_{i,m+2}^{(3)} = -s_{i,m}^{*}, s_{i,m+3}^{(3)} = s_{i,m+1}^{*} \\
s_{i,m}^{(4)} &= s_{i,m+3}, s_{i,m+1}^{(4)} = -s_{i,m+2}, s_{i,m+2}^{(4)} = -s_{i,m+1}, s_{i,m+3}^{(4)} = s_{i,m} \\
m &= 1, 5, \ldots, M_i - 3,
\end{aligned} \tag{4.4.1}
$$

where $s_{i,m}$ is the input data sequence, $s_{i,m}^{(j)}, j = 1, 2, 3, 4$ denote the encoded data sequence for transmit antenna j. Following this, signals from each transmit antenna are all spread by the same spreading code. It's also assumed that the transmitted signal is corrupted by other users' interference and additive noise in the channel.

To increase temporal diversity, the receiver signal is typically sampled at the rate T_F faster than or equal to the chip rate T_C. In this case, the receiver signal $y(t)$ passes through the chip-matched filter, and is sampled at the chip rate. Stacking the chip rate samples, the discrete-time received signal vector is obtained. The receiver segment $\mathbf{y}_{im}$ which corresponds to the mth symbol of user i will be considered first. $\mathbf{y}_{im}$ is given by

$$
\mathbf{y}_{im} = \mathbf{T}_{im}[\mathbf{h}_i^{(1)} s_{i,m}^{(1)} + \mathbf{h}_i^{(2)} s_{i,m}^{(2)} + \mathbf{h}_i^{(3)} s_{i,m}^{(3)} + \mathbf{h}_i^{(4)} s_{i,m}^{(4)}] \tag{4.4.2}
$$

where $\mathbf{T}_{im}$ is the Toeplitz matrix whose first column is made of $(m-1)G_i + d_i$ zeros follows by the code vector c_{im}(the mth segment of G_i chips of the spreading code of user i) and additional zeros that make the size of y_{im} the total number of chips of the entire slot plus $max\{d_i, i =$

$1, \ldots, K\}$.

4.4.1 Simple Linear Matrix Transform Method in the Receiver

The output of the decorrelator is given in vector form by

$$\mathbf{z} = \mathbf{T}^{\dagger}\mathbf{y} = \vartheta(\mathbf{H})\mathbf{s} + \mathbf{n} = diag(\mathbf{I}_{Mi} \otimes \mathbf{H}_1, \ldots, \mathbf{I}_{MK} \otimes \mathbf{H}_K)\mathbf{s} + \mathbf{n}, \quad (4.4.3)$$

where $\mathbf{n} = \mathbf{T}^{\dagger}\mathbf{w}$ is now colored. The four subvectors corresponding to four consecutive symbols $m, m+1, m+2, m+3$ of the user i are given by

$$\mathbf{z}_{i,m} = [\mathbf{h}_i^{(1)}\mathbf{h}_i^{(2)}\mathbf{h}_i^{(3)}\mathbf{h}_i^{(4)}] \begin{bmatrix} s_{i,m} \\ -s_{i,m+1}^* \\ -s_{i,m+2}^* \\ s_{i,m+3} \end{bmatrix} \quad (4.4.4)$$

$$\mathbf{z}_{i,m+1} = [\mathbf{h}_i^{(1)}\mathbf{h}_i^{(2)}\mathbf{h}_i^{(3)}\mathbf{h}_i^{(4)}] \begin{bmatrix} s_{i,m+1} \\ s_{i,m}^* \\ -s_{i,m+3}^* \\ -s_{i,m+2} \end{bmatrix} \quad (4.4.5)$$

$$\mathbf{z}_{i,m+2} = [\mathbf{h}_i^{(1)}\mathbf{h}_i^{(2)}\mathbf{h}_i^{(3)}\mathbf{h}_i^{(4)}] \begin{bmatrix} s_{i,m+2} \\ -s_{i,m+3}^* \\ s_{i,m}^* \\ -s_{i,m+1} \end{bmatrix} \quad (4.4.6)$$

$$\mathbf{z}_{i,m+3} = [\mathbf{h}_i^{(1)}\mathbf{h}_i^{(2)}\mathbf{h}_i^{(3)}\mathbf{h}_i^{(4)}] \begin{bmatrix} s_{i,m+3} \\ -s_{i,m+2}^* \\ s_{i,m+1}^* \\ -s_{i,m} \end{bmatrix} \quad (4.4.7)$$

Now rewriting these four sub vectors $\mathbf{z}_{i,m}, \mathbf{z}_{i,m+1}, \mathbf{z}_{i,m+2}, \mathbf{z}_{i,m+3}$ as:

$$\mathbf{Z} = \begin{bmatrix} \mathbf{z}_{i,m} \\ \mathbf{z}^*_{i,m+1} \\ \mathbf{z}^*_{i,m+2} \\ \mathbf{z}_{i,m+3} \end{bmatrix} = \begin{bmatrix} \mathbf{h}_i^{(1)} & \mathbf{h}_i^{(2)} & \mathbf{h}_i^{(3)} & \mathbf{h}_i^{(4)} \\ \mathbf{h}_i^{*(2)} & -\mathbf{h}_i^{*(1)} & \mathbf{h}_i^{*(4)} & -\mathbf{h}_i^{*(3)} \\ \mathbf{h}_i^{*(3)} & \mathbf{h}_i^{*(4)} & -\mathbf{h}_i^{*(1)} & -\mathbf{h}_i^{*(2)} \\ \mathbf{h}_i^{(4)} & -\mathbf{h}_i^{(3)} & -\mathbf{h}_i^{(2)} & \mathbf{h}_i^{(1)} \end{bmatrix} \begin{bmatrix} s_{i,m} \\ -s^*_{i,m+1} \\ -s^*_{i,m+2} \\ s_{i,m+3} \end{bmatrix} \tag{4.4.8}$$

where $\mathbf{z}$ and $\mathbf{h}$ are all $Lh \times 1$ column vector, let $Lh = 5$, $\mathbf{z}_{i,m} = [z_{i,m,1} z_{i,m,2} \ldots z_{i,m,5}]^T$, and $\mathbf{h}_i^{(1)} = [h_{i,1}^{(1)} h_{i,2}^{(1)} \ldots h_{i,5}^{(1)}]^T$.

Applying matched filtering at the receiver,the overall matrix can be obtained as follows:

$$\mathbf{\Delta} = \mathbf{H}^H\mathbf{H} = \begin{bmatrix} \lambda & 0 & 0 & \alpha \\ 0 & \lambda & -\alpha & 0 \\ 0 & -\alpha & \lambda & 0 \\ \alpha & 0 & 0 & \lambda \end{bmatrix} \tag{4.4.9}$$

where $\lambda = \sum_{l=0}^{L-1} \sum_{j=1}^{4} |h_{i,l}^{(j)}|^2$, and $\alpha = 2\sum_{l=0}^{L-1} Re\{h_{i,l}^{*(1)} h_{i,l}^{(4)} - h_{i,l}^{*(2)} h_{i,l}^{(3)}\}$. From Equation (4.4.9), it is clear that some nonzero off-diagonal terms appear, which lead to some diversity loss. In order to achieve full diversity, feedback bits are used to rotate the phases to eliminate or reduce the off-diagonal element.

4.4.2 Transmission with Channel Feedback

The non-zero off diagonal elements in matrix Equation (4.4.9) reduce the diversity gain and the signal-to-noise ratio (SNR) at the receiver. The signals transmitted from certain antennas can be modified by rotating with proper phase angle such that the magnitude of the off-diagonal

elements α is minimized.

Without loss of generality, consider that the signals from the third and fourth transmit antennas are rotated by phaser θ and ϕ respectively and the rotation angle is selected from a range $\theta, \phi \in [0, 2\pi]$, the system diagram is illustrated in Figure 4.6. Which is equivalent to multiplying

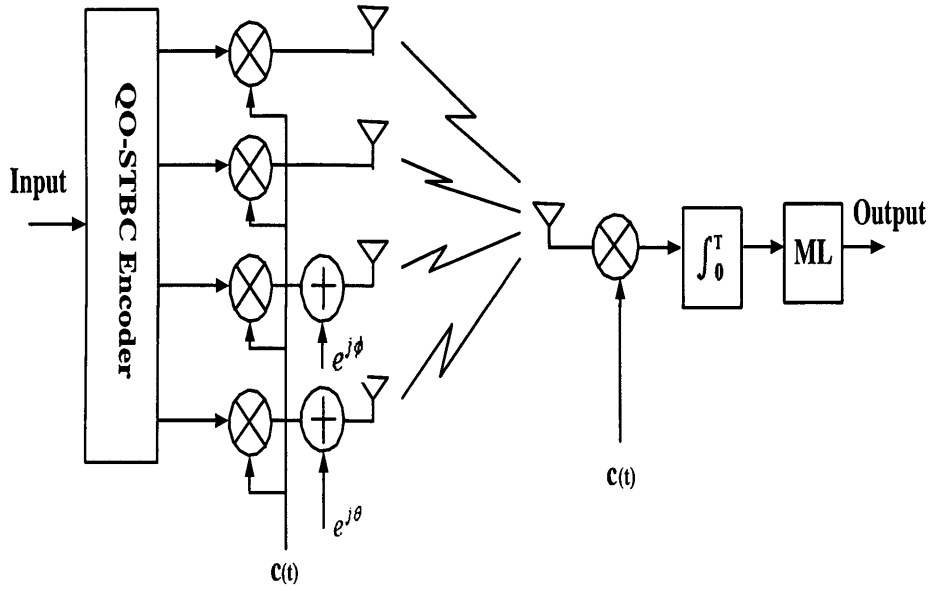

Figure 4.6. Block diagram of the baseband model of an WCDMA based two-phase feedback STBC scheme with four transmit antennas

the first and second term in equation 4.4.9 by $e^{j\theta}$ and $e^{j\phi}$,

$$\alpha' = Re\{\sum_{l=0}^{L-1} h_{i,l}^{*(1)} h_{i,l}^{(4)} e^{j\theta} - \sum_{l=0}^{L-1} h_{i,l}^{*(2)} h_{i,l}^{(3)} e^{j\phi}\} \tag{4.4.10}$$

Let $\kappa = \sum_{l=0}^{L-1} h_{i,l}^{*(1)} h_{i,l}^{(4)}$ and $\beta = \sum_{l=0}^{L-1} h_{i,l}^{*(2)} h_{i,l}^{(3)}$

$$\alpha' = |\kappa| cos(\theta + \angle\kappa) - |\beta| cos(\phi + \angle\beta) \tag{4.4.11}$$

where $|\cdot|$ and $\angle$ denote the absolute value and the angle (arctan) operators, respectively.

Then it is easy to find the rotated phasor parameter θ and ϕ after trigonometric manipulations (Let $\alpha^{'} = 0$). Those solutions are

$$\theta = arccos(\frac{|\beta|}{|\kappa|}cos(\phi + \angle\beta)) - \angle\kappa \tag{4.4.12}$$

provided that

$$\phi \in \begin{cases} [0, 2\pi), & \text{when } |\beta| < |\kappa| \\ [\pi\text{-}\xi\text{-}\angle\beta,\ \xi\text{-}\angle\beta] & \\ \bigcup[2\pi - \xi - \angle\beta, \pi + \xi - \angle\beta], & \text{otherwise} \end{cases} \tag{4.4.13}$$

where $\xi = \frac{|\kappa|}{|\beta|}$.

4.4.3 Simulations

In this section, the error performance of the proposed schemes in quasi-static frequency selective channels which vary independently from one frame to another is examined. For the previous system, the average BER against SNR is simulated using BPSK symbols, which was calculated using Monte Carlo runs. An uplink WCDMA system with two transmit antenna and a single receive antenna was adopted. For the multiuser case, a scenario with ($K = 2$) asynchronous users was considered, each user has equal power. The spreading codes were randomly generated with spreading gain $G = 32$ and fixed throughout the Monte Carlo simulation for BER. The slot size was $M = 80$, the symbol sequences were generated randomly for each Monte Carlo run in the simulation. The channel for each Tx-Rx pair had three fingers $L = 3$. The SNR is defined by $(\|\mathbf{h}^{(1)}\|^2 + \|\mathbf{h}^{(2)}\|^2)GE_c/\delta^2$, where E_c it the chip energy and δ^2 is the chip noise variance. Each frame consists

of 1000 symbols in the simulation.

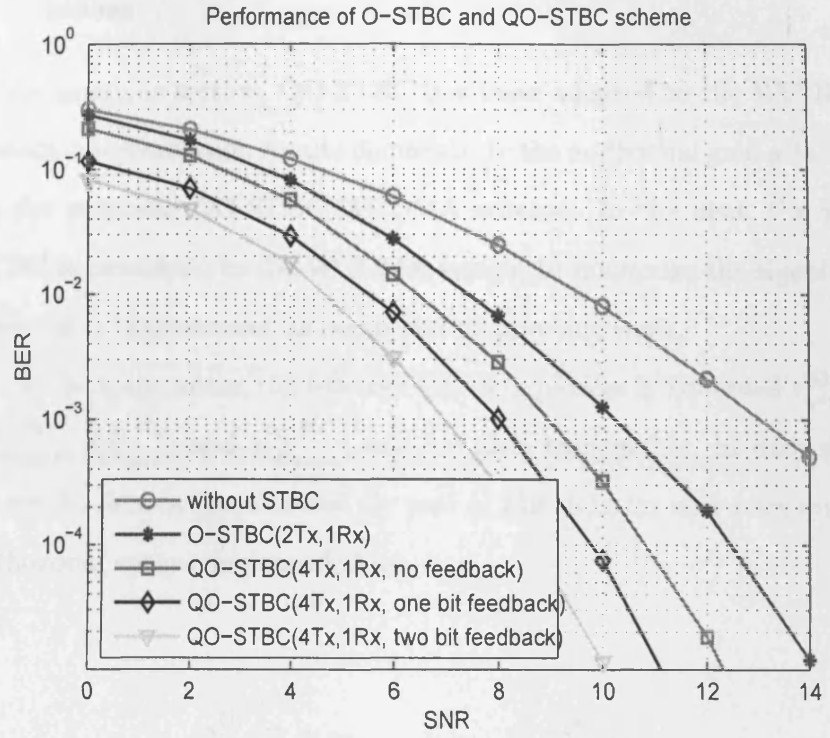

Figure 4.7. The BER vs. SNR performance for QO-STBC-WCDMA system

The BER performance for the proposed closed-loop QO-STBC WCDMA system with four transmit antennas and one receiver antenna is showed in Figure 4.7. The performance of the WCDMA system without STBC, combined with O-STBC and QO-STBC is shown in Figure 4.7 for comparison. It is clear that the proposed scheme is much better than without the STBC case. As shown in Figure 4.7, when the BER is 10^{-3}, it can get a $5dB$ gain in the signal bit feedback scheme, moreover, the two bits scheme outperforms the signal bit feedback nearly $1dB$ at the BER of 10^{-3}.

4.5 EO-STBC MIMO-WCDMA Transceiver Design with Four Antennas

In the previous section, QO-STBC has been adopted to the WCDMA system, the simulation results demonstrate the additional gain attained by the proposed QO-STBC WCDMA scheme. In the next, the EO-STBC is developed to the WCDMA system to maximize the signal-to-noise ratio improvement as compared to previous work.

At the transmitter, the *i-th* user's data sequences are denoted $s_{i,m_{m=1}}^{(1)\,M_i}$, $s_{i,m_{m=1}}^{(2)\,M_i}$, $s_{i,m_{m=1}}^{(3)\,M_i}$ and $s_{i,m_{m=1}}^{(4)\,M_i}$, one for each transmitter, in each slot, where M_i denotes the slot size for user i. The data for user i are quasi-orthogonal space-time encoded as:

$$\begin{aligned}
s_{i,m}^{(1)} &= s_{i,m}, \qquad s_{i,m+1}^{(1)} = -s_{i,m+1}^{*} \\
s_{i,m}^{(2)} &= s_{i,m}, \qquad s_{i,m+1}^{(2)} = -s_{i,m+1}^{*} \\
s_{i,m}^{(3)} &= s_{i,m+1}, \qquad s_{i,m+1}^{(3)} = s_{i,m}^{*} \\
s_{i,m}^{(4)} &= s_{i,m+1}, \qquad s_{i,m+1}^{(4)} = s_{i,m}^{*} \\
m &= 1, 3, \ldots, M_i - 1,
\end{aligned} \tag{4.5.1}$$

where $s_{i,m}$ is the input data sequence, $s_{i,m}^{(j)}, j = 1, 2, 3, 4$ denote the encoded data sequence for transmit antenna j.

Including all users and noise, the complete matrix model is given by

$$\begin{aligned}
\mathbf{y} &= [\mathbf{T}_1 \cdots \mathbf{T}_K] diag(\boldsymbol{I}_{M_1} \otimes \mathbf{H}_1, \ldots, \boldsymbol{I}_{M_K} \otimes \mathbf{H}_K)\mathbf{S} + \mathbf{w} \\
&= \mathbf{T}\boldsymbol{D}(\mathbf{H})\mathbf{S} + \mathbf{w}
\end{aligned} \tag{4.5.2}$$

After the despreading, the output is given in vector form by

$$\mathbf{z} = \mathbf{T}^{\dagger}\mathbf{y} = \vartheta(\mathbf{H})\mathbf{s} + \mathbf{n} = diag(\mathbf{I}_{Mi} \otimes \mathbf{H}_1, \ldots, \mathbf{I}_{MK} \otimes \mathbf{H}_K)\mathbf{s} + \mathbf{n}, \quad (4.5.3)$$

where $\mathbf{n} = \mathbf{T}^{\dagger}\mathbf{w}$ is also colored. The two subvectors of the user i are given by

$$\mathbf{z}_{i,m} = [\mathbf{h}_i^{(1)}\mathbf{h}_i^{(2)}\mathbf{h}_i^{(3)}\mathbf{h}_i^{(4)}] \begin{bmatrix} s_{i,m} \\ s_{i,m}^* \\ s_{i,m+1}^* \\ s_{i,m+1} \end{bmatrix} \quad (4.5.4)$$

$$\mathbf{z}_{i,m+1} = [\mathbf{h}_i^{(1)}\mathbf{h}_i^{(2)}\mathbf{h}_i^{(3)}\mathbf{h}_i^{(4)}] \begin{bmatrix} -s_{i,m+1}^* \\ -s_{i,m+1}^* \\ s_{i,m}^* \\ s_{i,m}^* \end{bmatrix} \quad (4.5.5)$$

Now rewriting these two sub vectors $\mathbf{z}_{i,m}, \mathbf{z}_{i,m+1}$ as:

$$\tilde{\mathbf{z}} = \begin{bmatrix} \mathbf{z}_{i,m} \\ \mathbf{z}_{i,m+1}^* \end{bmatrix} = \begin{bmatrix} \mathbf{h}_i^{(1)} + \mathbf{h}_i^{(2)} & \mathbf{h}_i^{(3)} + \mathbf{h}_i^{(4)} \\ \mathbf{h}_i^{*(3)} + \mathbf{h}_i^{*(4)} & -\mathbf{h}_i^{*(1)} - \mathbf{h}_i^{*(2)} \end{bmatrix} \begin{bmatrix} s_{i,m} \\ s_{i,m+1} \end{bmatrix} \quad (4.5.6)$$

where $\mathbf{z}$ and $\mathbf{h}$ are all $Lh \times 1$ column vector, let $Lh = 5$, $\mathbf{z}_{i,m} = [z_{i,m,1}z_{i,m,2} \ldots z_{i,m,5}]^T$, and $\mathbf{h}_i^{(1)} = [h_{i,1}^{(1)}h_{i,2}^{(1)} \ldots h_{i,5}^{(1)}]^T$.

Applying the match filtering, the Equation (4.5.6) is transform as:

$$\mathbf{r}_{mf} = \Delta\mathbf{s} + \mathbf{n}_{mf} \quad (4.5.7)$$

where the 2×2 matrix Δ can be obtained as follows

$$
\begin{aligned}
\Delta &= \begin{bmatrix} (\mathbf{h}_i^{*(1)} + \mathbf{h}_i^{*(2)})^T & (\mathbf{h}_i^{(3)} + \mathbf{h}_i^{(4)})^T \\ (\mathbf{h}_i^{*(3)} + \mathbf{h}_i^{*(4)})^T & (-\mathbf{h}_i^{(1)} - \mathbf{h}_i^{(2)})^T \end{bmatrix} \begin{bmatrix} \mathbf{h}_i^{(1)} + \mathbf{h}_i^{(2)} & \mathbf{h}_i^{(3)} + \mathbf{h}_i^{(4)} \\ \mathbf{h}_i^{*(3)} + \mathbf{h}_i^{*(4)} & -\mathbf{h}_i^{*(1)} - \mathbf{h}_i^{*(2)} \end{bmatrix} \\
&= \begin{bmatrix} |\mathbf{h}_i^{(1)} + \mathbf{h}_i^{(2)}|^2 + |\mathbf{h}_i^{(3)} + \mathbf{h}_i^{(4)}|^2 & 0 \\ 0 & |\mathbf{h}_i^{(1)} + \mathbf{h}_i^{(2)}|^2 + |\mathbf{h}_i^{(3)} + \mathbf{h}_i^{(4)}|^2 \end{bmatrix} \\
&= \begin{bmatrix} (\sum_{l=0}^{L-1} \sum_{j=1}^{4} |h_{i,l}^{(j)}|^2 + \varrho) & 0 \\ 0 & (\sum_{l=0}^{L-1} \sum_{j=1}^{4} |h_{i,l}^{(j)}|^2 + \varrho) \end{bmatrix} \\
&= (\sum_{l=0}^{L-1} \sum_{j=1}^{4} |h_{i,l}^{(j)}|^2) \boldsymbol{I}_2 + \varrho \begin{bmatrix} 1 & 0 \\ 0 & 1 \end{bmatrix}
\end{aligned} \tag{4.5.8}
$$

where

$$\varrho = 2Re\{h_{i,l}^{(1)} h_{i,l}^{*(2)} - h_{i,l}^{(3)} h_{i,l}^{*(4)}\} \tag{4.5.9}$$

4.5.1 Transmission with Channel Feedback

Assume that channel state information (CSI) is available at the transmitter. At first, by rotating the signals from the first and third antennas in the transmission were adopted to force ϱ to be positive and maximum magnitude, where the rotation is define by the following phasors

$$\mathbf{U} = [U_1, U_2]^T \tag{4.5.10}$$

where $U_1 = (-1)^i$ and $U_2 = (-1)^k$, $i, k = 0, 1$. Here i and k are two feedback parameters determined by the channel condition. In particular, when $i(ork) = 1$, $U_1(orU_2) = -1$, which means that s_1 and s_3 will be phase rotated by 180° before transmission. Otherwise, they can be

directly transmitted.

The feedback performance gain is

$$\varrho' = 2Re(U_1 h_{i,l}^{(1)} h_{i,l}^{*(2)}) + 2Re(U_2 h_{i,l}^{(3)} h_{i,l}^{*(4)}) \tag{4.5.11}$$

It is obvious that if $\varrho' > 0$, the designed closed-loop system can obtain additional performance gain, which leads to an improved SNR at the receiver. According to the above analysis, the design criterion of the two-bit feedback scheme can be proposed. That is, each element of the feedback performance gain in Equation (3.6.15) should be nonnegative

$$(i,k) = \begin{cases} (0,0), & if Re(h_{i,l}^{(1)} h_{i,l}^{*(2)}) \geq 0 \quad and \quad Re(h_{i,l}^{(3)} h_{i,l}^{*(4)}) \geq 0 \\ (0,1), & if Re(h_{i,l}^{(1)} h_{i,l}^{*(2)}) \geq 0 \quad and \quad Re(h_{i,l}^{(3)} h_{i,l}^{*(4)}) < 0 \\ (1,0), & if Re(h_{i,l}^{(1)} h_{i,l}^{*(2)}) < 0 \quad and \quad Re(h_{i,l}^{(3)} h_{i,l}^{*(4)}) \geq 0 \\ (1,1), & if Re(h_{i,l}^{(1)} h_{i,l}^{*(2)}) < 0 \quad and \quad Re(h_{i,l}^{(3)} h_{i,l}^{*(4)}) < 0 \end{cases} \tag{4.5.12}$$

4.5.2 Simulations

In this section, the simulations are performed between O-STBC, close-loop QO-STBC and close-loop EO-STBC MIMO WCDMS system, which is shown in Figure 4.8. The simulation environment is the same as in the previous section. It can be seen that at a BER of 10^{-3}, the performance improvement of the closed loop feedback QO-STBC scheme is approximately $3.8dB$ compared to the O-STBC WCDMA scheme. Furthermore, the proposed closed loop EO-STBC WCDMA scheme achieves the best performance, which outperforms closed loop QO-STBC scheme approximately $0.2dB$.

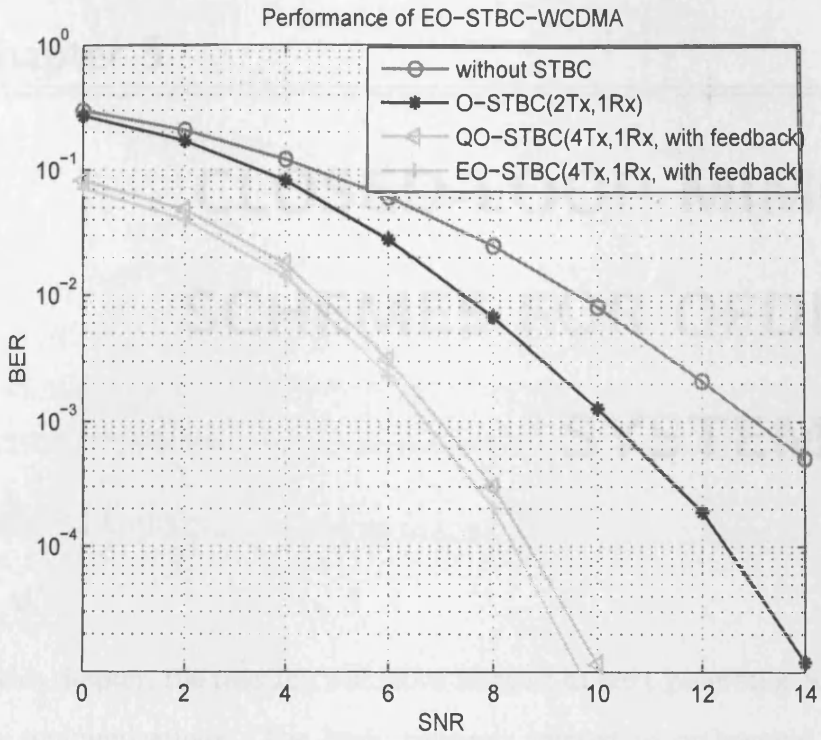

Figure 4.8. The BER vs. SNR performance for EO-STBC-WCDMA system

4.6 Summary

In this chapter, the full-rate STBC for four transmit antennas QO-STBC has been proposed in a long code WCDMA systems. A feedback method is also adopted to achieve the additional performance gain. The simulation results demonstrate the additional gain attained by the proposed QO-STBC and EO-STBC WCDMA method. The feedback method proved a surprising good performance.

Chapter 5

CLOSED-LOOP MIMO SCHEMES FOR OFDM SYSTEMS

In this chapter, the research will move forward to next generation wireless communications. The basic concepts related to orthogonal frequency division multiplexing (OFDM) are presented, which is considered as a key technique for 4G broadband wireless connection. A basic system model is given, common components for OFDM based systems are explained, and a simple transceiver based on OFDM modulation is presented. Important impairments in OFDM systems are mathematically analyzed. Bandwidth efficiency is then analyzed, and the insertion of a guard interval is identified as a method to overcome inter-symbol interference due to multipath propagation. Otherwise, the multiple input multiple output (MIMO) technique will be also introduced to combine with OFDM to form MIMO-OFDM systems in order to take advantage of both techniques.

5.1 A Brief Overview of the OFDM Technique

Frequency division multiplexing (FDM) has been a widely-used technique for signal transmission in frequency selective channels. In essence, FDM divides the channel bandwidth into subchannels and transmits multiple relatively low rate signals by carrying each signal on a separate carrier frequency. To facilitate separation of the signals at the receiver, the carrier frequencies are spaced sufficiently far apart so that signal spectra do not overlap. Further, in order to separate the signals with realizable filters, empty spectral regions are placed between the signals. As such, the resulting spectral efficiency of the system is quite low.

In order to solve the bandwidth efficiency problem, orthogonal frequency division multiplexing was proposed, which employs orthogonal tones to modulate the signals. Orthogonal frequency division multiplexing (OFDM) is a means to deal with the channel-induced linear distortion encountered when transmitting over a dispersive radio channel [60]. The idea of OFDM is to split the total transmit bandwidth into a number of orthogonal subcarriers in order to transmit the signals in these subcarriers in parallel. By doing that, a high rate data stream can be divided into a number of lower-rate streams because the symbol period increases with the number of subcarriers. Therefore, the effect of multipath delay decreases and the frequency selective fading channel is turned into a flat fading channel. Thus, OFDM is a solution to the frequency selectivity of fading channels. It takes advantage of a frequency-selective fading channel and turns the channel into a flat fading channel. In terms of the time-variation within a fading channel, it is assumed that the channel is fixed, or quasi-static, within the

OFDM symbol period. It is straightforward that by dividing the total bandwidth into a number of subcarriers, the subcarrier bandwidth is decreased with an increasing number of subcarriers in the frequency domain, and in the time domain, the symbol period increases. The higher the number of subcarriers, the longer the symbol period.

5.2 OFDM Principles

In a conventional serial data system, the symbols are transmitted sequentially, with the frequency spectrum of each data symbol allowed to occupy the entire available bandwidth.

A parallel data transmission system offers possibilities for alleviating many of the problems encountered with serial systems. A parallel system is one in which several sequential streams of data are transmitted simultaneously, so that at any instant many data elements are being transmitted. In such a system, the spectrum of an individual data element normally occupies only a small part of the available bandwidth.

In the OFDM scheme of Figure 5.1, the serial data stream of a traffic channel is passed through a serial-to-parallel convertor which splits the data into a number of parallel channels. The data in each channel are applied to a modulator, such that for N channels there are N modulators whose carrier frequencies are $f_0, f_1, \ldots, f_{N-1}$. The difference between adjacent channels is $\triangle_f$ and the overall bandwidth W of the N modulated carriers is $N\triangle_f$.

In the more conventional serial transmission approach, the traffic data are applied directly to the modulator, transmitting at a carrier frequency positioned at the center of the transmission band and the modulated signal occupies the entire bandwidth W. By contrast, dur-

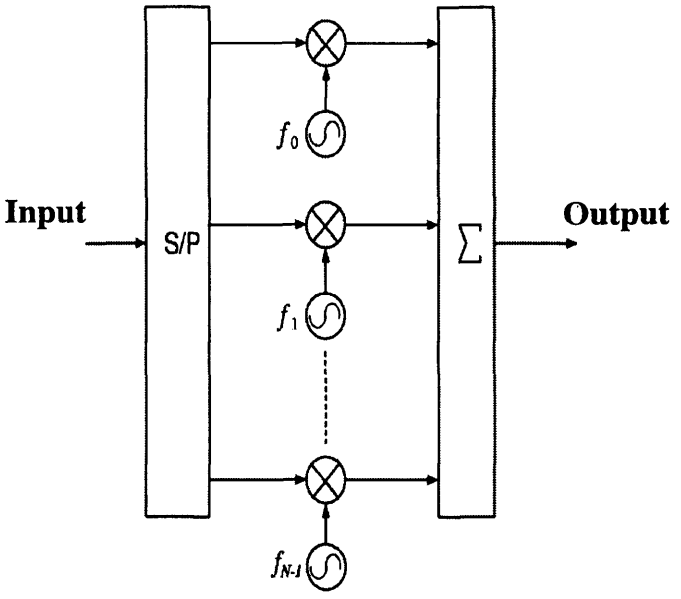

Figure 5.1. OFDM modulation block diagram.

ing a N-symbol period of the conventional system, each of the N OFDM subchannel modulators carries only one symbol, each of which has an N time longer duration.

The principal advantage of OFDM is that because the symbol period has been increased, the channel's delay spread becomes a significantly shorter fraction of a symbol period than in the serial system, potentially rendering the system less sensitive to channel-induced dispersion than the conventional serial design.

A drawback of OFDM systems is their complexity, because of the need for N modulators, receiver filters and demodulators. This is particularly relevant since, in order to achieve high resilience against fades in the channel, the block size N must be on the order of 100s, requiring a large amount of subchannel modems. This problem can be overcome by using the Fast Fourier Transform [61].

5.2.1 OFDM Employing FFT

Substantial hardware simplifications can be made with OFDM transmissions if the bank of subchannel modulators/demodulators is implemented using the computationally efficient pair of Inverse Fast Fourier Transform (IFFT) and Fast Fourier Transform (FFT) [62].

In fact, for the lth rectangular-shaped signalling interval of length T_s we can express the kth subchannel as:

$$c_{l,k} = (a_{l,k} + jb_{l,k})rect(\frac{t - lT_s}{T_s}) \tag{5.2.1}$$

where $a_{l,k}$ and $b_{l,k}$ are real numbers that depend on the input data and chosen constellation. The modulated signal corresponding to the lth signalling interval can thus be written as

$$m_l(t) = Re\{\sum_{k=0}^{N-1} c_{l,k}e^{j2\pi f_k t}\} \tag{5.2.2}$$

where $Re\{\cdot\}$ denotes real part. Writing $f_k = f_0 + k \triangle f$ and $t = nT_s$, with the orthogonality condition

$$\triangle f = 1/T_s \tag{5.2.3}$$

then the above equation becomes

$$m_l(nT_s) = Re\{e^{j2\pi f_o nT_s} \sum_{k=0}^{N-1} c_{l,k}e^{j2\pi kn}\} \tag{5.2.4}$$

in which the formula of DFT (inverse) transformation is exploited. The parameter N of OFDM systems is generally a power of two, thus a more computationally efficient IFFT algorithm can be employed.

With the orthogonality condition Equation (5.2.3) and employing rectangular pulse shaping, the spectrum of every subcarrier is a $sin(x)/x$ function, whose zeros correspond to the center of the other subcarriers, thus giving no inter-carrier interference (ICI). Successful operation depends upon perfect synchronization and no channel variation within the OFDM block. The overall spectrum is flat over the used bandwidth.

5.2.2 Bandwidth Efficiency

One important consideration about OFDM is related to bandwidth efficiency. Assume to use a serial system with one carrier, the minimum bandwidth required is $f_B = 1/T$ and the bandwidth efficiency is assumed as $\eta = 1bit/s/Hz(bps/Hz)$ because the spectrum of this pulse is represented by the sync function $sinc(\cdot)$ whose first zero is at $f_B = 1/T$. The approximate bandwidth of a $(2M + 1)$-carriers system using M sine and cosine carriers of length $(2M + 1)T$ becomes

$$B = \frac{M+1}{2M+1}\frac{1}{T} \tag{5.2.5}$$

yielding a bandwidth efficiency of

$$\eta = \frac{2M+1}{M+1} bps/Hz \tag{5.2.6}$$

For large M, the efficiency tends to $2bps/Hz$, e.g. for a value of $M = 512$, the bandwidth efficiency $\eta = 1.998bps/Hz$, which is almost two times larger than the bandwidth efficiency 1 of single carrier system. Hence multiple carrier system can achieve much more bandwidth efficiency than a single carrier system. Otherwise, in order to increase data rate, the data bits can be modulated on the subcarriers

for more efficiency.

5.2.3 Modulation

In an OFDM link, the data bits are modulated on the subcarriers by some form of phase shift keying (PSK) or quadrature amplitude modulation (QAM). To estimate the bits at the receiver, knowledge is required about the reference phase and amplitude of the constellation on each subcarrier. In general, the constellation of each subcarrier shows a random phase shift and amplitude change, caused by carrier frequency offset, timing offset and frequency-selective fading. To cope with these unknown phase and amplitude variations, two different approaches exist. The first one is coherent detection, which requires estimates of the reference amplitudes and phases to determine the best possible decision boundaries for the constellation of each subcarrier. The main issue with coherent detection is how to find the reference values without introducing too much training overhead [63]. The second approach is differential detection, which does not use absolute reference values, but only looks at the phase and/or amplitude differences between two QAM values. Differential detection can be performed both in the time domain or in the frequency domain; in the first case, each subcarrier is compared with the subcarrier of the previous OFDM symbol. In the case of differential detection in the frequency domain, each subcarrier is compared with the adjacent subcarrier within the same OFDM symbol. Both of these OFDM schemes require guard interval between the OFDM blocks to eliminate inter-symbol interference (ISI).

5.2.4 Guard Interval

One of the most important reasons to employ OFDM modulation is the efficient way it deals with multipath delay spread. By dividing the input data stream into N subcarriers, the symbol duration is made N times longer, which reduces the relative multipath delay spread, relative to the symbol time, by the same factor. To eliminate inter-symbol interference (ISI) almost completely, a guard time is introduced for each OFDM symbol. The guard interval is chosen larger than the expected delay spread, such that multipath components from one symbol cannot interfere with the next symbol. The method is best explained with reference to Figure 5.2. Every block of N samples as obtained by an IFFT is quasi-periodically extended by a length N_g, simply by repeating N_g samples of the useful information block.

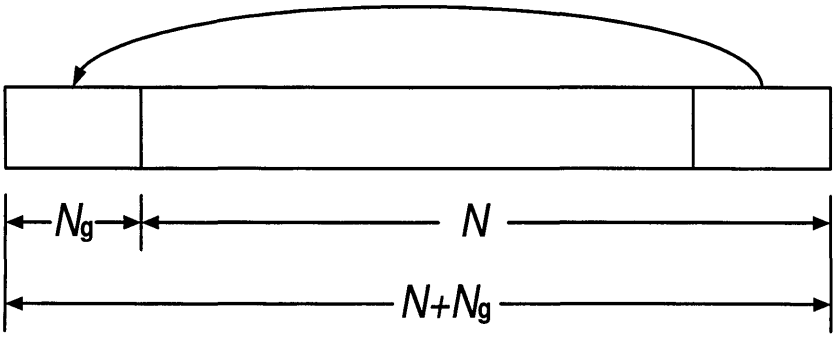

Figure 5.2. Guard interval by cyclic extension

The total sequence length becomes $N + N_g$ samples, corresponding to a duration of $T_s + T_g$. Trailing and leading samples of this extended block are corrupted by the channel transient response, hence the receiver should demodulate only the central N number of samples, essentially unaffected by the channel's transient response. It must be appreciated that cyclic extension actually wastes channel capacity as

well as transmitted power; however, if the useful information blocks are long, the extension length can be kept low relative to the useful information block length. Thus the efficiency in terms of bit rate capacity can be expressed as:

$$\eta_g = \frac{N}{N + N_g} \tag{5.2.7}$$

and can be kept as high as 97%.

Echo spread longer than the guard interval duration generates ISI. Poole [64] studied the effects of an echo longer than the guard interval duration and gives an expression for the equivalent noise floor (ENF) introduced; the results are extended to the case of multiple echoes. Benedetto et al. [65] studied the advantages of using waveform shaping in OFDM system to decrease the side lobes of the transmitted signal and to improve the performances in terms of $Eb/N0$. By their research, it is clear that taking advantage of guard interval larger than delay spread within OFDM will be useful to mitigate ISI in multipath channels.

5.3 OFDM System Model

A block diagram of a basic OFDM system is given in Figure 5.3. First of all, the source data bits are re-structured by a serial-to-parallel (S/P) converter, and then are modulated as a data block of N mapped symbols generally using a phase shift keying (PSK) or quadrature amplitude modulation (QAM) constellation. These mapped symbols are then converted into the time domain by applying an IFFT operation. After that, a cyclic prefix (CP) of length P is inserted at the head of the time

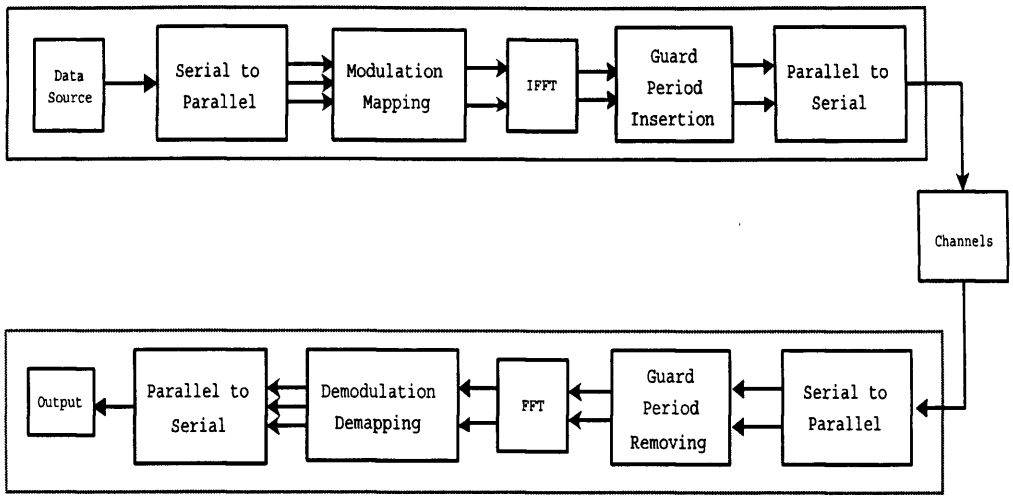

Figure 5.3. OFDM transceiver diagram consisting of the transmitter, channel and receiver.

interleaved samples; the CP length P should not be less than channel length $L(P \geq L)$ to guarantee that the ISI is completely removed.

Here the whole block of data is considered as a random-OFDM symbol. When the signal is propagating through the radio channel, the channel matrix can be represented as a circulant matrix H due to CP insertion [66], the columns of which are composed in the terms of cyclically shifted versions of a zero padded channel vector, i.e. the channel matrix is performed as a circular convolution matrix by introducing a CP in the time domain. An attractive property of a circulant matrix is that it can be exactly diagonalized by performing a DFT operation. The DFT is often simplified by using an FFT at the receiver with concomitant low computational complexity. The same process as the transmitting stage is inversely performed at the receiving end, with CP removal, FFT, demapping and parallel-to-serial converting.

As a result of the nature of the circulant matrix, only one-tap channel equalization is required for frequency domain for signal estimation,

with a static channel.

5.3.1 Signal Processing of OFDM Model in a Static Channel

As shown in Figure 5.3, assuming the transmitting signals are independent and identically distributed (i.i.d.), and that the mapped symbol set can be expressed as $\{s_k\}$, and the $\{x_n\}$ are the time samples after the IFFT operation, which can be described by the following N-point IDFT operation as,

$$x_n = \frac{1}{\sqrt{N}} \sum_{k=0}^{N-1} s_k e^{j\frac{2\pi}{N}kn} \tag{5.3.1}$$

where $n = 0, 1, 2, \ldots, N-1$ for x_n and the component of $\frac{1}{\sqrt{N}}$ represents the normalization of the FFT or IFFT operations. The vector form of the sequence $\{x_n\}$ can be written as

$$\mathbf{x} = \mathbf{F}^H \mathbf{s} \tag{5.3.2}$$

where $\mathbf{F}$ is the DFT matrix of size $N \times N$ and $\mathbf{s}$ is the transmitting mapped symbol vector in the frequency domain. After the insertion of a CP of length P, the transmitting guarded-OFDM symbol sequence $\{\tilde{x}_p\}$ can be defined as

$$\tilde{x}_p \in \{\tilde{x}_{N-P}, \tilde{x}_{N-P+1}, \ldots, \tilde{x}_{N-1}, \tilde{x}_0, \tilde{x}_1, \ldots, \tilde{x}_{N-1}\} \tag{5.3.3}$$

where $-P \leq p \leq N-1$ for $\tilde{x}_p$. As the signal is traversing an L path static channel where $L \leq P$, the received baseband signal at sample time n can be described after removing the CP as

$$r_n = \sum_{l=0}^{L-1} h(l)\tilde{x}_{n-l} + v_n \tag{5.3.4}$$

where $h(l)$ is the l-th tap of the complex channel and v_n is the complex white circular zero mean Gaussian noise at sample time n for r_n and v_n. Hence, the received signal in the time domain can be written in vector form of length N as

$$\mathbf{r} = \mathbf{Hx} + \mathbf{v} = \mathbf{HF}^H\mathbf{s} + \mathbf{v} \tag{5.3.5}$$

where $\mathbf{F}^H$ denotes IFFT operation matrix. Performing the FFT which is denoted as $\mathbf{F}$ on Equation (5.3.5), the received sample vector in the frequency domain becomes

$$\begin{aligned} \mathbf{Fr} &= \mathbf{FHx} + \mathbf{Fv} \\ &= \mathbf{FHF}^H\mathbf{s} + \mathbf{Fv} \\ &= \mathbf{H}_{df}\mathbf{s} + \mathbf{Fv} \end{aligned} \tag{5.3.6}$$

where $\mathbf{H}_{df} = \mathbf{FHF}^H$ is the inter-carrier interference (ICI) matrix, i.e. the "subcarrier coupling matrix", which is diagonal when the channel is static. Herein the signal and noise are assumed zero mean and mutually uncorrelated, thus,

$$E\{\mathbf{s}\} = E\{\mathbf{v}\} = 0$$

$$E\left\{\mathbf{ss}^H\right\} = \boldsymbol{I}$$

$$E\left\{\mathbf{sv}^H\right\} = \mathbf{0}$$

$$E\left\{\mathbf{vv}^H\right\} = \sigma^2\boldsymbol{I}$$

where σ^2 denotes noise variance. Hence, it only needs a one-step linear equalization algorithm for frequency domain operation with low com-

putational complexity, such as zero-forcing (ZF) [67] equalization and linear minimum mean squared error (L-MMSE) equalization [67]. The ZF equalization algorithm is given as

$$\hat{\mathbf{s}}_{ZF} = (\mathbf{H}_{df})^{+} \cdot \mathbf{Fr} \tag{5.3.7}$$

where $(\cdot)^{+}$ denotes the Moore-Penrose pseudo-inverse [68] and [69]. Figure 5.4 shows the performance of an uncoded OFDM system employing different types of QAM and PSK modulation, where the ZF algorithm is used for channel equalization.

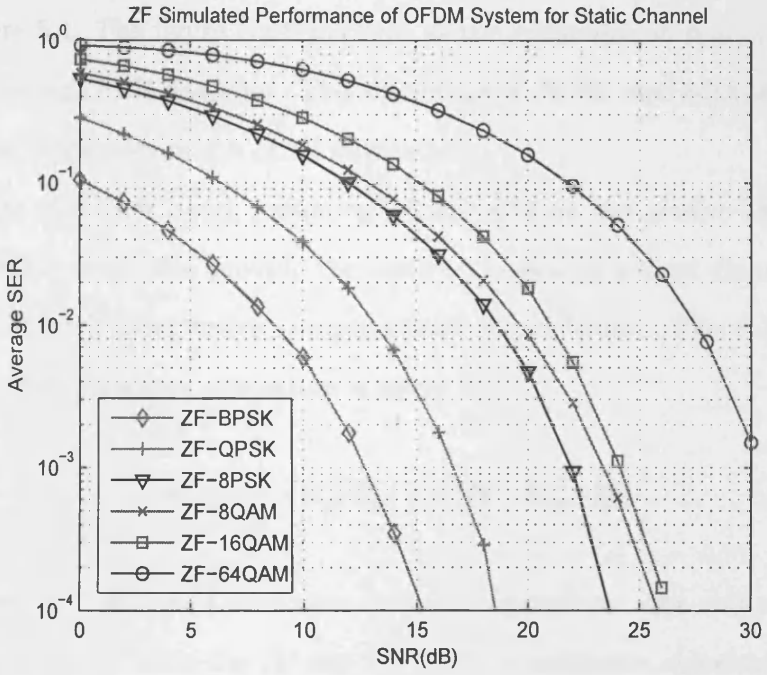

Figure 5.4. The average SER vs. SNR performance for an OFDM system: the simulation is implemented over a static channel and performs ZF channel equalization.

The OFDM system was simulated under static multipath channel conditions. The simulations were of length 200,000 symbols and were

taken from $0dB < SNR < 30dB$ for each type of modulation. Additionally, in this thesis, both BPSK and QPSK constellation are used in the simulations for average bit error rate (BER). In terms of SNR for BPSK, this is identical to Eb/N0 whereas for QPSK it is 2Eb/N0. But for relative comparisons of the proposed schemes, the relative ordering will be the same whether BPSK or QPSK is used, and therefore performance assessment is possible. The size of FFT and IFFT was chosen as 32, the length of cyclic prefix as 24 and channel length equal to 6. The results of simulation are given in terms of average transmitting symbol error rate (SER) versus signal-to-noise ratio (SNR) as shown in Figure 5.4. The figure confirms that as the constellation size increases the average SER degrades. The advantage of 8PSK over 8QAM is due to the larger separation of all its symbols.

On the other hand, assuming perfect CSI at the receive antenna, L-MMSE could also provide the ability to equalize a fixed channel for OFDM with inexpensive computational expenditure. The L-MMSE algorithm for signal estimation is given as

$$\hat{\mathbf{s}}_{MMSE} = \left(\mathbf{H}_{df}^{H}\mathbf{H}_{df} + \sigma^2 \boldsymbol{I}\right)^{-1} \mathbf{H}_{df}^{H} \cdot \mathbf{Fr} \tag{5.3.8}$$

where $(\cdot)^{-1}$ denotes the matrix inversion operation. For static channel conditions, both the ZF and L-MMSE equalization algorithm only require $\mathcal{O}(N)$ (the order of N) operations. Hence, they represent the classical motivation for the use of OFDM for multipath static channels. Figure 5.5 shows the average SER performance of an OFDM system performing L-MMSE algorithm for channel equalization for various symbol constellations is shown. The simulation of Figure 5.5 has been

initialized to be the same as the simulation of Figure 5.4. It clearly shows that for simple multipath static channels the L-MMSE and ZF can achieve essentially identically robust performance with the use of an OFDM system.

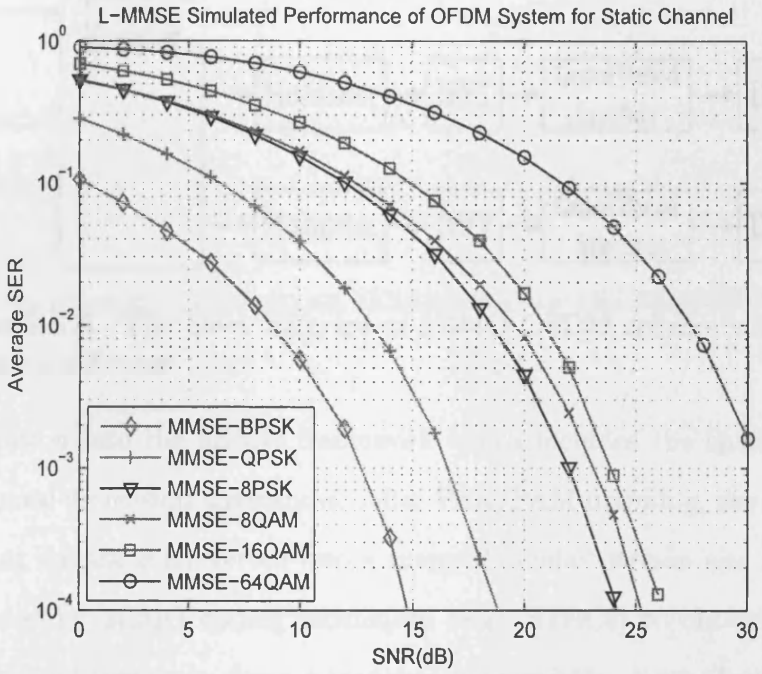

Figure 5.5. The average SER vs. SNR performance for an OFDM system: the simulation is implemented over static channels and performs L-MMSE channel equalization.

5.4 Introduction to MIMO-OFDM Systems

Figure 5.6 illustrates a block diagram of a basic baseband MIMO-OFDM system.

As discussed above, it is useful to combine OFDM with MIMO techniques to achieve further system performance improvement. Consider a MIMO-OFDM system with n_t transmit and n_r receive antennas. In this system, OFDM techniques add signal processing in the frequency

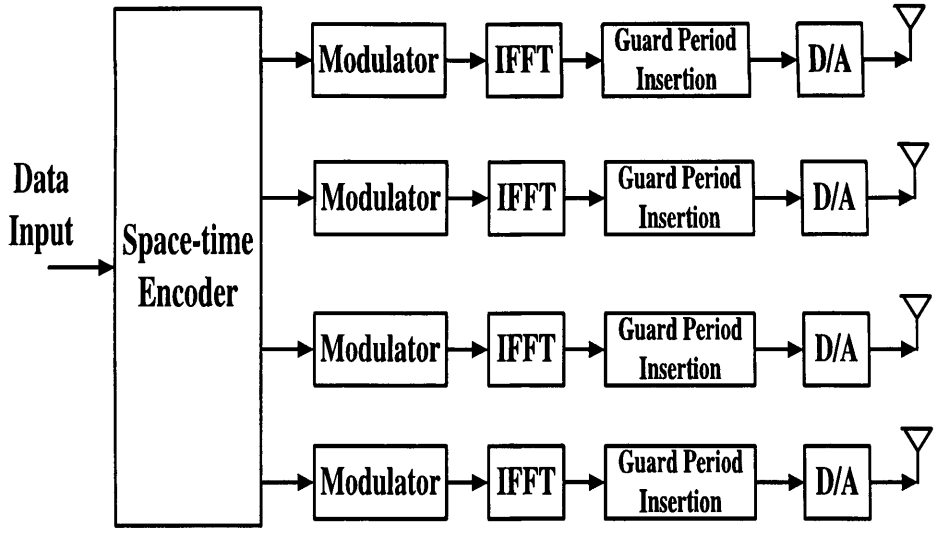

Figure 5.6. The block diagram of MIMO OFDM scheme with four transmit antennas.

dimension into the MIMO framework which includes the spatial and temporal dimension algorithms. After PSK/PAM mapping, the incoming bit stream is converted into a mapped symbol stream and is then encoded by MIMO coding techniques (e.g. STBCs) to obtain coded spatial and frequency domain transmitting symbols. A set of subcarriers can be chosen for signal transmission. Despite the fact these carriers effectively overlap in the frequency domain, all the signals can be distinguished at the receiver because of the orthogonality of the carriers. Thus, the whole system is spectrally efficient provided the problems of synchronization (frequency offset) and doubly selective channels are not severe. To provide the transmission with the appropriate frequency carriers, digital signal processing with an IFFT operation is applied at the transmitter for each branch of the output of the MIMO encoder, and then the cyclic prefix (CP) is added on to the OFDM symbols to mitigate ISI before transmission. A quasi-static channel environment for this system where each OFDM block experiences time-invariant

but different fading is assumed. The number of multipaths for every fading channel from each transmit antenna to each receive antenna is assumed the same, which is denoted by L. In such a MIMO system the maximum diversity gain is theoretically $n_t \times n_r \times L$, to exploit this temporal diversity additional coding is required at the transmitter [70]. Such coding is not considered in this thesis so only spatial diversity is exploited. Herein, perfect synchronization is assumed for all transmitters and receivers and the high peak-to-average power ratio of OFDM is ameliorated by perfect linear power amplifiers. Hence, at the receive end, the CP is removed and the complementary FFT is performed for each receive branch. Figure 5.7 shows the block diagram of an MIMO OFDM receiver with one receive antenna. Then, at

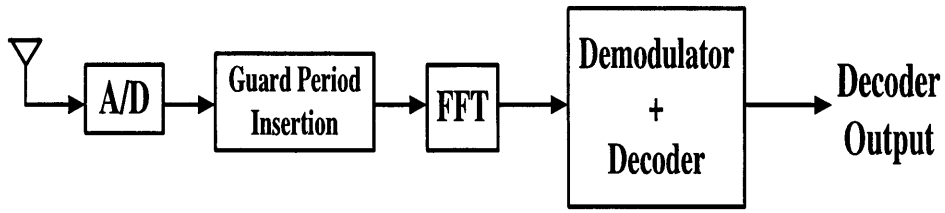

Figure 5.7. The block diagram of an MIMO OFDM receiver with one receive antenna.

this point, the MIMO decoder/detector must be applied to recover the frequency domain data stream, and then demapping/deinterleaving are implemented to obtain binary output data. It is typically assumed that perfect knowledge of channel state information (CSI) is available at the receiver. In principle, MIMO-OFDM can be considered as a parallel set of SISO-OFDM systems. Thus, the received signal across all the receive antennas at discrete frequency tone k after removing the CP

and taking the FFT can be written as

$$\mathbf{r}(k) = \mathbf{H}_f(k)\mathbf{x}(k) + \mathbf{v}_f(k) \tag{5.4.1}$$

where $\mathbf{r}(k) = [r_1(k), r_2(k), \ldots, r_{n_r}(k)]^T$, and $k = 0, 1, \ldots, N-1$. The vector $\mathbf{x}(k) = [x_1(k), x_2(k), \ldots, x_{n_t}(k)]^T$ is the frequency domain transmitting data symbol at the *k-th* subcarrier across the n_t'th transmit antenna, $n_t' = 1, 2, \ldots, n_t$; and $\mathbf{v}_f(k) = [\mathbf{v}_{f1}(k), \mathbf{v}_{f2}(k), \ldots, \mathbf{v}_{fn_r'}(k), \ldots, \mathbf{v}_{fn_r}(k)]$ denotes the frequency domain representation for the additive complex white Gaussian noise vector $\mathbf{v}$ at the *k-th* subcarrier. $\mathbf{H}_f(k)$ is the frequency domain channel matrix of the *k-th* tone written as

$$\mathbf{H}_f(k) = \begin{pmatrix} H_{11}(k) & H_{12}(k) & \cdots & H_{1n_t'}(k) & \cdots & H_{1n_t}(k) \\ H_{21}(k) & H_{22}(k) & \cdots & H_{2n_t'}(k) & \cdots & H_{2n_t}(k) \\ \vdots & \vdots & \ddots & \vdots & \ddots & \vdots \\ H_{m_r'1}(k) & H_{n_r'2}(k) & \cdots & H_{n_r'n_t'}(k) & \cdots & H_{n_r'n_t}(k) \\ \vdots & \vdots & \ddots & \vdots & \ddots & \vdots \cdots \\ H_{n_r1}(k) & H_{n_r2}(k) & \cdots & H_{n_rn_t'}(k) & \cdots & H_{n_rn_t}(k) \end{pmatrix} \tag{5.4.2}$$

where $H_{n_r'n_t'}(k) = \sum_{l=0}^{L-1} h_{n_r'n_t'}(l) e^{-\frac{2\pi j}{N} lk}$ and $h_{n_r'n_t'}(l)$ is the *l-th* tap of the fading channel from the n_t'th transmit antenna to the n_r'th receive antenna. From Equation (5.4.1), assuming the CP is greater than the channel length L, there is no ISI during transmission.

5.5 Capacity of MIMO-OFDM Systems

From the discussion introduced in the previous section, it is known that in OFDM-based systems statistically independent data streams are transmitted from different antennas and different tones, and the to-

tal available power is allocated uniformly across all space-frequency subchannels. Hence, in OFDM-based systems, an (n_t, n_r) MIMO frequency-selective channel can be divided into a number of narrowband MIMO subchannels for which the frequency response of the *k-th* subchannel is represented as $\mathbf{H}_f(k)$ in Equation (5.4.2). Assuming the CSI is not known at the transmitter, it has been shown in [28] and [26] that the open-loop capacity for MIMO OFDM over a frequency-selective wideband channel which is defined as bps/Hz can be obtained by averaging over the capacity of these narrowband MIMO subchannels. From the discussion in Chapter 3, the capacity of a narrowband MIMO channel of the kth tone is defined as

$$C = \log_2 \det \left[\boldsymbol{I}_{n_r} + \left(\frac{SNR}{n_t} \right) \mathbf{H}_f(k) \mathbf{H}_f^H(k) \right] \tag{5.5.1}$$

Herein, the frequency band is divided into a discrete number of N frequency-flat subchannels, where N denotes the number of subcarriers carried by an OFDM symbol. Then the open-loop system capacity of the (n_t, n_r) MIMO OFDM channel is given by

$$C = \frac{1}{N} \sum_{k=0}^{N-1} \log_2 \det \left[\boldsymbol{I}_{n_r} + \left(\frac{SNR}{n_t} \right) \mathbf{H}_f(k) \mathbf{H}_f^H(k) \right] \tag{5.5.2}$$

From Equation (5.5.2), the open-loop capacity of the (n_t, n_r) MIMO OFDM channel is presented as an average channel capacity determined by realizations of the subchannels for all subcarriers. Figure 5.8 illustrates the average channel capacity for different MIMO-OFDM configurations.

In this figure, the average capacity is determined by independent realizations of MIMO subchannels $\mathbf{H}_f(k)$ for 1024 subcarriers, where

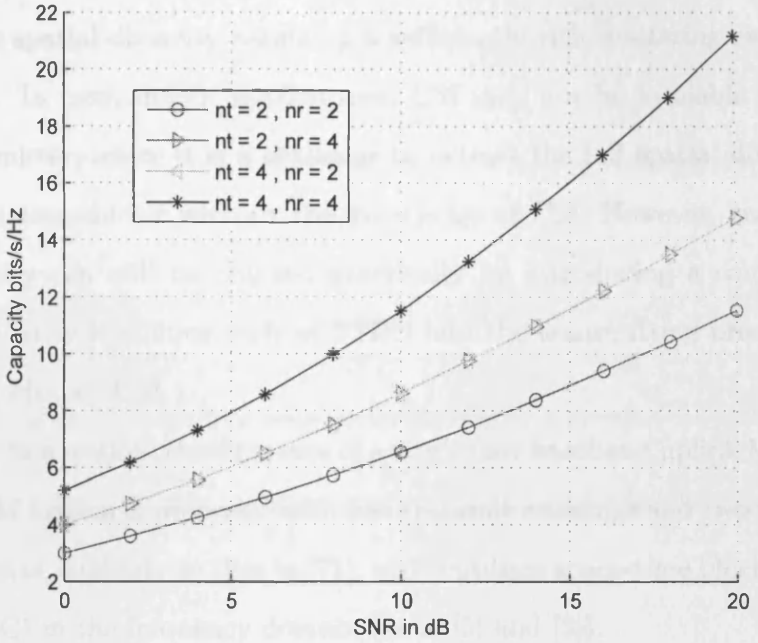

Figure 5.8. Average channel capacity for different MIMO-OFDM configurations.

the elements of $\mathbf{H}_f(k)$ are assumed to be independent and identically distributed (i.i.d.) circularly-symmetric complex Gaussian distributed. The capacity increasing with $min(n_t, n_r)$ can be observed in this figure. Therefore, in open-loop systems, it is observed that the theoretical capacity of the $(2, 4)$ MIMO frequency-selective channels is identical to the capacity of the $(4, 2)$ channels.

5.6 Space-Time Block Coded MIMO-OFDM Transceiver Design with Two Antennas

To increase the diversity gain and/or to enhance the system capacity, in practice, OFDM may be used in combination with antenna arrays at the transmitter and receiver to form a MIMO-OFDM system, which im-

proves the performance of communication in terms of taking advantage of the spatial diversity assuming a sufficiently rich scattering environment. In most mobile applications, CSI may not be available at the transmitter, hence it is a challenge to extract the full spatial diversity at the transmitter without the knowledge of CSI. However, transmit diversity can still be realized practically by introducing a controlled redundancy technique such as STBC into the transmitting processing stage without CSI.

In this section, the structure of a single user baseband uplink MIMO-OFDM system is proposed with two transmit antennas and two receive antennas, similarly to that in [71], which utilizes space-time block codes (STBC) in the frequency domain (as in [5] and [3]).

From the information source for the transmitter, it is assumed that a serial-to-parallel convertor collects a set of N bit BPSK symbols $\mathbf{x} = [x(0), \cdots, x(N-1)]^T$ to form a frequency domain signal symbol vector, BPSK is assumed but the results would apply equally for complex constellations such as QPSK, and in practice, an explicit OFDM modulating operation will be performed for each sub-channel. To avoid inter-symbol interference (ISI), a sufficiently long cyclic prefix (CP) must be chosen, i.e. the guard interval P should satisfy $P > L$, where L is the length of impulse response of each transmit-receive antenna sub-channel, which is the same for each sub-channel. From the previous section, the N time domain received symbols corresponding to the receive antenna can be obtained by an OFDM algorithm in terms of vector form as

$$\mathbf{r}_n = \mathbf{H}_c \mathbf{F}^H \mathbf{x} + \mathbf{v} \tag{5.6.1}$$

At each receive antenna, the samples corresponding to the cyclic prefix are first removed and then taking the FFT operation of received signal from Equation (5.6.1) yields

$$\mathbf{r} = \mathbf{F}\mathbf{r}_n = \mathbf{F}\mathbf{H}_c\mathbf{F}^H\mathbf{x}+\mathbf{F}\mathbf{v} = \mathbf{H}\mathbf{x} + \mathbf{v}_f \tag{5.6.2}$$

where $\mathbf{H}_c$ is the time-domain circular convolutional channel matrix of size $N \times N$, which has been described in [67]. Moreover, $\mathbf{F}$ denotes the $N \times N$ DFT matrix and therefore $\mathbf{F}^H$ denotes the IDFT matrix. $\mathbf{H}$ is defined as the *subcarrier coupling matrix* (diagonal for a static channel), and $\mathbf{v}_f$ is the frequency response of the additive complex Gaussian noise vector.

In the proposed MIMO-OFDM system, the STBC scheme which is similar to the scheme in [3] is adapted for the transmitting terminal. The two consecutive block signal vectors from the data source can be represented as $\mathbf{x}_1 = [x_1(0), \cdots, x_1(N-1)]^T$ and $\mathbf{x}_2 = [x_2(0), \cdots, x_2(N-1)]^T$. Herein, it is assumed that the time domain channel responses are constant during two consecutive signal block intervals, i.e. quasi-static. Here, $[\mathbf{H}_{qj}]$ is defined as *subcarrier coupling matrix* of size $N \times N$, experienced by the signal transmitted from the *q-th* transmit antenna to the *j-th* receive antenna, i.e. the diagonal matrix formed by the channel impulse response in the frequency domain, (as in [72]). The estimation of the time invariant channels is discussed in [73], and this issue is not addressed in this thesis. The coded signal transmitted from the transmit terminal during two block intervals in the frequency domain can be represented in matrix form as follows,

$$\begin{bmatrix} \mathbf{F}^H\mathbf{x}_1 & \mathbf{F}^H\mathbf{x}_2 \\ -\mathbf{F}^H\mathbf{x}_2^* & \mathbf{F}^H\mathbf{x}_1^* \end{bmatrix} \tag{5.6.3}$$

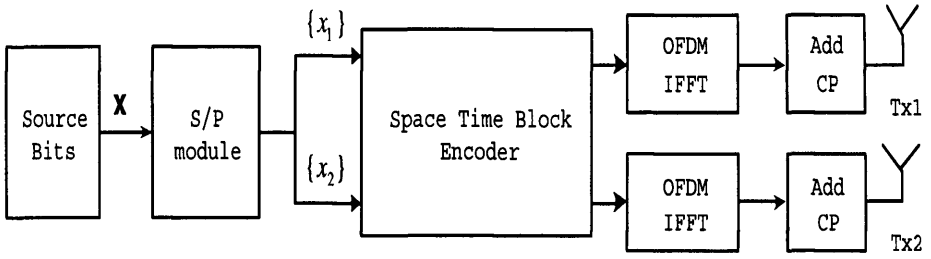

Figure 5.9. STBC MIMO-OFDM baseband transmitter diagram consisting of two transmit antennas.

The proposed STBC MIMO-OFDM transmitter is equipped with two transmit antennas for exploiting the above STBC scheme for wireless data transmission, which is shown in Figure 5.9, (as in [71] and [72]). In this transmitter, the source mapped information symbol stream is converted into two consecutive signal blocks of size N, then both signal blocks are encoded by an STBC encoder and each branch of the encoder output needs to be modulated by an OFDM module including IFFT and CP addition, and then these signals are sent from two transmit antennas in two consecutive OFDM time intervals. Two receive antennas are employed at the receiver for collecting the receive signals. If the output of the OFDM demodulator is considered at the first receive antenna after cyclic prefix removal, the frequency domain receive signal vectors during two sequential OFDM time-slots a and b for the first receive antenna could be obtained as in Equations (5.6.4) and (5.6.5), respectively.

$$\mathbf{r}_{1a} = \mathbf{H}_{11}\mathbf{x}_1 + \mathbf{H}_{21}\mathbf{x}_2 + \mathbf{v}_{f1a} \tag{5.6.4}$$

$$\mathbf{r}_{1b}^{*} = \mathbf{H}_{21}^{*}\mathbf{x}_1 - \mathbf{H}_{11}^{*}\mathbf{x}_2 + \mathbf{v}_{f1b}^{*} \tag{5.6.5}$$

For simplicity of notation, define signal vector $\mathbf{x} = \begin{bmatrix} \mathbf{x}_1 \\ \mathbf{x}_2 \end{bmatrix}$, received vector $\mathbf{r}_1 = \begin{bmatrix} \mathbf{r}_{1a} \\ \mathbf{r}_{1b}^{*} \end{bmatrix}$, and $\mathbf{v}_{f1} = \begin{bmatrix} \mathbf{v}_{f1a} \\ \mathbf{v}_{f1b}^{*} \end{bmatrix}$ which is the frequency response of the noise vector for the signal received by the first receive antenna. Therefore, write Equations (5.6.4) and (5.6.5) in a matrix form as

$$\mathbf{r}_1 = \tilde{\mathbf{H}}_1\mathbf{x} + \mathbf{v}_{f1} \tag{5.6.6}$$

The equivalent channel matrix of the transmitting data pipe from transmitter to the first receive antennas could be represented as

$$\tilde{\mathbf{H}}_1 = \begin{bmatrix} \mathbf{H}_{11} & \mathbf{H}_{21} \\ \mathbf{H}_{21}^{*} & -\mathbf{H}_{11}^{*} \end{bmatrix}$$

In a similar method, the frequency domain receive signal vectors could also be arranged during the two sequential OFDM time-slots a and b for the second receive antenna as in Equations (5.6.8) and (5.6.9), respectively.

$$\mathbf{r}_1 = \tilde{\mathbf{H}}_1\mathbf{x} + \mathbf{v}_{f1} \tag{5.6.7}$$

$$\mathbf{r}_{2a} = \mathbf{H}_{12}\mathbf{x}_1 + \mathbf{H}_{22}\mathbf{x}_2 + \mathbf{v}_{f2a} \tag{5.6.8}$$

$$\mathbf{r}_{2b}^{*} = \mathbf{H}_{22}^{*}\mathbf{x}_1 - \mathbf{H}_{12}^{*}\mathbf{x}_2 + \mathbf{v}_{f2b}^{*} \tag{5.6.9}$$

Equations (5.6.8) and (5.6.9) can simply be written in a matrix form as

$$\mathbf{r}_2 = \tilde{\mathbf{H}}_2\mathbf{x} + \mathbf{v}_{f2} \tag{5.6.10}$$

where the received vector for the second receive antenna $\mathbf{r}_2 = \begin{bmatrix} \mathbf{r}_{2a} \\ \mathbf{r}^*_{2b} \end{bmatrix}$, and $\mathbf{v}_{f2} = \begin{bmatrix} \mathbf{v}_{f2a} \\ \mathbf{v}^*_{f2b} \end{bmatrix}$, and the equivalent channel matrix $\tilde{\mathbf{H}}_2$ to the second receive antennas could be represented as

$$\tilde{\mathbf{H}}_2 = \begin{bmatrix} \mathbf{H}_{12} & \mathbf{H}_{22} \\ \mathbf{H}^*_{22} & -\mathbf{H}^*_{12} \end{bmatrix}$$

Finally, the overall receive vector can be arranged by combining Equations (5.6.7) and (5.6.10) as

$$\mathbf{r} = \begin{bmatrix} \mathbf{r}_1 \\ \mathbf{r}_2 \end{bmatrix} = \begin{bmatrix} \tilde{\mathbf{H}}_1 \\ \tilde{\mathbf{H}}_2 \end{bmatrix} .\mathbf{x} + \begin{bmatrix} \mathbf{v}_{f1} \\ \mathbf{v}_{f2} \end{bmatrix} = \tilde{\mathbf{H}}.\mathbf{x} + \mathbf{v}_f \qquad (5.6.11)$$

Let $N_b = 2N$, so that $\tilde{\mathbf{H}}$ is the overall equivalent channel matrix between transmitter and receiver of size $N_b \times N_b$ and $\mathbf{v}_f$ denotes the whole channel equivalent noise vector of size $N_b \times 1$ with variance σ_n^2.

5.6.1 Simulations

In this section, some simulations are implemented for the proposed schemes. For all simulations, in order to illustrate the performance of the proposed symbol detection algorithm, a STBC MIMO-OFDM system case with a single user terminal which is equipped with two transmit and one receive antennas is exploited.

A 1MHz transmitting data rate is assumed, i.e. the OFDM symbol duration is $T_s = 1\mu s$, which is divided into 128 sub-carriers by OFDM operation, and exploiting a BPSK signal constellation in this work and

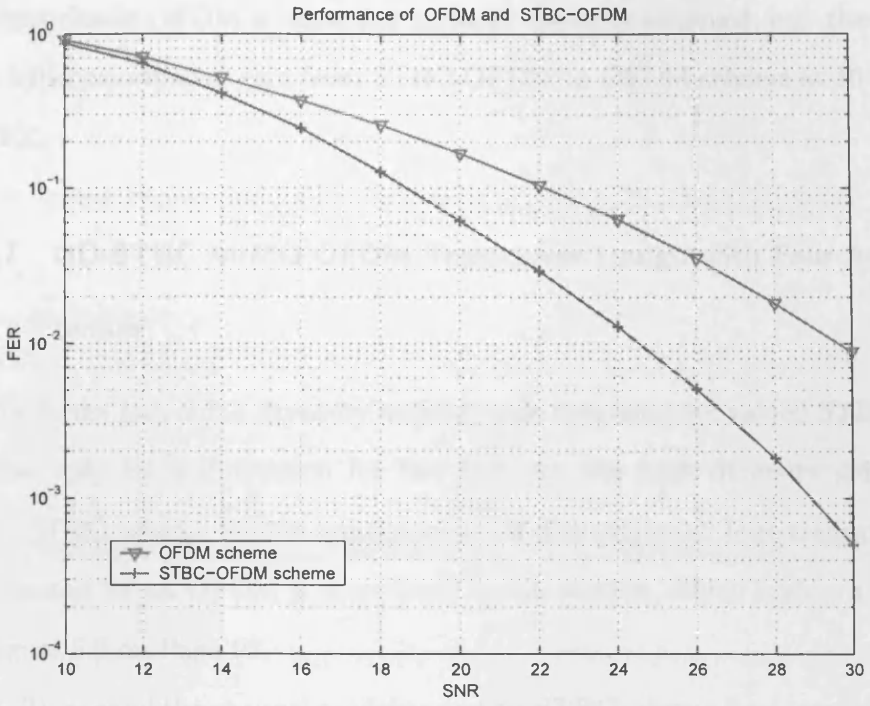

Figure 5.10. FER performance for an OFDM based STBC scheme with two transmit antennas and one receive antenna.

each serial data stream contains 256 symbols, which is coded into two OFDM blocks by a STBC encoding operation. Therefore, the user terminal could transmit two data blocks in parallel from two transmit antennas, from which the transmitting stream of $N_b = 256$ bits of information symbols are estimated in one detecting iteration.

For OFDM modulation, the length of the CP is kept equal to the order of the channel and the number of carriers is equal to the number of symbols in an OFDM block. Perfect knowledge of the channel state is available at the receiver at any time. However, there is no need for the knowledge of CSI at the transmitter. The simulation result of Figure 5.10 presents the frame error rate (FER) performance comparison between single transmit antenna OFDM scheme and two transmit antenna STBC-OFDM scheme. It is clear that STBC-OFDM outper-

forms classic OFDM scheme due to more diversity achieved, e.g. there is 5dB performance gain from STBC-OFDM to OFDM scheme at 10^{-2} FER.

5.7 QO-STBC MIMO-OFDM Transceiver Design with Four Antennas

Due to the fact of full diversity and full code rate complex valued STBC exist only for a dimension for two [23], for the high diversity gain, the STBC scheme for the enhancement of diversity with four transmit antennas for an OFDM is considered in this section, which is shown in Figure 5.6 on Page 93.

To expand the channel model to an QO-STBC scheme for 4 transmit antennas, the 4×4 code design with symbol rate 1 is used to construct the symbol matrix:

$$\mathbf{QO} = \begin{bmatrix} \mathbf{s}_1 & \mathbf{s}_2 & \mathbf{s}_3 & \mathbf{s}_4 \\ -\mathbf{s}_2^* & \mathbf{s}_1^* & -\mathbf{s}_4^* & \mathbf{s}_3^* \\ -\mathbf{s}_3^* & -\mathbf{s}_4^* & \mathbf{s}_1^* & \mathbf{s}_2^* \\ \mathbf{s}_4 & -\mathbf{s}_3 & -\mathbf{s}_2 & \mathbf{s}_1 \end{bmatrix} \tag{5.7.1}$$

where $\mathbf{s} = [s(0), \ldots, s(N-1)]^T$, is an N length size block of transmit symbols, and $(\cdot)^T$, $(\cdot)^*$ denote respectively transpose and conjugate operations. The output of the space-time encoder is then modulated by an IFFT into an OFDM symbol sequence, then transmitted through a frequency selective channel $h_{1,j}, h_{2,j}, h_{3,j}, h_{4,j}$ with channel taps q for the corresponding transmit antenna and *j-th* receiver antenna pair. Assume $\mathbf{H}_{1,j}(k), \mathbf{H}_{2,j}(k), \mathbf{H}_{3,j}(k), \mathbf{H}_{4,j}(k)$ denote the channel frequency re-

sponses of the *k-th* tone, related to the channel frequency responses of the *k-th* tone, related to the channel from the four transmit antennas in each terminal to the *j-th* receive antenna. It is assumed that all the channels have the same power-delay profile. The channel frequency response at the *k-th* frequency subcarrier for a MIMO-OFDM system can be expressed as

$$\mathbf{H}_{i,j}(k) = \sum_{l=0}^{L-1} h_{ij}(l) e^{-j2\pi l \frac{n}{N}} \tag{5.7.2}$$

where $k = 0, 1, \ldots, N-1$ and $\mathbf{H}_{i,j}(k)$ is the *ij-th* scalar element of the channel matrix quantity $\mathbf{H}$ which is defined as the *l-th* tap channel impulse response with zero mean complex Gaussian random variable with variance of the *k-th* tone signal picked up by each receive antenna during the time slots $1, 2, 3, 4$ can be written as:

$$\begin{bmatrix} \mathbf{r}_{1,j}(k) \\ \mathbf{r}_{2,j}(k) \\ \mathbf{r}_{3,j}(k) \\ \mathbf{r}_{4,j}(k) \end{bmatrix} = \begin{bmatrix} \mathbf{H}_{1,j}(k)\mathbf{s}_1(k) + \mathbf{H}_{2,j}(k)\mathbf{s}_2(k) + \mathbf{H}_{3,j}\mathbf{s}_3(k) + \mathbf{H}_{4,j}(k)\mathbf{s}_4(k) \\ \mathbf{H}_{2,j}(k)\mathbf{s}_1^*(k) - \mathbf{H}_{1,j}(k)\mathbf{s}_2^*(k) + \mathbf{H}_{4,j}\mathbf{s}_3^*(k) - \mathbf{H}_{3,j}(k)\mathbf{s}_4^*(k) \\ \mathbf{H}_{3,j}(k)\mathbf{s}_1^*(k) + \mathbf{H}_{4,j}(k)\mathbf{s}_2^*(k) - \mathbf{H}_{1,j}\mathbf{s}_3^*(k) - \mathbf{H}_{2,j}(k)\mathbf{s}_4^*(k) \\ \mathbf{H}_{4,j}(k)\mathbf{s}_1(k) - \mathbf{H}_{3,j}(k)\mathbf{s}_2(k) - \mathbf{H}_{2,j}\mathbf{s}_3(k) + \mathbf{H}_{1,j}(k)\mathbf{s}_4(k) \end{bmatrix} + \begin{bmatrix} \mathbf{v}_{1,j}(k) \\ \mathbf{v}_{2,j}(k) \\ \mathbf{v}_{3,j}(k) \\ \mathbf{v}_{4,j}(k) \end{bmatrix} \tag{5.7.3}$$

where $\mathbf{v}(k)$ denotes the frequency domain representation of the noise at the *k-th* tone. For simplicity of notation, define $\mathbf{r}_j(k) = [\mathbf{r}_{1,j} \quad \mathbf{r}_{2,j}^* \quad \mathbf{r}_{3,j}^* \quad \mathbf{r}_{4,j}]^T$, $\mathbf{s}(k) = [\mathbf{s}_1(k) \quad \mathbf{s}_2(k) \quad \mathbf{s}_3(k) \quad \mathbf{s}_4(k)]^T$, $\mathbf{v}_j(k) = [\mathbf{v}_{1,j}^* \quad \mathbf{v}_{2,j}^* \quad \mathbf{v}_{3,j}^* \quad \mathbf{v}_{4,j}^*]^T$,

and

$$\tilde{\mathbf{H}}_j(k) = \begin{bmatrix} \mathbf{H}_{1,j}(k) & \mathbf{H}_{2,j}(k) & \mathbf{H}_{3,j}(k) & \mathbf{H}_{4,j}(k) \\ \mathbf{H}_{2,j}(k)^* & -\mathbf{H}_{1,j}(k)^* & \mathbf{H}^*_{4,j}(k) & -\mathbf{H}_{3,j}(k)^* \\ \mathbf{H}_{3,j}(k)^* & \mathbf{H}_{4,j}(k)^* & -\mathbf{H}^*_{1,j}(k) & -\mathbf{H}_{2,j}(k)^* \\ \mathbf{H}_{4,j}(k) & -\mathbf{H}_{3,j}(k) & -\mathbf{H}_{2,j}(k) & \mathbf{H}_{1,j}(k) \end{bmatrix} \tag{5.7.4}$$

The Equation (5.6.13) can be rewrite as:

$$\mathbf{r}_j(k) = \tilde{\mathbf{H}}_j(k)\mathbf{s}(k) + \mathbf{v}_j(k) \tag{5.7.5}$$

Assuming only one receive antenna for simplicity, the matched filtering is performed by pre-multiplying by $\tilde{\mathbf{H}}$ in each subcarrier, as follows:

$$\mathbf{R}_{mf} = \tilde{\mathbf{H}}^H(k)\tilde{\mathbf{H}}(k)\mathbf{s}(k) + \tilde{\mathbf{H}}^H(k)\mathbf{v}(k) = \Delta\mathbf{s} + \mathbf{n} \tag{5.7.6}$$

where

$$\Delta = \tilde{\mathbf{H}}^H(k)\tilde{\mathbf{H}}(k) = \begin{bmatrix} \lambda & 0 & 0 & \partial \\ 0 & \lambda & -\partial & 0 \\ 0 & -\partial & \lambda & 0 \\ \partial & 0 & 0 & \lambda \end{bmatrix} \tag{5.7.7}$$

After match filtering at the receiver some non-zero off diagonal terms exist which reduce the diversity gain of the code. Where $\lambda = \sum_{l=0}^{L-1}\sum_{i=0}^{4}|H_{i,l}|^2(k)$, and $\partial = 2\sum_{l=0}^{L-1} Re\{H_{1,l}(k)^* H_{4,l}(k) - H_{2,l}(k)^* H_{3,l}(k)\}$, Re denotes the real part operator.

5.7.1 Transmission with Channel Feedback

When the transmitter does not have any knowledge of the channel state information, the signal transmission will be independent of the channel

information. However, if either full or partial channel information is available at the transmitter, both diversity gain can be obtained by exploiting the channel state information with low complexity. It has been proved that the capacity and system performance of a MIMO system can be substantially improved if partial channel state information is available at the transmitter.

If the first and second terms in the brackets of Equation (5.7.5) are multiplied by a phasor, it is possible to make it equalized easily.

Assuming that the signals from the third and fourth antennas are rotated by θ and ϕ respectively. Which is equivalent to multiplying the first and second term in Equation (5.7.5) by $e^{j\theta}$ and $e^{j\phi}$ respectively,

$$\alpha = |Re\{H_{1,l}(k)^* H_{4,l}(k)e^{j\theta} - H_{2,l}(k)^* H_{3,l}(k)e^{j\phi}\}| \tag{5.7.8}$$

Let $\kappa = H_{1,l}(k)^* H_{4,l}(k)$ and $\beta = H_{2,l}(k)^* H_{3,l}(k)$, then

$$\alpha = |\kappa| cos(\theta + \angle\kappa) - |\beta| cos(\phi + \angle\beta)) \tag{5.7.9}$$

In here, $|\cdot|$ and $\angle$ denote the absolute value and the angle (arctan) operators, respectively.

Since $\alpha = 0$ has infinite solutions for θ and ϕ. The solutions are

$$\theta = arccos(\frac{|\beta|}{|\kappa|} cos(\phi + \angle\beta)) - \angle\kappa \tag{5.7.10}$$

provided that

$$\phi \in \begin{cases} [0, 2\pi), & \text{when } |\beta| < |\kappa| \\ [\pi\text{-}\xi\text{-}\angle\beta,\ \xi\text{-}\angle\beta] & \\ \bigcup[2\pi - \xi - \angle\beta, \pi + \xi - \angle\beta], & \text{otherwise} \end{cases} \tag{5.7.11}$$

where $\xi = \frac{|\kappa|}{|\beta|}$.

5.7.2 Simulation

In this section, the error performance of the proposed schemes in quasi-static frequency selective channels is evaluated. The fading is constant within a frame and changes independently from one frame to another, the multipath channels have three taps for each transmit-receive antenna pair. The perfect knowledge of the channel state information is assumed at the receiver at any time. During the simulation, the transmitter power of each user is assumed the same. For the closed-loop system, the average frame error rate (FER) against SNR is simulated using QPSK symbols for all subcarriers, where each user data stream contains 256 symbols. Each frame consists of 100000 symbols in the simulation. The system parameters where adopted in this simulation are the following: the signal bandwidth is $1MHz$, which is divided into 128 subcarrier by OFDM operation. In order to make the tones orthogonal to each other, IFFT operation is $128us$, the guard interval is set to 22.

Figure 5.11 shows the performance comparison for classic OFDM, two transmit antenna O-STBC OFDM and four transmit antenna and one receive antenna closed loop QO-STBC OFDM schemes over quasi-static channels. At 10^{-3} FER level, the four transmit antenna scheme can obtain the best performance due to most diversity achieved. The performance improvement of closed loop QO-STBC OFDM scheme compared to O-STBC OFDM scheme is approximately $9dB$ performance gain, and the proposed closed loop QO-STBC scheme can get increase near $13dB$ improvement compare which is adopted Orthog-

onal STBC-OFDM system at 10^{-2} FER level. Hence, to use single phase feedback method appears to be able to obtain good enough error performance.

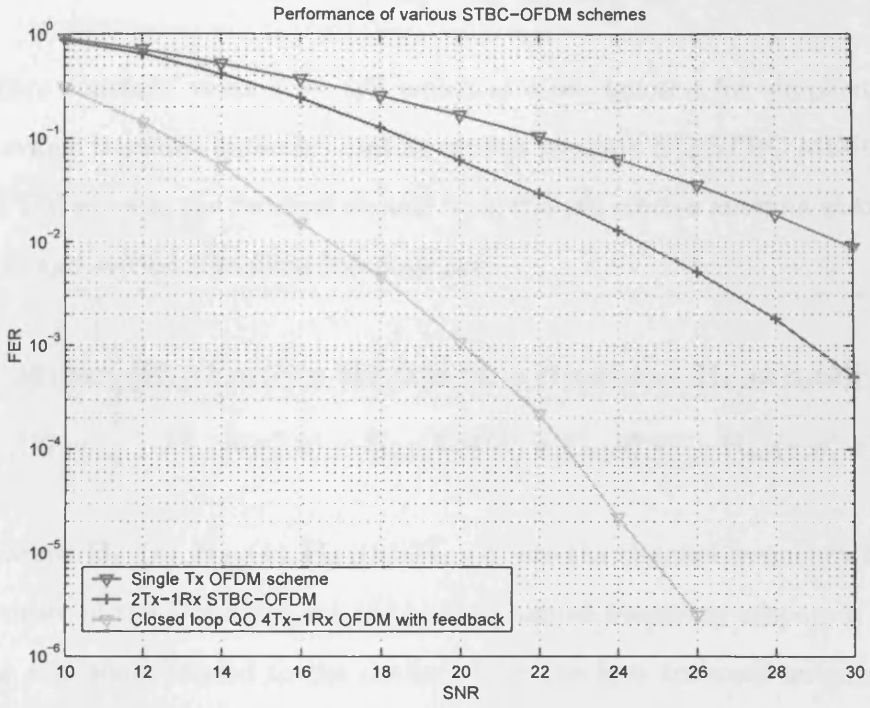

Figure 5.11. FER performance comparison between MIMO-OFDM system, O-STBC scheme and close-loop QO-STBC scheme with feedback.

5.8 EO-STBC MIMO-OFDM Transceiver Design with Four Antennas

The proposed MIMO-OFDM scheme can also be used combined with a building block to design the EO-STBC MIMO-OFDM system with four antennas and full rate. The scheme can achieve a full transmit

diversity with simple detection, given by

$$\mathbf{EO} = \zeta \begin{bmatrix} \mathbf{s}_1 & \mathbf{s}_1 & \mathbf{s}_2 & \mathbf{s}_2 \\ -\mathbf{s}_2^* & -\mathbf{s}_2^* & \mathbf{s}_1^* & \mathbf{s}_1^* \end{bmatrix} \tag{5.8.1}$$

where constant value $\zeta = 1/2$ which is often ignored for simplicity. For four transmit antennas and m receive antenna EO-STBC MIMO-OFDM system, the received signals from the jth receive antenna at the first and second signalling intervals are

$$\begin{aligned} \mathbf{r}_{1,j}(k) &= \frac{1}{2}[\mathbf{H}_{1,j}(k)\mathbf{s}_1(k) + \mathbf{H}_{2,j}(k)\mathbf{s}_1(k) + \mathbf{H}_{3,j}\mathbf{s}_2(k) + \mathbf{H}_{4,j}(k)\mathbf{s}_2(k)] + \mathbf{v}_1(k) \\ \mathbf{r}_{2,j}(k) &= \frac{1}{2}[-\mathbf{H}_{1,j}(k)\mathbf{s}_2^*(k) - \mathbf{H}_{2,j}(k)\mathbf{s}_2^*(k) + \mathbf{H}_{3,j}\mathbf{s}_1^*(k) + \mathbf{H}_{4,j}(k)\mathbf{s}_1^*(k)] + \mathbf{v}_2(k) \end{aligned}$$

Assume $\mathbf{H}_{1,j}(k), \mathbf{H}_{2,j}(k), \mathbf{H}_{3,j}(k), \mathbf{H}_{4,j}(k)$ are the channel frequency responses of the *k-th* tone, related to the channel frequency responses of the *k-th* tone, related to the channel from the four transmit antennas in each terminal to the *j-th* receive antenna. Herein, above equation can be written as the matrix notation as

$$\mathbf{r} = \begin{bmatrix} \mathbf{r}_{1,j}(k) \\ \mathbf{r}_{2,j}^*(k) \end{bmatrix} = \begin{bmatrix} \mathbf{H}_{1,j}(k) + \mathbf{H}_{2,j}(k) & \mathbf{H}_{3,j}(k) + \mathbf{H}_{4,j}(k) \\ \mathbf{H}_{3,j}^*(k) + \mathbf{H}_{4,j}^*(k) & -\mathbf{H}_{1,j}^*(k) - \mathbf{H}_{2,j}^*(k) \end{bmatrix} \begin{bmatrix} \mathbf{s}_1(k) \\ \mathbf{s}_2(k) \end{bmatrix} + \begin{bmatrix} \mathbf{v}_{1,j}(k) \\ \mathbf{v}_{2,j}^*(k) \end{bmatrix} \tag{5.8.2}$$

For simplicity, Equation (5.8.2) can be written as

$$\mathbf{r}_j(k) = \tilde{\mathbf{H}}_j(k)\mathbf{s}(k) + \mathbf{v}_j(k) \tag{5.8.3}$$

Assuming only one receive antenna for simplicity, the matched filtering

is performed by pre-multiplying by $\tilde{\mathbf{H}}$ in each subcarrier, as follows:

$$\mathbf{R}_{mf} = \tilde{\mathbf{H}}^H(k)\tilde{\mathbf{H}}(k)\mathbf{s}(k) + \tilde{\mathbf{H}}^H(k)\mathbf{v}(k) = \Delta\mathbf{s} + \mathbf{n} \tag{5.8.4}$$

where the 2×2 matrix Δ can be obtained as

$$\begin{aligned}
\Delta &= \mathbf{H}^H\mathbf{H} \\
&= \begin{bmatrix} |\mathbf{H}_{1,j}(k) + \mathbf{H}_{2,j}(k)|^2 & 0 \\ +|\mathbf{H}_{3,j}(k) + \mathbf{H}_{4,j}(k)|^2 & \\ 0 & |\mathbf{H}_{1,j}(k) + \mathbf{H}_{2,j}(k)|^2 \\ & +|\mathbf{H}_{3,j}(k) + \mathbf{H}_{4,j}(k)|^2 \end{bmatrix} \\
&= \begin{bmatrix} (\sum_{i=1}^{4} |\mathbf{H}_{i,j}(k)|^2 + \varrho) & 0 \\ 0 & (\sum_{i=1}^{4} |\mathbf{H}_{i,j}(k)|^2 + \varrho) \end{bmatrix} \\
&= (\sum_{i=1}^{4} |\mathbf{H}_{i,j}(k)|^2)\boldsymbol{I}_2 + \varrho \begin{bmatrix} 1 & 0 \\ 0 & 1 \end{bmatrix}
\end{aligned} \tag{5.8.5}$$

where

$$\varrho = 2Re\{\mathbf{H}_{1,j}(k)\mathbf{H}^*_{2,j}(k) + \mathbf{H}_{3,j}(k)\mathbf{H}^*_{4,j}(k)\} \tag{5.8.6}$$

Hence, with linear processing, the detected signals $\tilde{s_1}$ and $\tilde{s_2}$ can be obtained as

$$\begin{bmatrix} \tilde{\mathbf{s}}_1(k) \\ \tilde{\mathbf{s}}_2(k) \end{bmatrix} = \Delta \begin{bmatrix} \mathbf{s}_1(k) \\ \mathbf{s}_2(k) \end{bmatrix} + \begin{bmatrix} (\mathbf{H}^*_{1,j}(k) + \mathbf{H}^*_{2,j}(k))\mathbf{n}_1 + (\mathbf{H}_{3,j}(k) + \mathbf{H}_{4,j}(k))\mathbf{n}^*_2 \\ (\mathbf{H}^*_{3,j}(k) + \mathbf{H}^*_{4,j}(k))\mathbf{n}_1 - (\mathbf{H}_{1,j}(k) + \mathbf{H}_{2,j}(k))\mathbf{n}^*_2 \end{bmatrix} \tag{5.8.7}$$

In order to achieve full diversity, two feedback bits can be used to rotate the phase of the signals for certain antennas to ensure that ϱ is positive during the transmission block. The proposed feedback schemes

are explained in the following section.

5.8.1 Transmission with Channel Feedback

Herein, channel state information (CSI) is assumed available at the EO-STBC transmitter. At first, ϱ is adopted to be positive and maximum magnitude by rotating the signals from the first and third antennas in the transmission. The rotation is defined by the following phasors.

$$\mathbf{U} = [U_1, U_2]^T \tag{5.8.8}$$

In feedback scheme, the signals s_1 and s_3 are multiplied by $U_1 = (-1)^i$ and $U_2 = (-1)^k$, where $i, k = 0, 1$, and then they are transmitted from first antennas and third antenna, respectively. Herein i and k are defined as two feedback parameters determined by the channel condition. In particular, when $i(ork) = 1$, $U_1(orU_2) = -1$, which means that s_1 and s_3 will be phase rotated by 180° before transmission. Otherwise, they can be directly transmitted. Since the channel is assumed to be constant over a transmission block, hence the received signal becomes

$$\mathbf{r} = \begin{bmatrix} \mathbf{r}_{1,j}(k) \\ \mathbf{r}^*_{2,j}(k) \end{bmatrix} = \begin{bmatrix} \mathbf{H}'_{1,j}(k) + \mathbf{H}_{2,j}(k) & \mathbf{H}'_{3,j}(k) + \mathbf{H}_{4,j}(k) \\ \mathbf{H}'^*_{3,j}(k) + \mathbf{H}^*_{4,j}(k) & -\mathbf{H}'^*_{1,j}(k) - \mathbf{H}^*_{2,j}(k) \end{bmatrix} \begin{bmatrix} \mathbf{s}_1(k) \\ \mathbf{s}_2(k) \end{bmatrix} + \begin{bmatrix} \mathbf{v}_{1,j}(k) \\ \mathbf{v}^*_{2,j}(k) \end{bmatrix} \tag{5.8.9}$$

where $\mathbf{H}'_{1,j}(k)$ and $\mathbf{H}'_{3,j}(k)$ represent $U_1\mathbf{H}_{1,j}(k)$ and $U_2\mathbf{H}_{3,j}(k)$, respec-

tively. Furthermore, the new matrix $\tilde{\Delta}$ can be written as

$$\tilde{\Delta} = \begin{bmatrix} |\mathbf{H}'_{1,j}(k) + \mathbf{H}_{2,j}(k)|^2 & 0 \\ +|\mathbf{H}'_{3,j}(k) + \mathbf{H}_{4,j}(k)|^2 & \\ 0 & |\mathbf{H}'_{1,j}(k) + \mathbf{H}_{2,j}(k)|^2 \\ & +|\mathbf{H}'_{3,j}(k) + \mathbf{H}_{4,j}(k)|^2 \end{bmatrix} \quad (5.8.10)$$

From description above, the decision vector $\tilde{\mathbf{s}} = [\tilde{\mathbf{s}}_1, \tilde{\mathbf{s}}_2]^T$ with the receive vector $\mathbf{r} = [r_1, r_2^*]^T$ can be calculated as

$$\begin{aligned} \tilde{\mathbf{s}} &= \tilde{\mathbf{H}}^H \mathbf{r} = (|U_1|^2 |\mathbf{H}_{1,j}(k)|^2 + |\mathbf{H}_{2,j}(k)|^2 + |U_2|^2 |\mathbf{H}_{3,j}(k)|^2 + |\mathbf{H}_{4,j}(k)|^2 \\ &+ (2Re(U_1 \mathbf{H}_{1,j}(k) \mathbf{H}^*_{2,j}(k)) + 2Re(U_2 \mathbf{H}_{3,j}(k) \mathbf{H}^*_{4,j}(k)))\mathbf{s} + \mathbf{V} \end{aligned} \quad (5.8.11)$$

where $\mathbf{V} = \tilde{\mathbf{H}}^H \mathbf{v}$ is a noise component. Since $|U_1|^2 = |U_2|^2 = 1$

$$\alpha = \sum_{i=1}^{4} |\mathbf{H}_{i,j}(k)|^2 \quad (5.8.12)$$

which α corresponds to the conventional diversity gain for the four transmit and one receive antenna case. The feedback performance gain is

$$\varrho' = 2Re((U_1 \mathbf{H}_{1,j}(k) \mathbf{H}^*_{2,j}(k)) + 2Re(U_2 \mathbf{H}_{3,j}(k) \mathbf{H}^*_{4,j}(k)) \quad (5.8.13)$$

If $\beta' > 0$, the designed closed-loop system can obtain additional performance gain, which leads to an improved SNR at the receiver. Therefore, the design criterion of the two-bit feedback scheme can be proposed, and each element of the feedback performance gain should be nonneg-

ative, as

$$(i,k) = \begin{cases} (0,0), & if Re(\mathbf{H}_{1,j}(k)\mathbf{H}^*_{2,j}(k)) \geq 0 \quad and \quad Re(\mathbf{H}_{3,j}(k)\mathbf{H}^*_{4,j}(k)) \geq 0 \\ (0,1), & if Re(\mathbf{H}_{1,j}(k)\mathbf{H}^*_{2,j}(k)) \geq 0 \quad and \quad Re(\mathbf{H}_{3,j}(k)\mathbf{H}^*_{4,j}(k)) < 0 \\ (1,0), & if Re(\mathbf{H}_{1,j}(k)\mathbf{H}^*_{2,j}(k)) < 0 \quad and \quad Re(\mathbf{H}_{3,j}(k)\mathbf{H}^*_{4,j}(k)) \geq 0 \\ (1,1), & if Re(\mathbf{H}_{1,j}(k)\mathbf{H}^*_{2,j}(k)) < 0 \quad and \quad Re(\mathbf{H}_{3,j}(k)\mathbf{H}^*_{4,j}(k)) < 0 \end{cases} \tag{5.8.14}$$

5.8.2 Simulation

In this section, the simulations are performed between O-STBC, close-loop QO-STBC and close-loop EO-STBC MIMO OFDM system. The simulation environment is the same as setting in Section 5.7.2. Figure 5.12 shows the performance comparison for two transmit antenna O-STBC OFDM, four transmit antenna and one receive antenna closed loop QO-STBC OFDM scheme and EO-STBC OFDM schemes over quasi-static channels. It can be seen that at a FER of 10^{-3}, the performance improvement of the closed loop feedback QO-STBC scheme is approximately $9dB$ compared to the O-STBC OFDM scheme. Furthermore, the performance gain of both closed loop feedback QO-STBC and EO-STBC is only approximately $0.4dB$. The proposed closed loop EO-STBC OFDM scheme outperforms closed loop QO-STBC scheme slightly. Therefore, to use closed loop feedback QO-STBC method appears to be able to obtain good enough error performance.

5.9 Summary

In this chapter, a background review of key physical layer technology of next generation wireless communications, OFDM techniques, is pro-

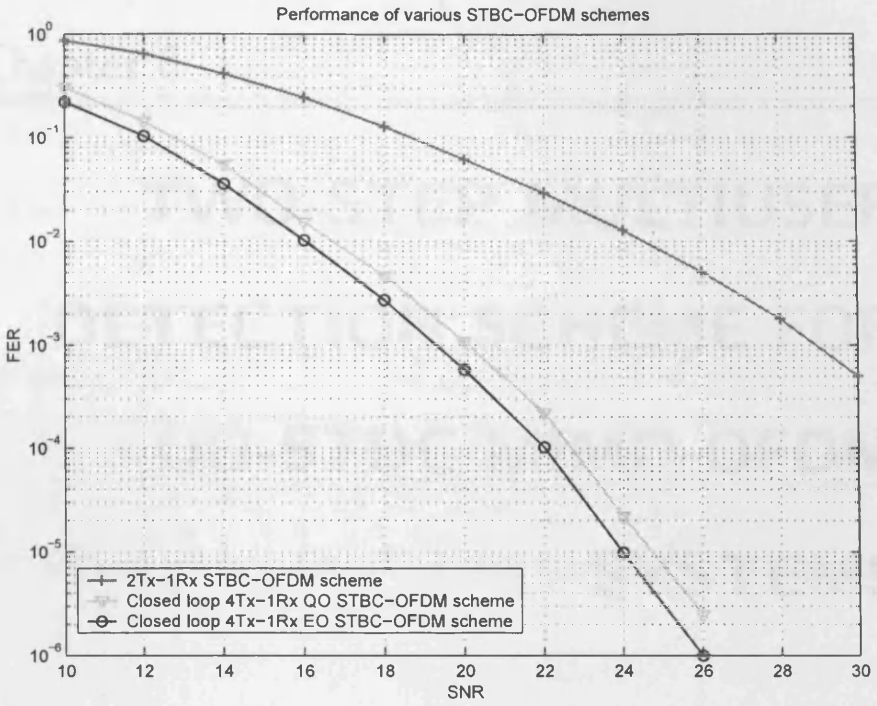

Figure 5.12. FER performance comparison for MIMO-OFDM system with O-STBC scheme, feedback close-loop QO-STBC scheme and feedback close-loop EO-STBC scheme.

vided. Certain representative classes of coherent STBCs for use in enhancing error performance of multi-antenna transmission systems over frequency selective fading channels have also been utilized. The Alamouti code is applied on the MIMO-OFDM system firstly and a system with four transmit antennas which adopts the QO-STBCs is considered in particular for more system diversity. Moreover, quasi-orthogonal STBC-OFDM system jointly optimizes a phase feedback method. The extended orthogonal STBC-OFDM system is also proposed for performance comparison. They improve the error rate performance of the system by providing diversity gain.

Chapter 6

TWO-STEP MULTIUSER DETECTION SCHEME FOR QO-STBC MIMO-OFDM SYSTEMS

6.1 Introduction

In the previous chapter, signal detection was investigated for single user usage over a multiple input multiple output (MIMO) wideband channel. In this chapter the multiuser detection problem is addressed for a multicarrier MIMO system. In particular, the topic of multiuser quasi-orthogonal space-time block coding MIMO-orthogonal frequency division multiplexing (QO-STBC MIMO-OFDM) systems is addressed by performing a parallel interference cancellation (PIC) algorithm.

The outline of this chapter is as follows. In Section 6.2, a brief review of multiuser detection is given and the interference occurring in the multiuser application is introduced. Then the PIC algorithm is discussed to mitigate multiuser interference for signal detection in Section 6.3. A novel two-step multiuser interference cancellation scheme

for QO-STBC MIMO-OFDM systems based on the PIC algorithm is designed in Section 6.4, which was also described in [74]. Simulation results and analysis are also presented. Finally, conclusions are provided in Section 6.5.

6.2 Multiuser Interference and Multiuser Detection

6.2.1 Multiuser Detection

During the past decade, multiuser detection (MUD) has become a major research topic to deal with interference in multiuser MIMO-OFDM applications by jointly detecting signals from different users.

A multiuser MIMO-OFDM system allows multiple users to exploit the spatial resources based on advanced transmit or receiver processing. Hence such OFDM-based MIMO structures are explicitly developed for situations where the number of users is more than one. In the associated receiver processing, the multiuser receiver can detect all the users' data simultaneously by exploiting the structure of the multiuser signal. Such MUD improves upon conventional single-user receivers which are only designed to operate in thermal noise without considering multiuser interference. Therefore, multiuser receivers can potentially substantially outperform single-user receivers in a multiuser environment. Effective multiuser receivers can extract and detect a desired user data from the multiuser signal efficiently.

There are some basic multiuser detection algorithms and their variants which are well reviewed in the overview book by Verdu [59]. Although these methods were originally proposed for code division multiple access (CDMA) systems [75,76], it can also be employed in TDMA

systems [77] and OFDM systems [78]. Recently, various MUD schemes have been proposed for MIMO-OFDM systems. Among these MUDs, the classic linear-least squares (LS) [59,79], and minimum mean square error (MMSE) [59,79,80] approaches are popular schemes for multiuser interference suppression due to their low computational complexity.

6.2.2 Multiuser Interference Cancellation

In wireless communication systems, data can be transmitted over the radio spectrum resource by reusing frequency bands. However, when multiple transmitters operate in one frequency-division channel, interference will occur between each other, which represents co-channel interference (CCI). In practical wireless communications, there are possibly strong interferers occurring in urban areas where the base stations (BS) are closely spaced. Therefore effectively suppressing CCI is important to improve the service quality or minimize the allowable distance among nearby co-channel BSs, and thus increase the system capacity [81] and [77].

CCI is an inherent problem for most multiple access schemes, for example orthogonal frequency division multiple access (OFDMA) and time division multiple access (TDMA). Otherwise, there is also multiple access interference (MAI) presented in a CDMA system. MAI occurs between users, both in the uplink and downlink. Furthermore, the MAI can also come from other cells (intercell MAI). Hence suppressing the MAI due to each user can provide the ability to allocate a larger number of users in the cell and among cells. On other hand, the transmit power will be reduced by suppressing MAI and CCI, which is required to meet the target SNR, and more channels can be used for transmitting

with a fixed power budget, thereby resulting in capacity increase and environmental advantages, as in so-called green radio. Hence the design of interference-suppression receivers has become very important target of interest for future multiuser mobile systems.

The optimal approaches of MUD are based on maximum likelihood (ML) or the maximum a posteriori probability (MAP) algorithm and can provide performance close to the single-user bound, however, these schemes require high computational complexity [59]. Therefore, some sub-optimal MUD algorithms which have much lower complexity have been developed. As introduction in previous chapters, zero-forcing (ZF) detection and MMSE detection are referred to as linear detection methods. On the other hand, there is another class of sub-optimal MUD referred to nonlinear detection such as decision-feedback MUD, successive interference cancellation (SIC) and parallel interference cancellation (PIC). The PIC detector is an iterative multiuser detector, which can perform more accurate estimation during iterations than linear scheme, which will be introduced in the following sections.

6.3 PIC scheme in Multiuser Detection

As description in the last section, nowadays, researchers normally prefer the low complexity linear schemes exploited in multiuser detections. On the other hand, nonlinear detection schemes could also be proposed to exploit the data from the interfering user to detect the signal of the desired user. This strategy is defined as interference cancellation (IC) detection which reconstructs the multiuser interference by temporary data estimations, and then cancels it from the received signal. The IC detection scheme normally includes two types: SIC scheme and PIC

scheme.

In the SIC detection scheme [82], the detector firstly detects the most likely reliable user by using conventional matched filtering (MF). Then the interference caused by this user is reconstructed and subtracted from the received signal. If the interference is cancelled effectively from received stream, then the resulting signal term contains one fewer major interfering users. Next the receiver will repeat the process to find the strongest user among the remaining ones until the last users is left. This class of detectors has the almost paradoxical feature that interference cancellation can be performed most reliably when the interference is strong relative to the desired signal, i.e. when there is a significant power difference between each of the user signals. However its performance is poor when power levels are approximately equal. At the same time, the signals need to be sorted by power correctly, and signal reordering is required whenever the power profile changes. This will be a particular risk in a high capacity system (with widely variable power levels). Finally, serial cancellation one-by-one will lead to a relatively long processing delay.

In PIC detection as illustrated in [83, 84], it illustrates that the receiver simultaneously firstly detects each user's data separately. In order to cancel the MAI for each user, the detector employs the first stage estimations to remove the remaining users' interference for each user from the received signal. Compared with SIC, since the IC is performed in parallel for all users, it is defined as parallel interference cancellation and the delay required to complete the process is dramatically reduced. In this detector, each user in the system receives equal treatment in the attempt to cancel its MAI. It is clear that the parallel

cancellation process should be divided into two stages: (1) perform the estimation of all users' signals; (2) reconstruct the MAI and subtract it from the received signal for each user. Thus the PIC is also called multi-stage IC. The first stage of PIC can be provided by an MF or linear detector such as MMSE.

Figure 6.1 illustrates the structure of the PIC detector in a two-user scenario.

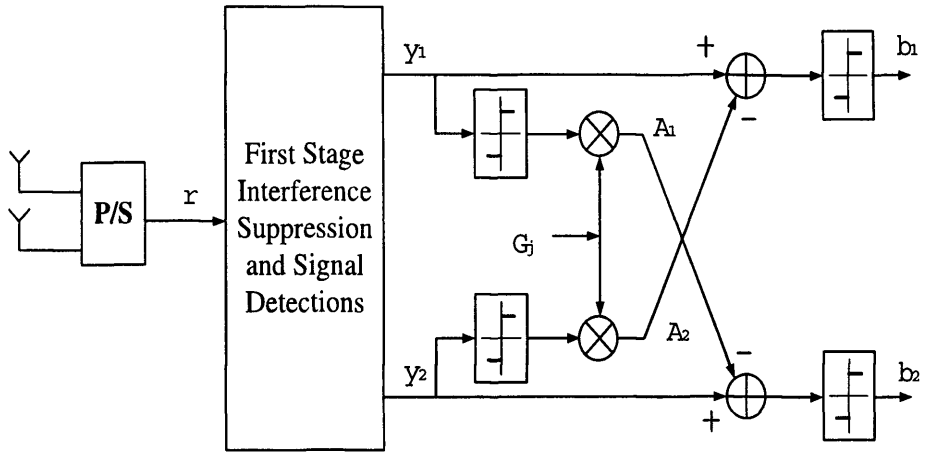

Figure 6.1. The structure of the parallel interference cancellation (PIC) scheme for the two user signal detection.

Suppose that users are demodulated by the conventional MF in the first stage and there are K users which are detected in the first stage. Then the signal estimation of the users is given by

$$\mathbf{y} = \mathbf{W}^H \mathbf{r} \tag{6.3.1}$$

where $\mathbf{W}$ is the detection weight matrix where $\mathbf{W} = [\mathbf{w}_1, \mathbf{w}_2, \ldots, \mathbf{w}_K]$ and $\mathbf{w}_k$ is the column weight vector for the kth user. The vector $\mathbf{y} = [y_1, y_2, \ldots, y_K]^T$ is the first stage detection, it is assumed that the complex scalar G_j is reconstructing the MAI parameter of the jth

interfering user, so the kth user's MAI caused by the jth interfering user is obtained as

$$A_j = G_j y_j \tag{6.3.2}$$

where $j \neq k$. The MAI can be cancelled from the received signal as

$$\tilde{y}_k = y_k - \sum\nolimits_{j \neq k} A_j \tag{6.3.3}$$

Supposing that a hard decision is employed, the output of the two-stage PIC detector is:

$$\begin{aligned} b_k &= sgn(\tilde{y}_k) \\ &= sgn\left(y_k - \sum\nolimits_{j \neq k} G_j y_j\right) \end{aligned} \tag{6.3.4}$$

From the discussion above, PIC detection can avoid the long delay derived from the serial processing in the SIC. It is unnecessary to order the users by power for the PIC. The iterative scheme [85, 86] can be performed for many iterations to achieve the best performance. Finally, using channel decoding following the PIC detection in every iteration is also a desirable approach to reduce the risk of oscillation. A powerful channel decoder (such as Turbo decoder) can substantially improve the temporary data estimates and achieve more accurate interference reconstruction and subtraction. Hence PIC detection is considered as one of the most promising MUD techniques [87, 88].

6.4 Two-Step PIC MUD for QO-STBC MIMO-OFDM Systems

In this section, a new two-step interference cancellation (IC) technique for an orthogonal frequency division multiplexing system with multiple transmitter and receiver antennas linked over a frequency selective channel is explored. Firstly, a recently proposed type of full code rate space-time block code is utilized, which is a quasi-orthogonal space-time block code (QO-STBC) scheme to exploit temporal and spatial diversity within a multiuser environment with k co-channel users. Herein, four transmit antennas are adopted for each user and two antennas in the receiver. The scheme has a combined interference suppression scheme based on a minimum mean-square error (MMSE), followed by an interference cancellation step and symbol-wise detection. The frame error rate (FER) performance for the proposed algorithm is compared with an orthogonal space-time block code (O-STBC) scheme for two transmitter antennas in slow fading frequency selective channels. Simulation results are shown in the last part of this section.

6.4.1 System Model

Consider a block or vector transmission OFDM system, where K synchronous users are communicating with a base station. Four antennas are employed in each transmit terminal and two antennas in the receiver. The baseband transmitter structure is illustrated in Figure 6.2. The IFFT-FFT blocks implicitly include the addition/removal of the cyclic prefix.

When the ith terminal user transmits the four consecutive block vectors $\mathbf{S}_1^i, \mathbf{S}_2^i, \mathbf{S}_3^i, \mathbf{S}_4^i$, according to QO-STBC, the symbol matrix becomes:

$$QO = \begin{bmatrix} \mathbf{S}_1^i & \mathbf{S}_2^i & \mathbf{S}_3^i & \mathbf{S}_4^i \\ -(\mathbf{S}_1^i)^* & (\mathbf{S}_1^i)^* & -(\mathbf{S}_4^i)^* & (\mathbf{S}_3^i)^* \\ -(\mathbf{S}_3^i)^* & -(\mathbf{S}_4^i)^* & (\mathbf{S}_1^i)^* & (\mathbf{S}_2^i)^* \\ \mathbf{S}_4^i & -\mathbf{S}_3^i & -\mathbf{S}_2^i & \mathbf{S}_1^i \end{bmatrix} \tag{6.4.1}$$

where $\mathbf{S} = [S(0), \ldots S(N-1)]^T$ is an N length size block of transmit symbols, and $(\cdot)^T$, $(\cdot)^*$ denote respectively transpose and conjugate operations. The output of the space-time encoder is then modulated by an IFFT into an OFDM symbol sequence, which is then transmitted through a frequency selective channel with coefficients $\{h_{n,j}\}$ with maximum order q for the *n-th* transmit antenna and *j-th* receiver antenna pair. $H_{1,j}^i(k), H_{2,j}^i(k), H_{3,j}^i(k), H_{4,j}^i(k)$ denote the channel fre-

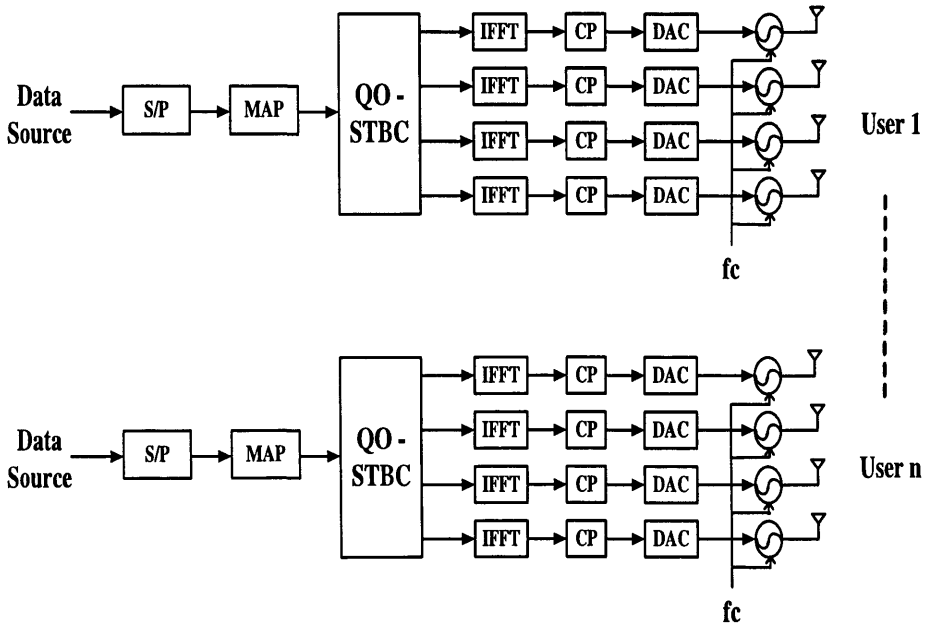

Figure 6.2. Multiuser QO-STBC MIMO-OFDM transmitters for K users, where each user terminal is equipped with $n_t = 4$ transmit antennas.

quency responses of the *k-th* tone, related to the channel from the four

transmit antennas in each terminal to the jth receive antenna, where $k = 0, 1, \ldots, N-1$. The kth tone signal is picked up by each receive antenna during the time slot and can be written as:

$$\begin{bmatrix} r_{1,j}(k) \\ r_{2,j}(k) \\ r_{3,j}(k) \\ r_{4,j}(k) \end{bmatrix} = \begin{bmatrix} \eta_{1,j}(k) \\ \eta_{2,j}(k) \\ \eta_{3,j}(k) \\ \eta_{4,j}(k) \end{bmatrix}$$

$$+ \begin{bmatrix} \sum_{i=1}^{K} \{H_{1,j}^i(k) S_1^i(k) + H_{2,j}^i(k) S_2^i(k) + H_{3,j}^i(k) S_3^i(k) + H_{4,j}^i(k) S_4^i(k)\} \\ \sum_{i=1}^{K} \{H_{2,j}^i(k) \left(S_1^i(k)\right)^* - H_{1,j}^i(k) \left(S_2^i(k)\right)^* + H_{4,j}^i(k) \left(S_3^i(k)\right)^* - H_{3,j}^i(k) \left(S_4^i(k)\right)^*\} \\ \sum_{i=1}^{K} \{H_{3,j}^i(k) \left(S_1^i(k)\right)^* + H_{4,j}^i(k) \left(S_2^i(k)\right)^* - H_{1,j}^i(k) \left(S_3^i(k)\right)^* - H_{2,j}^i(k) \left(S_4^i(k)\right)^*\} \\ \sum_{i=1}^{K} \{H_{4,j}^i(k) S_1^i(k) - H_{3,j}^i(k) s S_2^i(k) - H_{2,j}^i(k) S_3^i(k) + H_{1,j}^i(k) S_4^i(k)\} \end{bmatrix} \tag{6.4.2a}$$

where $\eta(k)$ denotes the frequency domain representation of the noise at the kth tone. For simplicity of notation, define

$$\mathbf{r}_j(k) = [r_{1,j}(k), r_{2,j}^*(k), r_{3,j}^*(k), r_{4,j}(k)]^T$$

$$\mathbf{S}^i(k) = [S_1^i(k), S_2^i(k), S_3^i(k), S_4^i(k)]^T$$

$$\eta_j(k) = [\eta_{1,j}(k), \eta_{2,j}^*(k), \eta_{3,j}^*(k), \eta_{4,j}(k)]^T$$

and

$$\tilde{\mathbf{H}}_j^i(k) = \begin{bmatrix} H_{1,j}^i(k) & H_{2,j}^i(k) & H_{3,j}^i(k) & H_{4,j}^i(k) \\ \left(H_{2,j}^i(k)\right)^* & -\left(H_{1,j}^i(k)\right)^* & \left(H_{4,j}^i(k)\right)^* & -\left(H_{3,j}^i(k)\right)^* \\ \left(H_{3,j}^i(k)\right)^* & \left(H_{4,j}^i(k)\right)^* & -\left(H_{1,j}^i(k)\right)^* & -\left(H_{2,j}^i(k)\right)^* \\ H_{4,j}^i(k) & -H_{3,j}^i(k) & -H_{2,j}^i(k) & H_{1,j}^i(k) \end{bmatrix} \tag{6.4.3}$$

So equation (6.4.2a) can be rewritten as

$$\mathbf{r}_j(k) = \sum_{i=1}^{K} \tilde{\mathbf{H}}_j^i(k)\mathbf{S}^i(k) + \eta_j(k), \quad k = 0, 1, \ldots, N-1 \tag{6.4.4}$$

In the sequel, only two terminal users will be considered for convenience of presentation. Consider that all the receiver antennas in the kth tone receive signal can be represented in matrix form as follows:

$$\begin{bmatrix} \mathbf{r}_1(k) \\ \mathbf{r}_2(k) \end{bmatrix} = \begin{bmatrix} \tilde{\mathbf{H}}_1^1(k) & \cdots & \tilde{\mathbf{H}}_1^K(k) \\ \tilde{\mathbf{H}}_2^1(k) & \cdots & \tilde{\mathbf{H}}_2^K(k) \end{bmatrix} \cdot \begin{bmatrix} \mathbf{S}^1(k) \\ \mathbf{S}^2(k) \\ \vdots \\ \mathbf{S}^K(k) \end{bmatrix} + \begin{bmatrix} \eta_1(k) \\ \eta_2(k) \end{bmatrix} \tag{6.4.5}$$

Eq.(6.4.5) can be re-written as

$$\mathbf{r}''(k) = \mathbf{H}''(k)\mathbf{S}''(k) + \eta''(k) \tag{6.4.6}$$

where $\mathbf{r}''(k)$ is the $\mathbf{8 \times 1}$ column vector corresponding to the overall receiver signals at all receive antennas, $\mathbf{H}''(k)$ has a code matrix of size $\mathbf{8 \times 8}$, $\mathbf{S}''(k)$ is the transmitting signal vector with dimension $\mathbf{8 \times 1}$

including all users at the k-th tone, and $\eta''(k)$ is the noise vector with 8 elements.

6.4.2 Linear MMSE IC Suppression and ML Decoding

For simplicity, the two users case is considered in this scheme. A two-user QO-STBC OFDM receiver is considered as illustrated in Figure 6.3, where the receiver is equipped with m receive antennas.

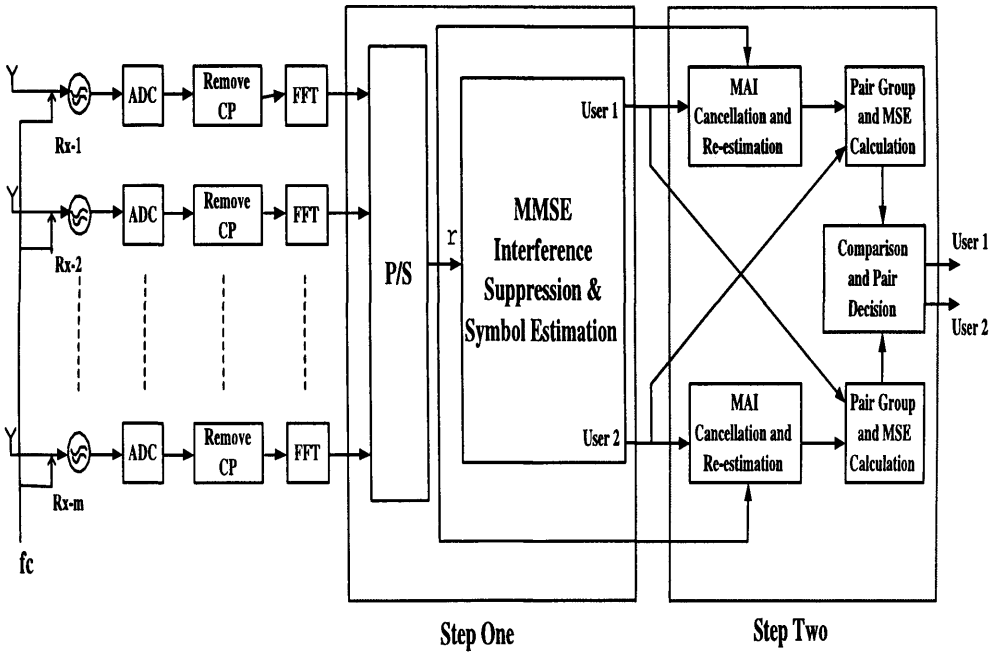

Figure 6.3. Two-step PIC Multiuser QO-STBC MIMO-OFDM receiver for two users, which is equipped with m receive antennas.

The receive signal at the receive antenna during four sequential signal slots is given by:

$$\begin{aligned} \mathbf{r}_1(k) &= \tilde{\mathbf{H}}_1^1(k)\mathbf{S}^1(k) + \tilde{\mathbf{H}}_1^2(k)\mathbf{S}^2(k) + \eta_1(k) \\ \mathbf{r}_2(k) &= \tilde{\mathbf{H}}_2^1(k)\mathbf{S}^1(k) + \tilde{\mathbf{H}}_2^2(k)\mathbf{S}^2(k) + \eta_2(k) \end{aligned} \tag{6.4.7}$$

Assume to define the ith user terminal, where i=1,2. Here use an MMSE interference cancellation and maximum likelihood decoder to estimate the transmitted symbols. The cost function for the user 1 to minimize the mean square error caused by co-channel interference and noise is given by:

$$J(w) = E\left\{\left\|S^i(k) - \mathbf{w}^H \mathbf{r}''(k)\right\|^2\right\} \tag{6.4.8}$$

where $E\{\cdot\}$ denotes the statistical expectation operation, $\{\cdot\}^H$ denotes Hermitian transpose operator, and $\|\cdot\|$ denotes Euclidean Norm. By using the standard minimization technique:

$$\frac{\partial J(\mathbf{w})}{\partial \mathbf{w}} = 0 \tag{6.4.9}$$

it can be shown that the weights $\mathbf{w}_{4i-3}, \mathbf{w}_{4i-2}, \mathbf{w}_{4i-1}, \mathbf{w}_{4i}$, corresponding to user i, can be computed respectively, as:

$$\begin{aligned}
\mathbf{w}_{4i-3} &= \mathbf{M}^{-1}\mathbf{h}_{4i-3} \\
\mathbf{w}_{4i-2} &= \mathbf{M}^{-1}\mathbf{h}_{4i-2} \\
\mathbf{w}_{4i-1} &= \mathbf{M}^{-1}\mathbf{h}_{4i-1} \\
\mathbf{w}_{4i} &= \mathbf{M}^{-1}\mathbf{h}_{4i}
\end{aligned}$$

where $\mathbf{M} = \tilde{\mathbf{H}}(k)\tilde{\mathbf{H}}(k)^* + \frac{1}{\Gamma}\mathbf{II}_{2m}$ and $\Gamma = E_s/N_0$ is the signal-to-noise ratio, $\mathbf{h}_{4i}$ is the $4i$-th column vector of $\tilde{\mathbf{H}}(k)$, then the maximum likelihood decoding equation can be written as:

$$\tilde{\mathbf{S}}^{(i)}(k) = \arg \min_{S_n^{(i)} \in \mathbf{S}} \sum_{n=1}^{4} \left\{\left\|\mathbf{w}_{4i-4+n}^* \mathbf{r}''(k) - S_n^{(i)}\right\|^2\right\} \tag{6.4.10}$$

where $S_n^{(i)}$ is one of all possible choices of symbols from a QPSK constellation. From the first step symbol estimation, the reliability value of estimation can be measure by Euclidean Norm. So the reliability functions of all symbols from the user terminal will be given by:

$$\triangle_i = \sum_{n=1}^{4} \left\{ \left\| \mathbf{w}_{4i-4+n}^{*} \mathbf{r}''(k) - \tilde{S}_n^{(i)} \right\|^2 \right\} \tag{6.4.11}$$

where $\tilde{\mathbf{S}}^{(i)}(k)$ is the overall receiver signals at all receive antennas, $\mathbf{r}''(k)$ includes all possible symbol pairs of the *i-th* user in the transmit signal.

6.4.3 Two-step Approach for IC and ML Decoding

If the original performance is not good enough, there is another arithmetic step that can be used, that is a two-step IC. In this two-step approach, the receiver decodes signals from the two terminal users using the linear MMSE decoding scheme, herein define these two block symbols as $\tilde{\mathbf{S}}^1(k)$ and $\tilde{\mathbf{S}}^2(k)$. Without loss of generality, assume that the detection scheme is addressed on decoding the symbols from the first terminal user, then:

$$\begin{aligned} \mathbf{r}_1(k) - \tilde{\mathbf{H}}_1^1(k)\tilde{\mathbf{S}}^1(k) &= \tilde{\mathbf{H}}_1^2(k)\tilde{\tilde{\mathbf{S}}}^2(k) + \eta_1(k) \\ \mathbf{r}_2(k) - \tilde{\mathbf{H}}_2^1(k)\tilde{\mathbf{S}}^1(k) &= \tilde{\mathbf{H}}_2^2(k)\tilde{\tilde{\mathbf{S}}}^2(k) + \eta_2(k) \end{aligned}$$

Now these equations are decoded to obtain the signal $\tilde{\tilde{\mathbf{S}}}^2(k)$ corresponding to $\tilde{\mathbf{S}}^1(k)$.

$$\tilde{\tilde{\mathbf{S}}}^2(k) = \arg \min_{\mathbf{S}_n^2 \in \mathbf{S}} \sum_{n=1}^{2} \left\{ \left\| \mathbf{r}_n(k) - \tilde{\mathbf{H}}_n^1(k)\tilde{\mathbf{S}}^1(k) - \tilde{\mathbf{H}}_n^2(k)\tilde{\tilde{\mathbf{S}}}^2(k) \right\|^2 \right\} \tag{6.4.12}$$

The reliability function of the pair of result $\left\{\tilde{\mathbf{S}}^1(k), \tilde{\tilde{\mathbf{S}}}^2(k)\right\}$ is given by:

$$\triangle(\tilde{\mathbf{S}}^1) = \sum_{n=1}^{2} \left\{ \left\| \mathbf{r}_n(k) - \tilde{\mathbf{H}}_n^1(k)\tilde{\mathbf{S}}^1(k) - \tilde{\mathbf{H}}_n^2(k)\tilde{\tilde{\mathbf{S}}}^2(k) \right\|^2 \right\} \quad (6.4.13)$$

Similarly, using $\tilde{\mathbf{S}}^2(k)$ to estimate $\tilde{\tilde{\mathbf{S}}}^1(k)$, the equation and the corresponding reliability function are straightforward to write from the equations above, as

$$\tilde{\tilde{\mathbf{S}}}^1(k) = \arg \min_{\mathbf{S}_n^1 \in \mathbf{S}} \sum_{n=1}^{2} \left\{ \left\| \mathbf{r}_n(k) - \tilde{\mathbf{H}}_n^1(k)\tilde{\tilde{\mathbf{S}}}^1(k) - \tilde{\mathbf{H}}_n^2(k)\tilde{\mathbf{S}}^2(k) \right\|^2 \right\} \quad (6.4.14)$$

$$\triangle(\tilde{\mathbf{S}}^2) = \sum_{n=1}^{2} \left\{ \left\| \mathbf{r}_n(k) - \tilde{\mathbf{H}}_n^1(k)\tilde{\tilde{\mathbf{S}}}^1(k) - \tilde{\mathbf{H}}_n^2(k)\tilde{\mathbf{S}}^2(k) \right\|^2 \right\} \quad (6.4.15)$$

To achieve better performance, the smaller of the two values $\triangle_1 + \triangle(\tilde{\mathbf{S}}^1)$ and $\triangle_2 + \triangle(\tilde{\mathbf{S}}^2)$ is selected. If $\left(\triangle_1 + \triangle(\tilde{\mathbf{S}}^1)\right) < \left(\triangle_2 + \triangle(\tilde{\mathbf{S}}^2)\right)$, the symbol pair $\left\{\tilde{\mathbf{S}}^1(k), \tilde{\tilde{\mathbf{S}}}^2(k)\right\}$ will be chosen for final estimation, otherwise, $\left\{\tilde{\mathbf{S}}^2(k), \tilde{\tilde{\mathbf{S}}}^1(k)\right\}$ will be used.

The Table 6.1 shows the proposed two-step PIC and multiuser detection algorithm for two user QO-STBC-OFDM system.

6.4.4 Simulations and Results

In simulations, QO-STBC is exploited with four antennas in each transmit terminal and two receive antennas together with the proposed two-step parallel interference cancellation MIMO-OFDM detection scheme. The system is considered based on perfect synchronization. An O-

Table 6.1. Two-step PIC algorithm for two user QO-STBC-OFDM Detection.

for $k = 0 : N-1$

for $i = 1, 2$

$\mathbf{M} = \tilde{\mathbf{H}}(k)\tilde{\mathbf{H}}(k)^* + \frac{1}{\Gamma}\mathbf{II}_{2m}$

$\mathbf{w}_{4i-3} = \mathbf{M}^{-1}\mathbf{h}_{4i-3}, \ \mathbf{w}_{4i-2} = \mathbf{M}^{-1}\mathbf{h}_{4i-2}$

$\mathbf{w}_{4i-1} = \mathbf{M}^{-1}\mathbf{h}_{4i-1}, \ \mathbf{w}_{4i} = \mathbf{M}^{-1}\mathbf{h}_{4i}$

$\tilde{\mathbf{S}}^{(i)}(k) = \arg \min_{\mathbf{S}_n^{(i)} \in \mathbf{S}} \sum_{n=1}^{4} \left\{ \left\| \mathbf{w}_{4i-4+n}^* \mathbf{r}''(k) - \tilde{S}_n^{(i)} \right\|^2 \right\}$

$\triangle_i = \sum_{n=1}^{4} \left\{ \left\| \mathbf{w}_{4i-4+n}^* \mathbf{r}''(k) - \tilde{S}_n^{(i)} \right\|^2 \right\}$

$\mathbf{r}_1(k) - \tilde{\mathbf{H}}_1^1(k)\tilde{\mathbf{S}}^1(k) = \tilde{\mathbf{H}}_1^2(k)\tilde{\tilde{\mathbf{S}}}^2(k) + \eta_1(k)$

$\mathbf{r}_2(k) - \tilde{\mathbf{H}}_2^1(k)\tilde{\mathbf{S}}^1(k) = \tilde{\mathbf{H}}_2^2(k)\tilde{\tilde{\mathbf{S}}}^2(k) + \eta_2(k)$

$j \in \{1, 2\}$ and $j \neq i$

$\tilde{\tilde{\mathbf{S}}}^i(k) = \arg \min_{\mathbf{S}_n^j \in \mathbf{S}} \sum_{n=1}^{2} \left\{ \left\| \mathbf{r}_n(k) - \tilde{\mathbf{H}}_n^i(k)\tilde{\tilde{\mathbf{S}}}^i(k) - \tilde{\mathbf{H}}_n^j(k)\tilde{\mathbf{S}}^j(k) \right\|^2 \right\}$

$\triangle(\tilde{\mathbf{S}}^i) = \sum_{n=1}^{2} \left\{ \left\| \mathbf{r}_n(k) - \tilde{\mathbf{H}}_n^i(k)\tilde{\tilde{\mathbf{S}}}^i(k) - \tilde{\mathbf{H}}_n^j(k)\tilde{\mathbf{S}}^j(k) \right\|^2 \right\}$

$\triangle_i = \triangle_i + \triangle(\tilde{\mathbf{S}}^i)$

end

if $\triangle_1 < \triangle_2$

choose $\left[\tilde{\mathbf{S}}^1(k), \tilde{\tilde{\mathbf{S}}}^2(k) \right]$

else

choose $\left[\tilde{\mathbf{S}}^2(k), \tilde{\tilde{\mathbf{S}}}^1(k) \right]$

end

end

STBC technique is also implemented based on similar simulation environment for comparison. During simulations, assume that the transmitter power of each user is the same. The system parameters are considered as follows: the signal bandwidth is 1 MHz, which is divided into 128 sub-carriers by OFDM operation, and the data modulation is considered to be QPSK for all subcarriers, where each user data stream contains 256 symbols. In order to make the tones orthogonal to each other, IFFT operation is 128 us, an additional 22 cyclic prex symbols are used as a guard interval after each data block.

The data transmission is implemented simply over a MIMO frequency selective channel with slow time variant fading, generated by the typical Jakes' fading model (see in [89]) and the multipath channels have 6 taps for each transmit-receive antenna pair, i.e. frequency-selective sub-channel tap length $L = 6$ and $\sum_{l=1}^{L} \sigma_l^2 = 1$, where σ_l^2 is the variance of the lth path. Herein, the channel fading is assumed to be uncorrelated among different transmitting antennas of different users. Moreover, the perfect knowledge of the channel state information will be assumed at the receiver at any time.

In Figure 6.4, the frame error rate (FER) performance comparison for two user QO-STBC-OFDM system multiuser detection is shown. The simulations are implemented as a comparison between L-MMSE interference suppression and two-step multiple access interference (MAI) cancellation over slowly fading channels which are at 20Hz maximum Doppler frequency. SNR is used in the simulation for consistency but E_b/N_0 would simply be a 3dB shift for QPSK caused from error floor at this slow fading.

As a benchmark, the performance of MAI-free bound is also evalu-

ated with two-step processing in Figure 6.4, assuming *perfect knowledge of the multiple access interfering symbols* [90] at maximum Doppler frequency of 20Hz. The benchmark shows the limitation of performance that the scheme can achieve when the MAI can be evaluated perfectly. From the result, it is clear that the two-step PIC scheme performs very close to the so-called MAI-free bound (MAIFB), e.g. there is only 1dB shift at 10^{-3} FER between two-step scheme and MAIFB, but 5dB for one-step scheme, i.e. the proposed two-step PIC scheme performs MAI cancellation more effectively rather than LMMSE.

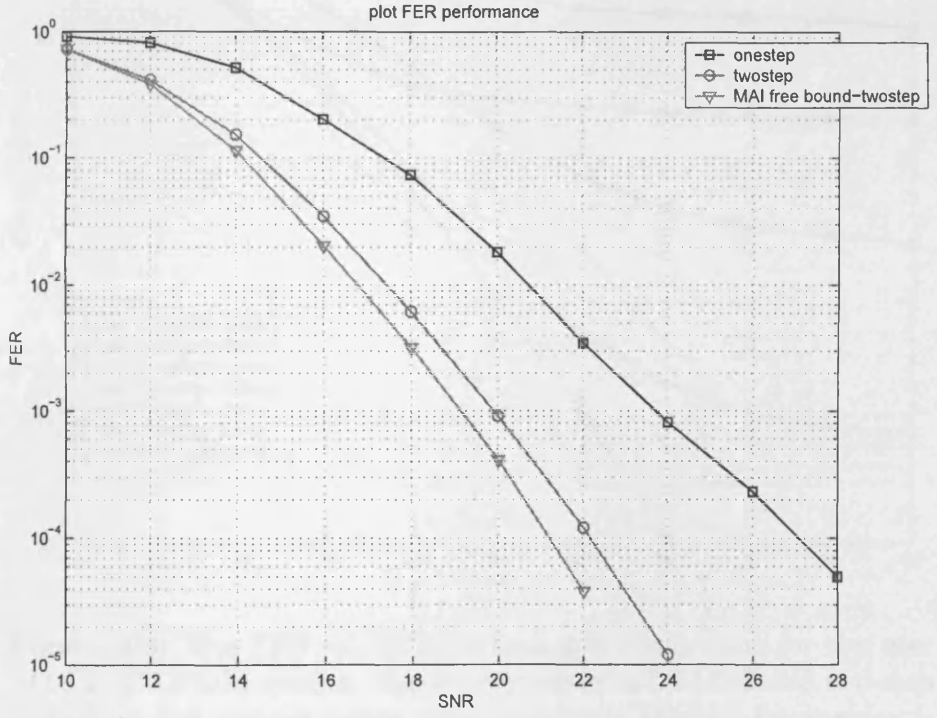

Figure 6.4. The FER vs. SNR performance comparison for two user QO-STBC-OFDM system: LMMSE and two-step schemes over slow fading MIMO channels where channel tap length $L = 3$ and Doppler frequency $f_d = 20Hz$. MAI-free bound is also shown.

Figure 6.5 illustrates the comparison of system performance between L-MMSE interference suppression and two-step processing when the

system is working over various fading rate channel environments. The best performance is given at the channel of 20Hz maximum Doppler frequency, which means small value of Doppler shift can avoid an error floor in the proposed QO-STBC-OFDM system. Otherwise, the performance degrades at higher SNR values with increasing maximum Doppler frequency, e.g. two-step scheme has 3dB SNR shift at 10^{-4} FER between $f_d = 20Hz$ and $f_d = 50Hz$.

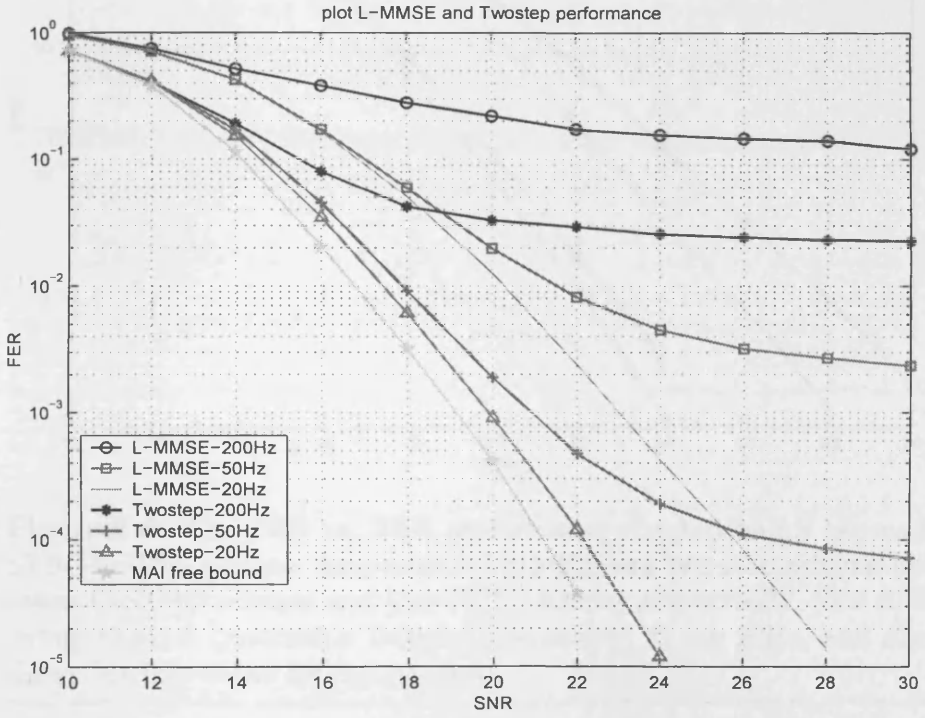

Figure 6.5. The FER vs. SNR performance comparison for two user QO-STBC-OFDM system: implements between LMMSE and two-step processing over various fading rates (maximum Doppler frequencies f_d are 20Hz, 50Hz and 200Hz respectively), and MAIFB is also performed at 20Hz for comparison.

Recall that the channel is assumed to be quasi-static over four OFDM symbol periods in order to employ the QO-STBC codes. This assumption will be violated in the time-variant channel case and the or-

thogonality of Qo-STBC can not be obtained between the antennas and the carriers which will cause an error floor. This problem can be further solved by using closed-loop optimization to obtain orthogonality.

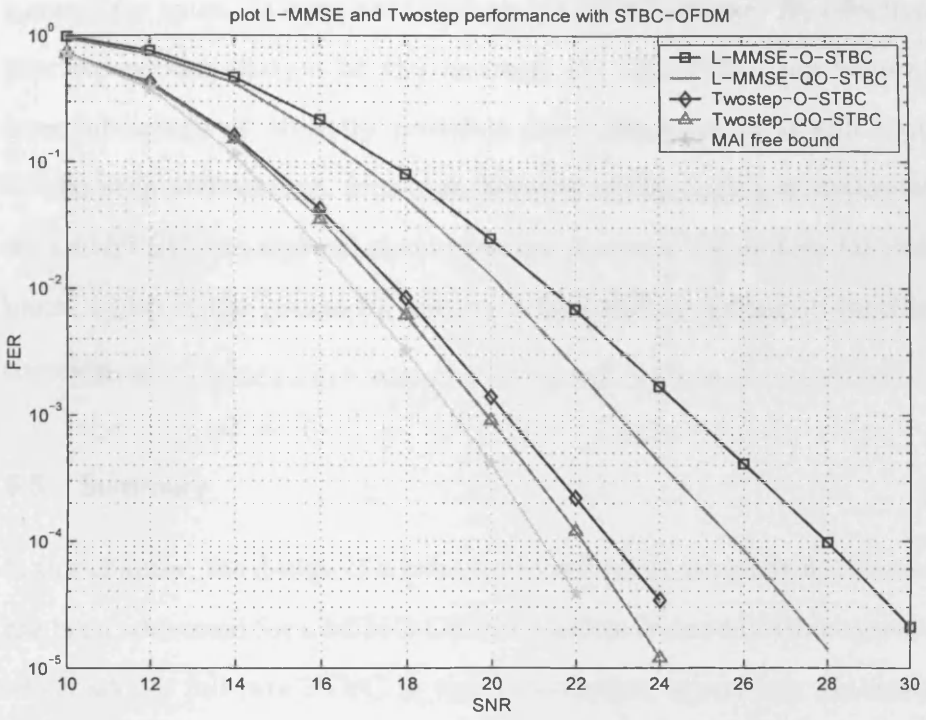

Figure 6.6. The FER vs. SNR performance comparison for two user STBC-OFDM system: implements LMMSE and two-step scheme between O-STBC scheme and QO-STBC scheme respectively, over slow fading channel (maximum Doppler frequencies f_d are 20Hz, and also shows MAIFB curve for comparison.

In Figure 6.6, a performance comparison for a two user STBC-OFDM system which uses the LMMSE and two-step scheme and a O-STBC scheme and the proposed QO-STBC scheme is given for slow fading channels. Herein maximum Doppler frequencies of the channel f_d is considered as 20Hz, and the MAIFB curve is also shown for comparison. From the simulation result, it is clear that the QO-STBC scheme outperforms the O-STBC scheme, particularly, when the value

of SNR is high, e.g. the proposed two-step QO-STBC outperforms two-step O-STBC more than 3dB SNR at 10^{-4} FER.

The QO-STBC is best due to the diversity increase through more transmitter antennas compared with the O-STBC scheme. By effective interference cancellation at the receiver, the QO-STBC can achieve more advantage of diversity provided that orthogonality is still kept for the proposed scheme. However, because of the coding structure of the QO-STBC, the channel should remain constant within four OFDM block, which is the reason for the error-floor still occurring in varying channels.

6.5 Summary

In this chapter, the design of a two-step interference cancellation scheme has been addressed for a MIMO-OFDM wireless communication system which adopts full-rate STBC in the transmission, where four transmit antennas in each terminal user and two receive antennas in the receiver are exploited. The receiver is based on a linear MMSE interference suppression in the first step and a two-step parallel interference cancellation approach is also considered based on hard decision.

Simulation results show a considerable performance improvement of the proposed full-rate STBC over the two-step interference cancellation methods over slow fading channels. It is clear that MAI can be suppressed and cancelled effectively. However, the performance of the scheme still suffers significant degradation from the effect of time variant MIMO channels. Due to error detection, the proposed two-step MAI scheme based on hard decisions could induce the risk of oscillation such that the performance becomes worse with increasing number

of iterations. If the temporary decision is wrong, the error will be doubled after the interference stages, especially in the early stages of the iterative processing.

A straightforward enhancement is to use a soft decision rather than a hard decision after the first detection stage which may cause the amplitude of a symbol estimate to represent its reliability more correctly. Moreover, a weight factor to scale can be used for the MAI estimates for further improvement of MAI cancellation. By proper improvement, the proposed scheme can be considered as a promising technique for high data wireless transmission over frequency selective multi-path fading channels for multiuser broadband wireless communication systems.

Chapter 7

CONCLUSION

In this final chapter of the thesis, the work and results presented in the previous chapters are summarized. In addition several directions for future work are discussed.

7.1 Summary of the Thesis

In this thesis, the design of space-time block coding scheme for frequency-flat channels is developed for point-to-point wireless communications. The proposed scheme is then extended to WCDMA and OFDM systems with four transmit antennas. Moreover, it also provides a first step to introducing more sophisticated interference cancellation and signal detection techniques into synchronous MIMO-OFDM systems and multiuser applications. In particular, the combination of STBC, MIMO, WCDMA and OFDM are addressed to improve transmission performance of broadband wireless communication systems.

STBCs from orthogonal design or orthogonal space-time block codes for MIMO wireless communications systems are a very powerful means of increasing the reliability of communication links. But a complex orthogonal design of OSTBCs which provides full diversity and full transmission rate is not possible for more than two transmit antennas. QO-STBC and EO-STBC have been introduced as a family of STBCs

with four transmit antennas, which can achieve full data rate at the expense of diversity order loss.

In the first part of the thesis, QO-STBC and EO-STBC for four transmit antennas are considered. In Chapter 3, loss of the diversity is questioned and it is found that this is due to an "interference factor". A novel method rotates the signals from one or two transmit antennas with phasers based on full and partial CSI. This CSI can possibly consist of feedback information from the receiver to the transmitter. Simulation results show that the QO-STBC and EO-STBC outperform the O-STBCs which adopted two transmit antenna, otherwise, the proposed closed-loop methods can provide substantial performance improvement than the open-loop. In particular, at 10^{-3}, the QO-STBC with feedback provides nearly $2dB$ improvement compared with O-STBC with two transmit antennas, and nearly $1dB$ degradation in the performance between QO-STBC and EO-STBC.

In Chapter 4, a novel combination of STBCs and the current third generation communication system - WCDMA is proposed. In this approach, a robust system model is adopted and the proposed STBC-WCDMA system is analyzed with the two transmit antennas and four transmit antennas. The feedback schemes are provided to orthogonalize QO-STBC and EO-STBC by rotating the transmitted signals from certain antennas in a prescribed way, based upon the information fed back from the receiver in the STBC-WCDMA system. The simulation result indicated that the performance can be enhanced when combined with STBCs and WCDMA wireless communication system. The proposed QO-STBC feedback scheme could obtain substantial performance improvement over quasi-static channel rather than the O-STBC

scheme with two transmit antennas, especially the EO-STBC scheme with feedback can achieve the best performance.

In Chapter 5, the previous schemes are successfully extended as full rate space time block codes within a beyond 3G communication multiuser system, OFDM system. The simulation results show that the new novel system can improve the performance, especially the close-loop method.

In Chapter 6, a novel and robust MUD technique called parallel interference cancellation was introduced for multiuser STBC-OFDM detection. The design of a two-step interference cancellation receiver was addressed to cancel MAI in a multiuser MIMO wideband wireless communications system within the quasi-static channel environment. In this approach, the transmitter serially concatenate STBC with OFDM for each user terminal and the receiver was based on a two-step hard-interference cancellation algorithm. The simulation results indicate that the proposed scheme could obtain substantial performance without increasing the complexity compared with the L-MMSE scheme for quasi-static channels with four transmit antennas.

7.2 Future Work

There are several possibilities for future research. In the following, some research directions are mentioned.

7.2.1 Robustness of Space Time Codes

1. The phase rotation algorithm proposed in the third chapter is considered only for a four transmit antenna scheme. This scheme can be generalized to a larger number of transmit antenna, e.g.,

five or six antennas. However, more feedback bits are required for a large number of antennas. Therefore, there is still an open point to reduce the amount of feedback bits for QO-STBCs or EO-STBCs employing more than four transmit antennas.

2. Throughout the thesis, CSI at the receiver is assumed to be known perfectly. However, in a real world application, CSI can only be estimated which obviously will introduce an error in the CSI. An interesting study would examine the proposed method in this thesis with channel estimation imperfections, and design robust algorithms.

3. Only one receive antenna is adopted in the thesis. However, multiple antennas also mean multiple radio frequency (RF) chains (analog-digital converters, low noise amplifiers, and down converters). But in some cases it may be impractical or even undesirable to have multiple RF chains at the receiver. A promising approach for reducing the cost and complexity while retaining a reasonably large fraction of the high potential data rate of a MIMO system is to employ a reduced number of RF chains at the receiver and attempt to optimally allocate each chain to one of a larger number of receive antennas. Actually, in this way, only the best set of antennas is used, while the remaining antennas are not employed, thus reducing the number of required RF chains.

7.2.2 Robustness of STBC MIMO-OFDM system

1. For future work of improving two-step multiuser detection scheme, soft estimation can be introduced into symbol estimate stage.

2. In recent years, iterative processing techniques with soft-input soft-output components have received considerable attention. Therefore, multiuser detection by iterative signal estimation scheme will be an effective approach in my work.

3. By concatenating the interference cancellation and detection process with channel decoding in every estimation stage, the approach can provide reduction of the risk of oscillation and improvement of system performance. A powerful channel decoder (for example, convolutional coding technique) can substantially improve the temporary data estimates and achieve more accurate interference reconstruction and subtraction. In addition to the multiple transmit and receive antenna diversities, the frequency selective diversity of order L can also be gained if an appropriate channel decoding algorithm is used.

4. More users can be simply introduced into the proposed STBC MIMO-OFDM systems by adding transmit terminals. Moreover this can also be realized by combining the interference cancellation and cooperative base station technique on receiving stage for more coverage and capacity.

BIBLIOGRAPHY

[1] T. Company, "Space-time block coded transmit antenna diversity for WCDMA," *SMG2 document*, p. 581/98, 1998.

[2] B. Hochwald, T. L. Marzetta, and C. B. Papadias, "A transmitter diversity scheme for wideband CDMA system based on space-time spreading," *IEEE Journal Selection Area on COmmun.,*, vol. 19, pp. 48–60, 2001.

[3] A. F. Naguib, N. Seshadri, and A. R. Calderbank, "Applications of space-time block codes and interference suppression for high capacity and high data rate wireless systems," *Proc. 32nd Asilomar Conf. Signals, Systems, and Computers*, vol. 2, pp. 1803–1810, Nov. 1998.

[4] T. S. Rappaport, *Wireless Communications Principles and Practice.* Upper Saddle River, NJ, Prentice Hall PTR, 1996.

[5] S. M. Alamouti, "A simple transmit diversity technique for wireless communications," *IEEE Journal on Selected Areas in Communications*, vol. 16, pp. 1451–1458, Sept. 1998.

[6] A. Lozano, F. R. Farrokhi, and R. A. Valenzuela, "Lifting the Limits on High-Speed Wireless Data Access Using Antenna Arrays," *IEEE Commun. Mag.*, vol. 39, pp. 156–162, Sep. 2001.

[7] A. J. Paulraj, D. A. Gore, R. U. Nabar, and H. Boelcskei, "An Overview of MIMO Communications - A Key to Gigabit Wireless," *Proc. IEEE*, vol. 92, pp. 198–218, Feb. 2004.

[8] G. Foschini, "Layered space-time architecture for wireless communication in a fading environment when using multi-element antennas," *Bell Labs Tech J.*, vol. 1, no. 2, pp. 41–59, 1996.

[9] N. Balaban and J. Salz, "Dual diversity combining and equalization in digital cellular mobile radio," *IEEE Transactions on Vehicular Technology*, vol. 40, pp. 342–354, May 1994.

[10] S. Catreux, V. Erceg, D. Gesbert, and J. R. W. Heath, "Adaptive Modulation and MIMO Coding for Broadband Wireless Data Networks," *IEEE Commun. Mag.*, vol. 40, pp. 108–115, Jun. 2002.

[11] V. Tarokh, N. Seshadri, and A. R. Calderbank, "Space-Time Codes for High Data Rate Wireless Communication: Performance Criterion and Code Construction," *IEEE Trans. Inform. Theory*, vol. 44, pp. 744–765, Mar. 1998.

[12] D. G. Brennan, "Linear Diversity Combining Techniques," *Proceedings of the IEEE*, vol. 91, pp. 331–356, Feb. 2003.

[13] S. Haykin, *Array Signal Processing.* Englewood Cliffs (NJ):Prentice-Hall, 1985.

[14] R. T. Compton, *Adaptive Antennas: Concepts and Performance.* Englewood Cliffs (NJ):Prentice-Hall, 1988.

[15] W. F. Gabriel, "Adaptive Processing Array Systems," *Proceedings of the IEEE*, vol. 80, pp. 152–162, Jan. 1992.

[16] L. Zheng and D. N. C. Tse, "Diversity and Multiplexing: A Fundamental Tradeoff in Multiple-Antenna Channels," *IEEE Trans. Inform. Theory*, vol. 49, pp. 1073–1096, May 2003.

[17] V. Tarokh, H. Jafarkhani, and A. R. Calderbank, "Space-time block codes from orthogonal designs," *IEEE Trans. Inform. Theory*, vol. 45, pp. 1456–1467, Jul. 1999.

[18] O. Tirkkonen and A. Hottinen, "Complex Space-time block codeds for four TX antennas," *Globecom 2000*, vol. 2, pp. 1005–1009, Dec. 2000.

[19] M. Rupp and C. F. Mechlenbrauker, "On Extended Alamouti Schemes for Space-Time Coding," *WPMC, Honolulu*, pp. 115–118, Oct. 2002.

[20] G. Ganesan and P. Stoica, "Space-time deiversity using orthogonal and amicable orthogonal design," *Wireless Personal communications*, vol. 18, pp. 165–178, 2001.

[21] O. Tirkknen, A. Boariu, and A. Hottinen, "Minimal Nonorthogonality Rate One Space-Time Block Codes for 3+ Tx Antennas," *IEEE International Symposium on Spread Spectrum Techniques and Application (ISSSTA), New Jersey, USA*, vol. 2, pp. 429–432, Sep. 2000.

[22] C. F. Mechlenbräuker and M. Rupp, "On Extended Alamouti Schemes for Space-Time Coding," *WPMC'02, Honolulu*, pp. 115–119, Oct. 2002.

[23] H. Jafarkhani, "A Quasi Orthogonal Space-Time Block Code," *IEEE Trans. Comm.*, vol. 49, pp. 1–4, Jan. 2001.

[24] J. Hou, M. H. Lee, and J. Y. Park, "Matrices analysis of quasi-orthogonal space-time block code," *IEEE Comm. Letters*, vol. 7, no. 8, pp. 385–387, 2003.

[25] K. F. Lee and D. B. Williams, "A Space-Frequency Transmitter Diversity Technique for OFDM Systems," *Proc. IEEE GLOBECOM, San Francisco, CA*, pp. 1473–1477, Nov. 2000.

[26] L. Teletar, "Capacity of multi-antenna Gaussian channels," *European Trans. Telecommunications*, vol. 10, pp. 585–595, Nov./Dec. 1999.

[27] A. Hottinen, O. Tirkkonen, and R. Wichman, *Multi-Antenna Transceiver Techniques for 3G and Beyond.* John Wiley and Son Ltd, 2003.

[28] G. Foschini and M. Gans, "On Limits of Wireless Communications in a Fading Environment when Using Mlutiple Antennas," *Wireless Personal Communications*, vol. 6, pp. 331–335, Mar. 1998.

[29] J. H. Winters, "On the Capacity of Radio Communication Systems with Diversity in a Rayleigh Fading Environment," *IEEE Journal on Selected Areas in Communications*, pp. 871–878, 1987.

[30] A. Wittneben, "A New Bandwidth Efficient Transmit Antenna Modulation Diversity Scheme for Linear Digital Modulation," *IEEE Int. Conference on Com., Geneva*, vol. 3, pp. 1630–1634, May 1993.

[31] M. K. Simon and M. S. Alouini, *Digital Communication over Fading Channel: A Unified Approach to Performance Analysis.* John Wiley and Son Ltd, 2000.

[32] N. Morinaga, R. Kohno, and S. Samnei, *Wireless Communication Technologies: New Multimedia.* Springer, 2000.

[33] C. Chuah, J. M. Kahn, and D. Tse, "Capacity of Multi-Antenna Array Systems in Indoor Wireless Environment," *Globecom, Sydney, Australia*, vol. 4, pp. 1894–1899, Nov. 1998.

[34] C. Shannon, "A mathematical theory of communication," *Bell Syst. Tech. J.*, vol. 27, pp. 379–423, Nov. 1948.

[35] A. Paulraj, R. Nabar, and D. Gore, *Introduction to Space-time Communications.* Cambridge, UK: Cambridge Univ. Press, 2003.

[36] A. Annamalai, "Selection diversity reception of spread-spectrum signals with unequal mean strengths," *IEEE 47th Vehicular Technology Conference*, vol. 2, pp. 1153–1157, May 1997.

[37] W. C. Jakes, *Microwave Mobile Communications.* New York: John Wiley and Sons, 1974.

[38] S. N. Diggavi, N. Al-Dhahir, A. Stamoults, and A. R. Calderbank, "Great expectations: the value of spatial diversity in wireless networks," *Proc. of the IEEE*, vol. 92, pp. 219–270, Feb. 2004.

[39] M. Tarkiainen and T. Westman, "Predictive Switched Diversity for Slow Speed Mobile Terminals," *IEEE Vehicular Technology Conference*, vol. 3, pp. 2042–2044, May 1997.

[40] S. R. Saunders, *Antennas and Propagation for Wireless Communication Systems.* Wiley, 1999.

[41] M. Jankiraman, *Space-time codes and MIMO systems.* Artech House, 2004.

[42] J. Radon, *Lineare scharen orthogonaler matrizen.* Abhandlungen aus dem Mathematischen Seminar der Hamburgishen Universitat, 1922.

[43] A. V. Geramita and J. Seberry, *Orthogonal Designs, Quadratic Forms and Hadamard Matrices, Lecture Notes in Pure and Applied Mathematics.* New York and Basel: Marcel Dekker, 1979.

[44] B. Vucetic and J. Yuan, *Space-Time Coding.* John Wiley and Sons, 2003.

[45] G. Larsson and P. Stoica, *Space-time Block Coding for Wireless Communication.* Cambridge University press, 2003.

[46] H. Jafarkhani, *Space-Time Coding: Theory and Practice.* Cambridge University press, 2005.

[47] C. Papadias and G. Goschini, "Capacity-Approaching Space-Time Codes for System Employing Four Transmitter Antennas," *IEEE Trans. Inf. Theory*, vol. 3, pp. 726–733, Mar. 2003.

[48] C. F. Mechlenbräuker and M. Rupp, "Flexible Space-Time Block Codes for Trading Quality of Service Against Data Rate in MIMO UMTS," *EURASIP J. on Appl. Signal Proc.*, pp. 662–675, May 2004.

[49] F. C. Zheng and A. G. Burr, "Robust Non-Orthogonal Space-Time Block Codes Over Highly Correlated Channels: a Generalisation," *IEE E1. Lettters*, vol. 39, pp. 1190–1191, Aug. 2003.

[50] C. Toker, S. Lambotharan, and J. A. Chambers, "Space-time block coding for four transmit antennas with closed loop feedback over frequency selective fading channels," *IEEE Information Theory Workshop*, pp. 195 – 198, Apr. 2003.

[51] Y. Yu, S. Keroueden, and J. Yuan, "Closed-Loop Extended Orthog-

onal Space-Time Block Codes for Three and Four Transmit Antennas," *IEEE Signal Processing Letters*, vol. 13, May 2006.

[52] P. W. Wolniansky, G. J. Roschini, G. D. Golden, and R. A. Valenzuela, "V-BLAST: an architecture for realizing very high data rates over the rich-scattering wireless channel," *In Proc. 1998 Int. Symp. Sig. Sys. Elect. (ISSSE'98), Pisa, Italy*, Sep. 1998.

[53] L. Zheng and D. N. C. Tse, "Diversity and multiplexing: A fundamental tradeoff in multiple-antenna channels," *IEEE Trans. Information Theory*, vol. 49, pp. 1073–1096, May 2003.

[54] A. J. Paulraj and T. Kailath, *Increasing capacity in wireless broadcast systems using distributed transmission/directional reception.* U.S. Patent Storm, 1994.

[55] G. G. Raleigh and J. M. Cioffi, "Spatio-Temporal Coding for Wireless Communication," *IEEE Transactions on Communications*, vol. 46, no. 3, pp. 357–366, 1998.

[56] D. G. H. Bölcskei and A. J. Paulraj, "On the Capacity of OFDM-based Spatial Multiplexing Systems," *IEEE Trans. Commun.*, vol. 50, p. 225C234, Feb. 2002.

[57] T. Ojanpera and R. Prasad, *Widerband CDMA for Third Generation Mobile Communications.* Artech House, Norwood, MA, 1998.

[58] L. Tong, A. J. V. der Veen, P. Dewilde, and Y. Sung, "Blind decorrelating Rake Receivers for long-code WCDMA," *IEEE Trans. Signal Processing*, vol. 51, pp. 1642–1655, Nov. 2003.

[59] S. Verdu, *Multiuser detection.* Cambridge; New York: Cambridge University Press, 1998.

[60] L. Hanzo, W. Webb, and T. Keller, *Single- and Multi-Carrier Quadrature Amplitude Modulation.* John Wiley and Sons Ltd, 2000.

[61] N. Brenner and C. Rader, "A New Principle for Fast Fourier Transformation," in *Proc. IEEE Acoustics Speech and Signal Processing*, 1976.

[62] S.B.Weinstein and P.M.Ebert, "Data transmission by Frequency-Division Multiplexing using the Discrete Fourier Transform," *IEEE Transactions on Communication Technology*, vol. 19, pp. 628–634, Oct. 1971.

[63] P. Stavroulakis, *Interference analysis and reduction for wireless systems* . Boston, MA : Artech House, 2003.

[64] R. Poole, "The echo performance of DVB-T receivers," *EBU technical review*, vol. 3, pp. 1241–1245, Sept. 2001.

[65] V. Benedetto, G. D'Aria, L. Scarabosio, "Performance of COFDM systems with waveform shaping," in *Proc. IEEE International Conference on Communications, ICC'97*, 1997.

[66] R. A. Horn and C. R. Johnson, *Matrix Analysis.* Cambridge, U.K.:Cambridge University Press, 1985.

[67] P. Schniter, "Low-complexity equalization of OFDM in doubly selective channels," *IEEE Trans. Signal Processing*, vol. 52, pp. 1002–1011, Apr. 2004.

[68] E. H. Moore, "On the reciprocal of the general algebraic matrix," *Bulletin of the American Mathematical Society*, vol. 26, pp. 394–395, 1920.

[69] R. Penrose, "A generalized inverse for matrices," *Proceding of the Cambridge Philosophical Society*, vol. 51, pp. 406–413, 1955.

[70] Z. Liu, Y. Xin, and G. B. Giannakis, "Space-time-frequency coded OFDM over frequency-selective fading channels," *IEEE Transactions on Signal Processing*, vol. 50, pp. 2465–2476, 2002.

[71] S. Suthaharan, A. Nallanathan, and B. Kannan, "Space-Time Coded MIMO-OFDM for high capacity and high data-rate wireless communication over frequency selective fading channels," *Proc. Mobile and Wireless Communications Network 2002, 4th International Workshop*, pp. 424–428, 2002.

[72] P. L. Kafle and A. B. Sesay and J. McRory, "An Iterative MMSE-decision Feedback Multiuser Detector for Space-time Coded Multicarrier CDMA System," May 2004.

[73] Y. S. Choi and P. J. Voltz and F. A. Cassara, "On Channel Estimation and Detection for Multi-carrier Signals in Fast and Selective Rayleigh Fading Channels," *IEEE Transactions on Communications*, vol. 49, pp. 1375–1387, Aug. 2001.

[74] C. Shen, L. Zhang, and J. A. Chambers, "A two-step interference cancellation technique for a mimo-ofdm system with four transmit antennas," in *Proc. 2007 15th International Conference on Digital Signal Processing*, (Cardiff, UK), 1-4 July 2007.

[75] A. Duel-Hallen, J. Holtzman, and Z. Zvonar, "Multiuser detection for CDMA systems," *IEEE Personal Communications*, vol. 2, pp. 46–58, Apr. 1997.

[76] S. Moshavi, "Multi-user detection for DS-CDMA communications," *IEEE Communications Magazine*, vol. 12, pp. 124–136, Oct. 1996.

[77] F. Nordstorm, *Interferer Detection and Cancellation in TDMA-Systems.* PhD thesis, Centre for Mathematical Sciences, Lund University, Sweden, 2002.

[78] M. Jiang and L. Hanzo, "Multiuser MIMO-OFDM for Next-Generation Wireless Systems," *Proceedings of the IEEE*, vol. 95, pp. 1430–1469, July 2007.

[79] L. Hanzo, M. Münster, B. J. Choi, and T. Keller, *OFDM and MC-CDMA for Broadband Multi-User Communications, WLANs and Broadcasting.* Piscataway, NJ: IEEE Press/Wiley, 2003.

[80] L. Giangaspero, L. Agarossi, G. Paltenghi, S. Okamura, M. Okada, and S. Komaki, "Co-channel interference cancellation based on MIMO OFDM systems," *Wireless Commun.*, vol. 9, pp. 8–17, Dec. 2002.

[81] B. Hagerman, *Single-User Receivers for Partly Known Interference in Multi-User Environments.* PhD thesis, Royal Institute of Technology, Sweden, Sept. 1995.

[82] P. Patel and J. Holtzman, "Analysis of a simple successive interference cancellation scheme in a DS/CDMA system," *IEEE Journal on Selected Areas on Communications*, pp. 976–807, June 1994.

[83] M. K. Varanasi and B. Aazhang, "Multistage detection in asynchronous code division multiple access communications," *IEEE Transactions on Communications*, vol. 38, pp. 509–519, Apr. 1990.

[84] R. K. Y. C. Yoon and H. Imai, "A spread-spectrum multiaccess system with cochannel interference cancellation for multipath fading channels," *IEEE Journal on Selected Areas in Communications*, vol. 11, pp. 1067–1075, Sept. 1993.

[85] P. Alexander, A. Grant, and M. Reed, "Iterative detection in Code-Division Multiple Access," *European Transactions on Telecommunications*, vol. 9, pp. 419–425, Sept. 1999.

[86] H. El Gamal and E. Geraniotis, "Iterative multiuser detection for coded CDMA signals in AWGN and fading channels," *IEEE Journal on Selected Areas in Communications*, vol. 18, 2000.

[87] D. Guo, L. K. Rasmussen, and T. J. Lim, "Linear parallel interference cancellation in long-code CDMA multiuser detection," *IEEE Journal on Selected Areas in Communications*, vol. 17, pp. 2074–2081, Dec. 1999.

[88] A. Nahler, R. Irmer, and G. Fettweis, "Reduced and differential parallel interference cancellation for CDMA systems," *IEEE Journal on Selected Areas in Communications*, vol. 20, no. 2, 2002.

[89] W. C. Jakes, *Microwave Mobile Communications.* Wiley IEEE Press, May 1994.

[90] P. Schniter, "Low-complexity equalization of OFDM in doubly selective channels," *IEEE Transactions on Signal Processing*, vol. 52, pp. 1002–1011, April 2004.